Modeling of characteristics and methodology for testing lithium-ion batteries for electric vehicle applications

Bašić, Hrvoje

University of Zagreb

FACULTY OF ELECTRICAL ENGINEERING AND COMPUTING

Hrvoje Bašić

MODELING OF CHARACTERISTICS AND METHODOLOGY FOR TESTING LITHIUM-ION BATTERIES FOR ELECTRIC VEHICLE APPLICATIONS

DOCTORAL THESIS

Zagreb, 2023

University of Zagreb

FACULTY OF ELECTRICAL ENGINEERING AND COMPUTING

Hrvoje Bašić

MODELING OF CHARACTERISTICS AND METHODOLOGY FOR TESTING LITHIUM-ION BATTERIES FOR ELECTRIC VEHICLE APPLICATIONS

DOCTORAL THESIS

Supervisor: Professor Hrvoje Pandžić, PhD

Zagreb, 2023

Sveučilište u Zagrebu

FAKULTET ELEKTROTEHNIKE I RAČUNARSTVA

Hrvoje Bašić

MODELIRANJE ZNAČAJKI I METODOLOGIJA ISPITIVANJA LITIJ-IONSKIH BATERIJA ZA PRIMJENU U ELEKTRIČNIM VOZILIMA

DOKTORSKI RAD

Mentor: prof. dr. sc. Hrvoje Pandžić

Zagreb, 2023.

The doctoral thesis was completed at the University of Zagreb Faculty of Electrical Engineering and Computing, Department of Energy and Power Systems, Zagreb, Croatia.

Supervisor: Professor Hrvoje Pandžić, PhD

Doctoral thesis has: 84 pages

Doctoral thesis number: _____

About the Supervisor

Hrvoje Pandžić (www.fer.unizg.hr/hrvoje.pandzic) was born in 1984 in Zagreb, Croatia. He received his Masters and PhD degrees from the University of Zagreb Faculty of Electrical Engineering and Computing (UNIZG-FER) in 2007 and 2011, respectively. After being a postdoctoral researcher at the University of Washington, Seattle, 2012-2014, he became an Assistant Professor at UNIZG-FER in 2014. Currently, he is a Professor at UNIZG-FER and Head of the Department of Energy and Power Systems, as well as Head of the Demand Response Laboratory (drlab.fer.hr). He has coordinated and participated in many European and national projects focused on electricity markets, energy storage, electric vehicles, microgrids and demand response. He published over 70 papers in journals categorized as Q1/Q2 according to JCR. He received numerous awards, including the Award Science by the Government of the Republic of Croatia, 2018; Award for the highest scientific and artistic achievements in Croatia by the Croatian Academy of Science and Arts for 2018; Award Vera Johanides by the Croatian Academy of Engineering for 2015. He has been an Associate Member of the Croatian Academy of Science and Arts since 2020 and an Associate Member of the Croatian Academy of Engineering since 2023. He has been an Editor of IEEE Transactions on Power Systems journal since 2019. He is an IEEE Senior Member, as well as a member of INFORMS and CIGRE. Besides research achievements, he has led over 20 technical studies for commercial partners.

orcid.org/0000-0003-4121-4702

scholar.google.com/citations?user=cbFwhhkAAAAJ

www.researchgate.net/profile/Hrvoje-Pandzic-2

www.scopus.com/authid/detail.uri?authorId=24438098800

www.webofscience.com/wos/author/record/2706650

O mentoru

Hrvoje Pandžić (www.fer.unizg.hr/hrvoje.pandzic) rođen je 1984. godine u Zagrebu. Završio je diplomski studij 2007. i doktorski studij 2011. godine na Sveučilištu u Zagrebu Fakultetu elektrotehnike i računarstva (UNIZG-FER). Nakon pozicije poslijedoktoranda na Sveučilištu Washington u Seattleu 2012-2014., postaje docent na UNIZG-FER 2014. godine. Trenutno je redoviti profesor i predstojnik Zavoda za visoki napon i energetiku te voditelj Laboratorija za odziv potrošnje. Vodio je mnoge europske i nacionalne istraživačke projekte usmjerene na energetska tržišta, spremnike energije, električna vozila, mikromreže i odziv potrošnje. Objavio je preko 70 znanstvenih radova u znanstvenim časopisima kvalificiranima kao Q1 ili Q2 prema JCR. Dobitnik je mnogih nagrada, uključujući nagradu Znanost Republike Hrvatske za 2018. godinu, Nagradu za najviše znanstvene i umjetničke uspjehe Hrvatske akademije znanosti i umjetnosti za 2018. godinu te nagradu Vera Johanides Hrvatske akademije tehničkih znanosti za 2015. godinu. Član-suradnik je Hrvatske akademije znanosti i umjetnosti od 2020. godine. Član je uređivačkog odbora časopisa IEEE Transactions on Power Systems. Član je profesionalnih udruženja IEEE (Senior Member), INFORMS i CIGRE. Osim znanstvenih uspjeha, vodio je preko 20 projekata za komercijalne naručitelje.

orcid.org/0000-0003-4121-4702

scholar.google.com/citations?user=cbFwhhkAAAAJ

www.researchgate.net/profile/Hrvoje-Pandzic-2

www.scopus.com/authid/detail.uri?authorId=24438098800

www.webofscience.com/wos/author/record/2706650

Acknowledgement

Special thanks to my supervisor professor Hrvoje Pandžić for his ongoing support and for his dedicated mentorship.

Abstract

Lithium-ion batteries are gradually expanding their use in a wide range of applications, from consumer electronics to electric vehicles and stationary energy storage. Besides personal cars, there is a growing demand for electrification of special-purpose vehicles. These vehicles are characterized by low production numbers and specific limitations such as restricted volume for battery placement, specific working conditions, requirement to supply electro-hydraulic systems, etc. Therefore, the selection of optimal battery cell and identification of its required characteristics is not a straightforward task. This thesis presents a methodology for selecting optimal battery cell for special purpose electric vehicles. Methodology consists of several laboratory testing procedures established to measure the electric and temperature characteristics of the candidate battery types. By evaluation of the experimental test results using the Analytic Hierarchy Process, the most appropriate battery cell is selected.

This thesis focuses on derivation and analysis of battery characteristics. Specifically, the energy efficiency of lithium-ion batteries is targeted, which is an important but often overlooked metric that can be used to assess charging and discharging energy losses. This thesis presents a method for obtaining individual one-way charging and discharging efficiencies dependent on the charging/discharging power. A method is based on a solution to an optimization problem, a decomposition of the roundtrip efficiencies into the charging and the discharging efficiency for different power rates, resulting in one-way (charging/discharging) efficiency characteristics.

Finally, a novel method for determination of battery capacity actually stored in the battery is presented is well. The method accounts for both the charging and discharging losses in battery use in different operational and ambient conditions. The proposed method is tested in a laboratory and compared against two existing baseline methods at different ambient temperatures. The results indicate that the proposed method significantly outperforms the baseline methods in terms of accuracy of the determined battery energy capacity and state-of-energy.

Keywords:

Lithium-ion batteries, experimental testing, electric vehicles, analytic hierarchy process, roundtrip efficiency, one-way efficiency, battery capacity, energy capacity, state-of-charge, state-of-energy

Modeliranje značajki i metodologija ispitivanja litij-ionskih baterija za primjenu u električnim vozilima

Litij-ionske baterije mogu djelovati kao prikladan spremnik energije u raznim primjenama, od potrošačke elektronike do električnih vozila i sustava pohrane energije. Električna vozila s baterijskim spremnicima energije postupno šire svoje tržište izvan tipičnog sektora javnog i privatnog prijevoza. Dobar primjer je rastuća potražnja za elektrifikacijom vozila posebne namjene kao što su kompaktne vakumske ulične čistilice. Ova vozila karakterizira mali proizvodni broj i specifična ograničenja kao što su ograničen volumen za smještaj baterija, specifični radni uvjeti, zahtjev za napajanjem elektrohidrauličkih sustava itd. Stoga odabir optimalne baterije i identifikacija potrebnih karakteristika nije jednostavan zadatak.

Prvi dio istraživanja bavi se razvojem metodologije za odabir optimalne baterije za električna vozila specifične namjene. Uspostavljen je postupak laboratorijskog ispitivanja za mjerenje električnih i termalnih karakteristika različitih tipova baterija.

Litij kobalt oksid baterije imaju nizak energetski kapacitet u usporedbi s drugim tipovima, tako da su očekivanja energetskih testova za ovu ćeliju niska. Maksimalna struja pražnjenja je prilično niska, što može rezultirati lošim performansama pri velikim opterećenjima. Litij nikal kobalt aluminij oksid baterije imaju slične tehničke karakteristike kao i litij kobalt oksid baterije. Litij mangan oksid baterije imaju sposobnost izdržati visoke struje pražnjenja, dok same ćelije imaju visok energetski kapacitet. Prema tehničkim karakteristikama očekuju se natprosječni rezultati i na energetskim i na toplinskim ispitivanjima. Litij željezo fosfat ima visoku maksimalnu dopuštenu struju i dug životni ciklus, ali mali energetski kapacitet. Stoga se očekuju dobre karakteristike grijanja i specifični rezultati punjenja i pražnjenja, ali loši rezultati ispitivanja energetskog kapaciteta. Litij nikal mangan kobalt oksid ćelije s visokim energetskim kapacitetom i visokom maksimalnom dopuštenom strujom punjenja/pražnjenja trebale bi dati dobre rezultate i u ispitivanju termalnih karakteristika i u ispitivanju energetskog kapaciteta. Ne očekuje se da će litij nikal mangan kobalt oksid ćelije s nižim energetskim kapacitetom imati dobre rezultate u energetskim testovima, ali se očekuje da će njihove termalne karakteristike biti dobre.

Predložena metodologija za određivanje optimalne baterije za primjenu u električnom vozilu posebne namjene podijeljena je u dva dijela. Prvo se provode testovi u skladu s europskim standardima za određivanje potrošnje te dodatni testovi razvijeni posebno prema zahtjevima rada vozila. Drugo, multikriterijska metoda odabira, Analitički hijerarhijski proces (AHP), koristi se za procjenu i kategorizaciju karakteristika baterijskih ćelija i rezultata eksperimentalnih ispitivanja.

Odabir najprikladnije baterije provodi se s dva različita pristupa (Slika 1). Prvo, evaluacija se temelji na analizi tehničkih podataka proizvođača, a drugo na temelju podataka dobivenih iz

predloženih eksperimentalnih ispitivanja.

Slika 1: Metodologija za određivanje optimalne baterijske ćelije

Analitički hijerarhijski proces (AHP) koristi se za određivanje optimalnog tipa baterijske ćelije na temelju sljedećih kriterija:

- Na temelju podataka proizvo đača: deklariran energetski kapacitet, maksimalna struja pražnjenja, maksimalna struja punjenja i cijena
- Na temelju podataka dobivenih eksperimentalnim ispitivanjima (izmjeren energetski kapacitet i povećanje temperature) i cijena

Nakon evaluacije rezultata eksperimentalnog ispitivanja korištenjem analitičkog hijerarhijskog procesa, odabire se najprikladnija baterijska ćelija.

Svi predloženi testovi nisu jednako važni za primjenu u električnom vozilu, gdje energetski test i prilagođeni test potrošnje imaju ključnu ulogu u odabiru optimalne baterijske ćelije. S druge strane, testovi sporog i brzog punjenja koriste se kao kontrolni testovi gdje ćelija može pasti samo ako su postignuti rezultati znatno ispod prosjeka. Stoga se AHP koristi za usporedbu rezultata provedenih testova i odabir optimalne baterije za vozilo. Kriteriji koji se koriste za usporedbu su izmjereni energetski kapacitet i porast temperature u četiri provedena testa, tj. energetski test, prilagođeni test potrošnje i dva testa punjenja.

Optimalna litij-ionska baterijska ćelija odabrana predloženom metodologijom razlikuje se od baterijske ćelije odabrane isključivo na temelju analize tablica s podacima proizvođača. Dakle, iako podatkovne tablice proizvođača sadrže mnoge korisne informacije, pokazalo se da analiza koja se temelji isključivo na takvim podacima može rezultirati suboptimalnim odabirom baterijskih ćelija. Međutim, predložena metoda rješava taj problem i identificira optimalnu baterijsku ćeliju za danu namjenu.

Drugi dio istraživanja bavi se eksperimentalnim određivanjem parametara baterija i njihovom primjenom.

Razvojem tehnologije baterije su često su dio većih, složenih sustava. Kako bi se očuvala rješivost zadanih računalnih problema (računalna sposobnost), modeli baterija se obično pojednostavljuju. Većina takvih modela baterija zanemaruje ovisnost učinkovitosti punjenja/pražnjenja o razini snage punjenja/pražnjenja i umjesto toga koristi konstantnu učinkovitost u cijelom rasponu razina snaga punjenja/pražnjenja. Stoga, ovo istraživanje predstavlja i metodu za određivanje pojedinačnih jednosmjernih učinkovitosti punjenja i pražnjenja ovisnih o snazi punjenja/pražnjenja. Kad god se baterija puni ili prazni, gubi se dio energije. Ti su gubici povezani

s unutarnjim otporom elektroda i elektrolita baterije, što se uglavnom očituje u disipaciji topline (Slika 2).

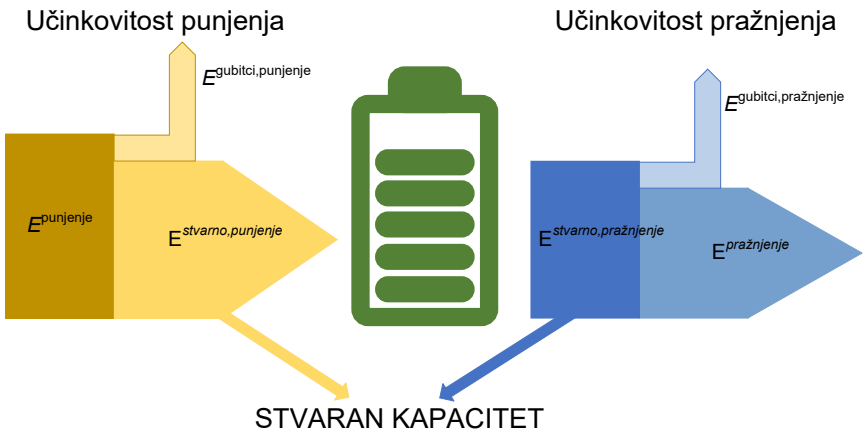

Slika 2: Učinkovitost punjenja/pražnjenja baterije

Kvantifikacija tih gubitaka naziva se učinkovitost baterije. Postoji više vrsta učinkovitosti baterija i sve su promjenjive, budući da ovise o različitim uvjetima punjenja/pražnjenja (C-stopa, P-stopa, temperatura okoline itd.), kao i o stanju zdravlja baterije (SOH, eng. state of health) i stanju napunjenosti (SOC, eng. state of charge) / stanju energije (SOE, eng. state of energy). C-stopa je brzina kojom se baterija puni ili prazni. Pri 1C baterija se puni (prazni) strujom koja odgovara njezinom kapacitetu u Ah (npr. 1C za bateriju od 10 Ah je 10 A, 0.5C je 5 A, itd.). P-stopa je postotak nominalne snage baterije pri kojoj se puni ili prazni. Kod 1P baterija se puni (prazni) brzinom koja odgovara njezinoj nominalnoj snazi (npr. 1P za bateriju kapaciteta 10Ah i nominalnog napona 10 V nominalna snaga iznosi 100 W, 0.5P je 50 W, itd.). SOC baterije je mjera za količinu naboja pohranjenog u bateriji u odnosu na puni kapacitet (pohranjeni naboj kada je baterija potpuno napunjena). SOE baterije je mjera za količinu energije pohranjene u bateriji s obzirom na puni energetski kapacitet (pohranjena energija kada je baterija potpuno napunjena). SOH baterije je mjera za cjelokupno stanje zdravlja baterije. Nova, zdrava baterija ima 100% SOH.

Podjela učinkovitosti baterije može biti prema mjerenim električnim veličinama: kulonska (η^{I}), naponska (η^{U}) i energetska (η^{E}) učinkovitost.

Učinkovitost baterije također se može podijeliti prema smjeru protoka energije: učinkovitost punjenja (η^{punjenje}), učinkovitost pražnjenja ($\eta^{\mathrm{pranjenje}}$) i kružna učinkovitost (η^{ciklus}).

C-stope i P-stope punjenja i pražnjenja baterije mogu se uvelike razlikovati, tako da uporaba odvojenih učinkovitosti punjenja i pražnjenja (umjesto kružne učinkovitosti) može omogućiti točniju procjenu SOE (i/ili SOC) baterije u stvarnom vremenu, kao i točnije predviđanje gubitaka energije pri planiranju rada baterije ili čak pri dimenzioniranju baterije. Međutim, određivanje učinkovitosti punjenja i pražnjenja (jednosmjerne učinkovitosti) nije jednostavno.

Učinkovitost se može eksperimentalno odrediti podvrgavanjem baterije ciklusu ili polucik-

lusu. Ciklus podrazumijeva i punjenje i pražnjenje u istom rasponu SOC (protok energije u oba smjera) i koristi se za određivanje kružne učinkovitosti. Poluciklus podrazumijeva ili punjenje ili pražnjenje (protok energije samo u jednom smjeru) i koristi se za određivanje jednosmjerne učinkovitosti punjenja ili pražnjenja. Određena učinkovitost može biti potpuna ili djelomična. Puni (polu)ciklus podrazumijeva punjenje od 0% na 100% SOC i/ili obrnuto, dok djelomični (polu)ciklus podrazumijeva pokrivanje određenog dijela SOC. Prilikom određivanja učinkovitosti baterije, puni (polu)ciklus treba započeti (i završiti, u slučaju kružne učinkovitosti) s potpuno ispražnjenom (0% SOC) ili potpuno napunjenom (100% SOC) baterijom. Ovaj pristup osigurava fiksnu početnu (i završnu) točku u smislu mjerljivih električnih veličina (napon na stezaljkama i struja). Ipak, SOC se obično koristi kao referenca za određivanje raspona parcijalnih (polu)ciklusa (koji također mogu biti udaljeni od 0% i 100% SOC). U tu svrhu, SOC se može odrediti najjednostavnijim oblikom brojanja kulona:

$$soc(t) = soc(t-1) + \frac{100}{C} \cdot \int_{t-1}^{t} I(\tau) d\tau, \tag{1}$$

gdje je $soc(t)$ izražen u postocima, C je kapacitet ćelije (Ah), a I je struja (A), pretpostavljena pozitivna za punjenje i negativna za pražnjenje. Kako bi se izbjeglo integriranje pogreške povezane s brojanjem kulona, preporučljivo je prvo potpuno napuniti ili isprazniti bateriju (100% ili 0% SOC), te ju zatim dovesti na ciljani SOC.

Postojeće metodologije za određivanje kulonske, naponske i energetske učinkovitosti objašnjene su kako slijedi:

•Kulonska u činkovitost

Kulonska učinkovitost je povezana s nabojem u amper satima (Ah) ispražnjenim iz baterije ili napunjenim u bateriju. Kulonska učinkovitost punjenja je omjer stvarnog naboja pohranjenog u bateriji (C^{stvarno}) i ukupnog naboja napunjenog u bateriju (C^{punjenje}) tijekom djelomičnog ili punog ciklusa punjenja. Kulonska učinkovitost pražnjenja je omjer ukupnog naboja ispražnjenog iz baterije ($C^{\text{praznjenje}}$) i stvarnog naboja pohranjenog u bateriji (C^{stvarno}) tijekom djelomičnog ili punog ciklusa pražnjenja. Kružna kulonska učinkovitost je omjer ukupnog naboja pražnjenog iz baterije ($C^{\text{praznjenje}}$) i ukupnog naboja punjenog u bateriju (C^{punjenje}) tijekom djelomičnog ili punog ciklusa.

•Naponska u činkovitost

Naponska učinkovitost je povezana s prosječnim naponom punjenja/pražnjenja. U ovom kontekstu, važno je razlikovati napon otvorenog kruga (U^{OC}) i napon zatvorenog kruga (U^{punjenje}, $U^{\text{praznjenje}}$). OCV je napon u stanju praznog hoda (nakon što je baterija duže vremena u stanju mirovanja), dok je napon zatvorenog kruga napon u stanju opterećenja, tj. tijekom punjenja ili pražnjenja. Napon zatvorenog kruga raste sa strujom punjenja i opada sa strujom pražnjenja, tako da naponska učinkovitost jako ovisi o vrijednosti struje punjenja/pražnjenja baterije. Naponska učinkovitost punjenja je omjer prosječnog napona

otvorenog kruga ($\overline{U^{\text{OC}}}$) i prosječnog napona punjenja ($\overline{U^{\text{punjenje}}}$) tijekom djelomičnog ili punog ciklusa punjenja. Naponska učinkovitost pražnjenja je omjer prosječnog napona pražnjenja ($\overline{U^{\text{praznjenje}}}$) i prosječnog napona otvorenog kruga ($\overline{U^{\text{OC}}}$) tijekom djelomičnog ili punog ciklusa pražnjenja. Kružna naponska učinkovitost je omjer prosječnog napona pražnjenja ($\overline{U^{\text{praznjenje}}}$) i prosječnog napona punjenja ($\overline{U^{\text{punjenje}}}$) tijekom djelomičnog ili punog kružnog ciklusa. Da bi se dobila jednosmjerna naponska učinkovitost mora biti poznata karakteristika napona otvorenog kruga u odnosu na stanje napunjenosti baterije (OCV-SOC), tj. potrebno ju je odrediti eksperimentalno.

•Energetska u činkovitost

Energetska učinkovitost je povezana s energijom u vat satima (Wh) ispražnjenom iz baterije ili napunjenoj u bateriju. Energetska učinkovitost definirana je analogno kulonskoj učinkovitosti, pri čemu E označava energiju u Wh.

Energetska učinkovitost punjenja:

$$\eta^{\text{punjenje,E}} = \frac{E^{\text{stvarno}}}{E^{\text{punjenje}}}. \tag{2}$$

Energetska učinkovitost pražnjenja:

$$\eta^{\text{praznjenje,E}} = \frac{E^{\text{praznjenje}}}{E^{\text{stvarno}}}. \tag{3}$$

Kružna energetska učinkovitost:

$$\eta^{\text{ciklus,E}} = \eta^{\text{punjenje,E}} \cdot \eta^{\text{praznjenje,E}} = \frac{E^{\text{praznjenje}}}{E^{\text{punjenje}}} \tag{4}$$

Jednosmjerna energetska učinkovitost može se odrediti na tri načina:

•Pomo ću mjerenja gubitaka topline - postojeća metoda

Moguće je izmjeriti toplinu oslobođenu iz baterije i izračunati jednosmjernu energetsku učinkovitost baterije pod različitim radnim i okolišnim uvjetima. Međutim, budući da je ukupno emitiranje topline iz baterije zbroj ireverzibilnog i reverzibilnog stvaranja topline, učinkovitost određena na ovaj način zanemaruje učinke reverzibilnog stvaranja topline.

•Korištenje OCV-SOC karakteristike - postoje ća metoda

Jednosmjerna energetska učinkovitost baterije može se odrediti na temelju karakteristika napona otvorenog kruga u odnosu na stanje napunjenosti. Prednosti ove metode su njezina jednostavnost i mogućnost određivanja ovisnosti jednosmjerne učinkovitosti o razini napunjenosti. Loše strane ove metode su zanemarivanje kulonskih gubitaka i ovisnost točnosti metode o jednom setu mjerenja spomenute karakteristike.

•Predložena metoda

Predložena metoda za određivanje jednosmjerne energetske učinkovitosti temelji se na

rješenju problema nelinearne optimizacije koji se sastoji od nekoliko relacija jednosmjerne učinkovitosti, gdje su kružne učinkovitosti eksperimentalno određeni parametri (Slika 3).

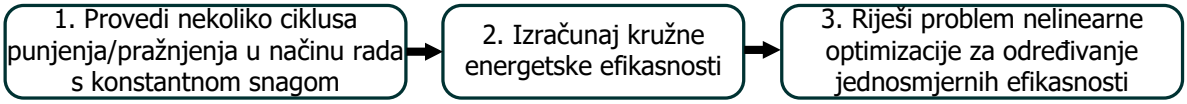

Slika 3: Metoda za određivanje jednosmjernih učinkovitosti

Prvo se eksperimentalno određuju kružne učinkovitosti ciklusa za različite parove snaga punjenja i pražnjenja. Svaki ciklus uvijek se započinje s ispražnjenom baterijom, gdje ispražnjena znači da se neispražnjena baterija prazni sve dok se ne dosegne granica niskog napona baterije uz uvjet da je P-stopa pražnjenja baterije jednaka P-stopi pražnjenja predmetnog kružnog ciklusa. Svako punjenje se izvodi u načinu rada s konstantnom snagom i prekida se čim se dosegne deklarirana naponska granica punjenja. Svako pražnjenje se izvodi u načinu rada s konstantnom snagom i prekida se čim se dosegne deklarirana granica napona pražnjenja baterije. Određeni broj P-stopa odabire se za pokrivanje očekivanih radnih snaga punjenja (C) i pražnjenja (D) baterije. Zatim se provodi $C \times D$ parcijalnih ciklusa u načinu rada s konstantnom snagom, za sve moguće kombinacije odabranih P-stopa punjenja/pražnjenja. Kako bi se povećala točnost i osigurala dosljednost, ciklus se može ponoviti J puta. Kružna učinkovitost za svaku kombinaciju P-stopa punjenja/pražnjenja računa se kao:

$$\eta_{c,d}^{\text{ciklus,E}} = \frac{\sum_{j=1}^{J} \eta_{c,d,j}^{\text{ciklus,E}}}{J}. \tag{5}$$

Da bismo dobili jednosmjernu učinkovitost iz izmjerenih kružnih učinkovitosti, formuliramo i rješavamo sljedeći problem nelinearne optimizacije:

$$\underset{\Xi=\{s_{c,d},\eta_c^{\text{punjenje,E,opt}},\eta_d^{\text{praznjenje,E,opt}}\}}{\text{Minimiziraj}} \quad \sum_{c\in\Omega^{\text{C}}} \sum_{d\in\Omega^{\text{D}}} s_{c,d}^2 \tag{6}$$

prema

$$\eta_c^{\text{punjenje,E,opt}} \cdot \eta_d^{\text{praznjenje,E,opt}} = \eta_{c,d}^{\text{ciklus,E}} + s_{c,d}, \quad \forall c \in \Omega^{\text{C}}, \forall d \in \Omega^{\text{D}}, \tag{7}$$

$$0 \leq \eta_c^{\text{punjenje,E,opt}} \leq 1, \quad \forall c \in \Omega^{\text{C}}, \tag{8}$$

$$0 \leq \eta_d^{\text{praznjenje,E,opt}} \leq 1, \quad \forall d \in \Omega^{\text{D}}. \tag{9}$$

Ovaj skup jednadžbi, uz pretpostavku $s_{c,d} = 0$, ne može se riješiti analitički, jer je pogrešno postavljen, tj. ili nema rješenja ili ima beskonačno mnogo rješenja. Drugim riječima, ne postoji kombinacija $\eta_c^{\text{punjenje,E,opt}}$ i $\eta_d^{\text{praznjenje,E,opt}}$ koja jednoznačno zadovoljava sve

$C \times D$ jednadžbe . Dakle, cilj ovog optimizacijskog problema je pronaći vrijednosti $\eta_c^{\text{punjenje,E,opt}}$ i $\eta_d^{\text{praznjenje,E,opt}}$, čiji umnošci najmanje odstupaju od izmjerene kružne učinkovitosti $\eta_{c,d}^{\text{ciklus,E}}$. Rješavanje optimizacijskog problema kojim se kružna učinkovitost razlaže na učinkovitosti punjenja i pražnjenja za različite razine snage, rezultira jednosmjernim učinkovitostima punjenja i pražnjenja. Jednosmjerne energetske učinkovitosti određene na ovaj način uzimaju u obzir i naponske i kulonske gubitke. Još jedna prednost predložene metode, u usporedbi s metodom temeljenom na OCV-u, je mogućnost bržeg određivanja jednosmjernih učinkovitosti (npr. za $C = D = 2$), te korištenjem manje preciznih instrumenata, budući da se izbjegavaju niske struje. Dodatno, prednost predložene metode je i mogućnost određivanja jednosmjernih kulonskih učinkovitosti na temelju izmjerenih kružnih kulonskih učinkovitosti. Loša strana ove metode je zanemarivanje nelinearnosti karakteristika punjenja/pražnjenja u cijelom rasponu SOC.

U radu s baterijskih sustava potrebno je dobro poznavanje radnih karakteristika baterija kako bi se mogle koristiti u punom kapacitetu. Jedna od takvih specifičnosti je ovisnost jednosmjerne učinkovitosti punjenja/pražnjenja o snazi punjenja/pražnjenja. Ovo istraživanje predlaže novu metodu za određivanje kapaciteta baterije temeljenu na eksperimentalnim ispitivanjima. Predložena metoda definira energetski kapacitet baterije kao energiju koja je stvarno pohranjena u bateriji, uzimajući u obzir gubitke prilikom punjenja i pražnjenja. Eksperimenti se sastoje od određivanja jednosmjernih učinkovitosti punjenja i pražnjenja na temelju višestrukih ciklusa koji se provode u različitim radnim i ambijentalnim uvjetima, s ciljem određivanja karakteristika ovisnosti jednosmjernih učinkovitosti o radnim uvjetima (snagama) i o temperaturi okoline. Nakon određivanja karakteristika jednosmjernih učinkovitosti, baterije se podvrgavaju višestrukim punim ciklusima punjenja/pražnjenja (0-100% SOC i/ili obrnuto) korištenjem različitih C-stopa (ili P-stopa). Izmjerene energije se zatim korigiraju za varijabilne jednosmjerne učinkovitosti kako bi se dobile vrijednosti stvarno pohranjene u bateriju tijekom punjenja ili stvarno ispražnjene iz baterije tijekom pražnjenja. Kapacitet se određuje kao srednja vrijednost korigiranih energija punjenja/pražnjenja svih punih ciklusa (različitim C- ili P-stopama). Laboratorijskim testiranjem predložena metoda uspoređena je s dvije postojeće metode pri različitim temperaturama okoline. Rezultati pokazuju da predložena metoda značajno nadmašuje postojeće metode u pogledu točnosti određenog kapaciteta baterije i stanja napunjenosti. Glavna prednost predložene metode je uzimanje u obzir i radnih (snaga) i ambijentalnih (temperatura) uvjeta.

Ključne riječi: Litij-ionske baterije, eksperimentalno testiranje, električna vozila, analitički hijerarhijski proces, kružna učinkovitost, jednosmjerna učinkovitost, kapacitet baterije, energetski kapacitet, stanje napunjenosti, stanje energije

Contents

Chapter 1

Introduction

1.1 Background, Motivation and Objective of the Thesis

Technological development and battery research is important both in the industry and the research community due to their increasing applications in home appliances, consumer electronics, transportation, and power system industry. Generally, this development consists of modelling and simulations, hardware-in-the-loop simulations and, finally, experimental testing. Currently, the most prominent battery technologies are based on lithium and this research will thus focus on lithium-based batteries. A large number of papers have been published on the subject of battery modelling and simulation.

A methodology for comparison of results of experimental testing and charge — discharge cycle efficiency of different lithium-ion batteries has not yet been performed in a systematic and rigorous manner. Thus, in this work procedures for testing of battery characteristics (charging and discharging tests, which represent a common way of using batteries in electric vehicles application) are developed. Laboratory tests on different types of batteries are carried out. Battery cell technologies that are evaluated in the research are mainly concentrated on lithium-ion technologies (lithium-cobalt-oxide, lithium-nickel-cobalt-aluminium-oxide, lithium-manganese-oxide, lithium-iron-phosphate, lithium-nickel-manganese-cobalt-oxide).

Development of a mathematical model of one-way charging and discharging efficiency for different types of lithium-ion batteries based on laboratory tests has not yet been described in the existing literature. Therefore, in the second phase, laboratory tests are carried out to determine charge — discharge cycle efficiency of lithium-ion battery cells, as well as the identification of the parameters of a mathematical model of one-way charging and discharging efficiencies under different operating and ambient conditions of charge and discharge of cells. The objective of the research is to define and evaluate a method for testing of different battery cells in a representative sample of conditions, both operating and environmental, that battery systems are exposed to in electric vehicles. These conditions are related to ambient temperature and humidity, which

are conditioned by the temperature chamber available at the Smart Grid Lab at the Faculty of Electrical Engineering and Computing.

The battery one-way charging and discharging efficiencies are derived based on the laboratory tests. The mathematical model of one-way efficiencies of the lithium-ion batteries suitable for use in simulation and optimization procedures is defined and developed.

To summarise, this thesis contribution is divided in two parts:

1. A methodology for experimental testing and evaluation of different types of lithium-ion batteries for the purpose of selecting the optimal battery for electric vehicles application
2. A model of lithium battery charge – discharge cycle efficiency in representative working conditions of electric vehicles based on laboratory testing

1.2 Structure of the Thesis

The thesis is structured as follows:

- Chapter 2 introduces relevant existing methods for battery evaluation and models of battery efficiency;
- Chapter 3 highlights the main contribution of the thesis and links them to the related publications;
- Chapter 4 presents the list of all relevant publications;
- Chapter 5 summarizes the author's contribution to the publications;
- Chapter 6 concludes the thesis and highlights the main findings.

Chapter 2

Concepts and State-of-the-art

This review section covers two research areas relevant to this thesis: the existing methodologies for evaluation of different types of lithium-ion batteries and the existing models of lithium-ion battery efficiencies.

2.1 Methodologies for evaluation of different types of lithium-ion batteries for vehicular application

The increase of applications of battery storage systems in many industries results in significant research and development efforts of the battery models and compositions.

The main drawbacks that slow down the rollout of electric vehicles are high investment cost, lack of public infrastructure and lower driving range as compared to the gasoline-powered vehicles, according to [1]. Energy density characteristics of lithium-ion batteries is highlighed as a significant drawback for their application in the vehicle industry in [2] and [3].

Therefore, detailed knowledge of battery characteristics is essential for their selection in application and use in electric vehicles. A detailed technical and theoretical description as well as a general overview of batteries is available in [4]. Currently dominant batteries are based on lithium and this research thus focuses on lithium-based batteries.

An overview of lithium-ion batteries used specifically for electric vehicles is presented in [5]. LCO, LMO, LFP and NMC battery types are presented and compared as the most promising batteries for electric vehicles.

An evaluation of performance of various lithium-ion batteries for use in electric vehicle applications is presented in [6]. The authors compare and evaluate capacity and efficiency performance, charging capabilities, Butler-Volmer phenomenon (electrical current dependence on the electrode potential), thermal characteristics, cycle life and cost of NCA, LFP and NMC batteries. The study shows that NMC batteries have the highest energy density, NCA and NMC batteries have the best charging and discharging capabilities in terms of ampere-hours and the

highest energy efficiency, while LFP batteries demonstrate the highest thermal stability.

A step toward real-life battery performance assessment is achieved by laboratory testing.

The authors of [7] share a valuable experience on usage and ageing testing of lithium-based and sodium-nickel-chloride-based batteries used for providing ancillary services to the power system. The experimental results show a significant difference in degradation of batteries depending on the types of test cycles for different types of batteries. An interesting research from the vehicular technology standpoint tests lithium-ion batteries under different temperature conditions, vibration frequencies and vibration directions [8]. NCA batteries were used in the tests and the results indicate that battery characteristics are significantly more affected by the ambient temperature than the road vibrations. Importance of an adequate and reliable management of parallel-connected lithium-ion battery cells is noted in [9], as the experimental tests showed that the management of parallel-connected lithium-ion battery cells with different levels of degradation causes further degradation of the whole battery pack. It is shown that the degraded cells in the parallel connection force the healthier cells to discharge at a higher current. The increased current and power lead to a higher polarization voltage drop and generation of more heat, which causes accelerated cell degradation.

Evaluation of LFP batteries for electric vehicle applications is presented in [10]. Five different commercial LFP batteries with different power and energy ratings were tested according to the recommendations from [11]. The following experimental procedures were conducted: commissioning (identification and weighting of the batteries), energy efficiency, specific energy (Wh/kg) and specific power (W/kg) capabilities tests at various C-rates, thermodynamic tests, fast-charging tests and aging tests. The results indicate that all of the tested batteries met the short-term U.S. Advanced Consortium goals [11], while the long-term results were achieved only for energy efficiency and cycle life under standard conditions. Specific power and fast charging capability test results did not meet the goals for most of the tested cells.

Additional experimental analyses of LFP battery for electric vehicle applications are presented in [12], [13] and [14]. In [12], the results of 50 moderate charging and discharging cycle tests of an LFP battery cell at the ambient temperature of 20°C are presented and analysed. The results demonstrate less than 0.5% loss of capacity, which can be used to extrapolate to the supplyer's claimed 1000 cycles before the capacity falls to 80%. The realistic road tests were conducted at ambient temperatures of -20°C, 0°C, +20°C and +40°C. The results reveal increased capacity and power degradation at low temperatures.

Two different test benches are used in the experiments described in [13], one for the tests in the steady state, and the other one under the dynamic operation conditions. Battery electrical characteristics, capacity-temperature dependence, ageing effects and energy storage efficiency under different currents and the dynamic performance are evaluated. It is shown that the charging / discharging efficiency at 1C rate is higher than charging / discharging efficiency at currents

much lower than 1C rate. Even though the value of the lost power in the internal resistance of the battery is low for lower C-rates, chemical reactions inside the battery are slower because of the material deterioration inside the cell.

Results of the capacity test, power capability test, open-circuit voltage test and voltage hysteresis test of an LFP battery are presented and evaluated for the hybrid electric vehicle application in [14]. Evaluation of the capacity tests and power capability tests at various states of charge and temperatures indicate degradation of cell performance at low ambient temperatures. Open-circuit voltage tests reveal only small variation at different ambient temperatures.

Electric vehicle application of LCO cells is evaluated in [15], where the results of cycling and loading tests are presented. The results demonstrate that cells perform well according to the manufacturer's specifications at ambient temperatures above 0°C in both Ah and Wh capacity, but a depression of capacity is revealed at temperatures lower than 0°C.

In [16], the authors conduct an experimental performance analysis of the lithium-polymer battery cell. Battery cell capacity, battery energy efficiency, temperature effects on performance of batteries, self-discharge, fast charging ability and realistic load tests were all conducted and analysed. It is determined that the resulting battery efficiency is over 96% at temperatures between +20°C and +40°C. The temperature test shows that the battery performs well at temperatures between 0°C and +40°C, but its efficiency and capacity decrease at temperatures below 0°C. The battery self-discharge is less than 5% per month. Results from the fast charging ability and realistic load tests are close to the values of the long-term United States Advanced Battery Consortium goals [11].

A state-of-health estimation method based on integration of the estimation effects of different health indicators and calculation of the weight coefficient of each indicator using the analytic hierarchy process is presented in [17].

The experimental life cycle tests on an NMC battery cells are performed to verify the presented method. An initial performance of the battery cells is determined using the static capacity test, resistance test, hybrid pulse test and three representative simulated driving schedule tests (federal urban driving schedule, inspection and maintenance driving schedule and dynamic stress test). The aging cycles consists of two patterns, the charging (constant current mode) and the discharging (several discharge steps with the same current excitation) pattern.

2.2 Battery characteristics

2.2.1 Models of lithium-ion battery efficiencies

Battery characteristics are investigated in a large number of scientific and professional works in different science and industry fields.

Battery models focused on vehicular applications can be categorized as electrochemical, stochastic, analytical and electrical-circuit models according to [18].

In [19], an in-depth analysis of the lithium-ion batteries is performed at the chemistry-material level. In this work, the importance of accounting for energy efficiency in battery materials is emphasized next to the high specific energy (Wh/kg) and energy density (Wh/L) anode and cathode materials. The importance of accounting for energy efficiency already during the development of new electrode materials is emphasized in [20], respectively. An analysis of Coulombic efficiency of lithium-metal batteries at a structural level is presented in [21].

A large number of papers analyze batteries based on electrical measurements. A relationship between the coulombic, the voltaic and the energy efficiency is studied in [22], with findings experimentally verified on nickel–metal hydride (Ni-MH) batteries. However, only roundtrip efficiencies with constant charging/discharging currents are considered. An analysis of one-way voltaic and energy efficiency is presented in [23], where the obtained characteristics are based on experimentally determined battery open-circuit voltage (OCV) characteristics. Contribution of parasitic reactions to the coulombic inefficiency is analyzed in [24], based on high-precision experimental testing on three commercial lithium-ion technologies. The results demonstrate that parasitic reactions cause coulombic inefficiency at a reaction rate independent of the cell cycling rate. Electrochemical reactions affecting coulombic efficiency and capacity fade are analyzed in [25] using high-precision experiments. The paper focuses on identification and evaluation of various parasitic coulombic losses. In [26], roundtrip coulombic and energy efficiencies, as well as capacity retention are analyzed for Ni-MH batteries, based on experimental measurements of the roundtrip efficiency. What is studied in this paper is the dependence of battery efficiency on the power rate, state-of-charge and battery operation duration. Differences in the electric vehicles' battery efficiency for constant-current (CC) and constant-power (CP) modes of operation are studied in [27]. Battery capacity efficiency in this study is defined as a roundtrip efficiency dependent on the charging power rate. An interesting research with experimental measurements of physical battery characteristics is presented in [28], where the concept of energy efficiency maps is introduced. The authors calculate one-way energy efficiencies based on measurements of the irreversible heat generated during charging and discharging, with these thermodynamic quantities determined from a detailed low-level multiphysics model of lithium-ion batteries. One-way charging and discharging characteristics are obtained by measuring irreversible heat using highly expensive equipment.

Besides the publications focused on electrical measurement analyses of batteries, another stream of research relevant for our work aims at developing battery models. Invention [29] claims a time-consuming method for calibration of a battery based on roundtrip charge/discharge cycles and power/energy measurements, resulting in a map of available discharge energy which is dependent on the discharging power and state-of-energy. This method does not determine

one-way charging/discharging efficiencies. Paper [30] is an extension of the invention [29] where the environmental temperature is accounted for. However, one-way efficiencies are still not considered. Invention [31] claims the method for obtaining the remaining energy in a battery, by utilizing the normalized state-of-energy dependence on power and temperature. Again, one-way efficiencies are not determined. A state-of-energy estimation method based on the back-propagation neural network model is presented in [32]. The model is trained using a large number of the measured voltage, current, temperature and state-of-energy samples. Additionally, it is combined with a particle filter for suppression of the measurement noise. An experimental verification of the model proved its high reliability and accuracy. As the model accounts for power states with dynamic discharge currents, only the roundtrip energy efficiency is indirectly accounted for, while the one-way charging and discharging efficiency is neglected. Furthermore, the energy efficiency characteristics are not evaluated in the review of the experimental results.

A model-based joint state estimator based on an adaptive unscented Kalman filter is developed in [33] for battery state-of-energy and power capability prediction. The model considers environmental temperature and aging of the battery, while it does not evaluate efficiency.

In [34], an equivalent circuit model and a life-cycle model of a lithium-ion battery are used to develop an energy management strategy for model predictive control of hybrid electric vehicles. These models account for the effect of the power rate on the efficiency and try to minimize high-power discharges that result in high energy losses. However, the models do not distinguish between the one-way charging and discharging efficiencies. The main drawback of relying only to the roundtrip efficiency is the inability to assess the amount of energy stored in the battery and the amount of energy that can be effectively discharged, which is especially relevant when charging and discharging at various P-rates, which directly affect the one-way charging and discharging efficiencies.

Battery one-way energy efficiencies can be determined from an open-circuit voltage characteristics. The OCV characteristic provides information about terminal voltage that a battery exhibits after being at rest for some time (typically few hours). OCV is state-of-charge or state-of-energy dependant so researchers typically consider OCV–SOC or OCV–SOE characteristics. In [35], the OCV-SOC characteristic is determined by subjecting a battery to a full cycle at low C-rates and then averaging the measured charging and discharging voltages. Two other, less time-consuming methods are described in [36]. They are based on periodical pausing of the charging and discharging processes. In the first method, the voltages reached during 1-minute pauses are measured and averaged over the charging and discharging processes. In the second method, exponential best-fit curves of the voltages measured during pauses are fitted and used to extrapolate the voltage steady-state values, which are again averaged over the charging and discharging processes to construct the OCV-SOC characteristic. Another, less time-consuming

method, is presented in [37], where one-way energy efficiencies are determined for a pulse charging/discharging half-cycles, with reference to the OCV estimated from the voltage levels measured after 10-minute rests following each pulse. An OCV-based method for determining battery one-way energy efficiency characteristics is presented in [38], where the OCV-SOC curve is determined as described in [35], while the mathematical OCV(SOC) function is obtained by a nonlinear fit. Experiments to evaluate battery aging parameters are conducted in [39], where the authors found that a loss of active material contributes to the coulombic inefficiency. The authors established the relationship between the coulombic efficiency and the capacity degradation based on incremental capacity analysis. Lithium-ion battery efficiency degradation is evaluated in [40] based on the OCV characteristic and accelerated calendar aging tests. Optimal SOC in terms of the efficiency is determined, while two efficiency degradation models are developed and evaluated. High correlation between the capacity fade and the energy efficiency degradation is reported.

The downside of using OCV characteristics to estimate one-way energy efficiencies is the fact that only voltaic efficiency is taken into account, while the effect of coulombic efficiency is neglected, as reported in [23]. This might not pose a big problem when talking about lithium-ion batteries which have high coulombic efficiency of 99% or more [21, 25, 39]. However, this renders the OCV-based method inappropriate for high-precision one-way energy efficiency measurements (as the current losses are neglected), while it is not possible to use it for one-way coulombic efficiency determination.

2.2.2 Determination of Lithium-ion Battery Capacity for Practical Applications

Battery systems are often considered as a source/sink with defined operational capabilities and fixed limitations in available capacity. In reality, battery systems consist of different connection combinations of battery cells with characteristics that depend on both operational and ambient conditions. Operational conditions are primarily related to the rate of charging and discharging current/power of the battery. In this work the focus is on battery power characteristics as the measures of power and energy are more convenient in the power system and automotive industries. The ambient temperature has the greatest effect on the performance characteristics of the battery comparing to other ambient parameters (humidity, vibration, etc.).

Different methods for estimation of the battery cell energy capacity are evaluated in large number of industry and scientific works [41].

The most common method is a calculation of the remaining battery energy capacity (in Wh) as a multiplication of the nominal energy capacity ($E^{\mathrm{n}} = U^{\mathrm{n}} \cdot Q^{\mathrm{n}}$, where U^{n} is the nominal voltage of the battery in V, Q^{n} is the nominal charge capacity of the battery in Ah, both de-

termined by the manufacturer) and the state-of-charge (SOC) determined by coulomb counting ($E_{\mathrm{SOC}}^{\mathrm{remaining}}(t) = U^{\mathrm{n}} \cdot Q^{\mathrm{n}} \cdot SOC(t)$), as stated in [42], [43]. However, this method neglects voltage charging and discharging characteristics, dynamic processes and battery capacity dependence on the power, the state-of-charge, the state-of-health, the ambient parameters, etc.

Another common method is defining the remaining battery energy capacity (in Wh) as a multiplication of state-of-energy with the nominal energy ($E_{\mathrm{SOE}}^{\mathrm{remaining}}(t) = E^{\mathrm{n}} \cdot SOE(t)$) where the state-of-energy is determined by the ratio of integrated charged or discharged power ($P^{\mathrm{ch}} = U^{\mathrm{ch}} \cdot I^{\mathrm{ch}}$, $P^{dis} = -U^{dis} \cdot I^{dis}$) and the nominal or maximum energy of the battery [30], [44], [45], [46], as follows $SOE(t) = SOE(t-1) + \frac{1}{E^{\mathrm{n}}} \cdot \int_{\mathrm{t}-1}^{\mathrm{t}} P^{\mathrm{ch/dis}}(\tau) d\tau$.

Both common methods neglect energy capacity dependence on operational and environmental parameters, as well. To reduce the error of operational losses, fixed operational roundtrip efficiency is commonly accounted for in the method presented in [47]. Many other, more complex methods have been developed for the determination of the remaining energy. Equivalent circuit models with implemented information about electrolyte characteristics [48], impedance and resistance experimental measurements [49] and other based on experimental and historical data [50]. Equivalent circuit models are highly dependent on input data (usually from controlled laboratory environment), so their application in real dynamic operation may result in inaccurate estimations of the remaining energy.

On the other hand, methods that use Kalman filters are able to provide more accurate results in dynamic situations. In [51], an online capacity estimation method based on the enhanced coulomb counting with the adaptive Kalman filter is applied to eliminate the capacity estimation error. The Kalman filter updates the covariance and noise from the error, and the capacity estimation is performed by the fusion of the Gaussian probability density functions of the predicted value (based on state-of-health estimation) and the measured capacity value. The reduced error in estimation is experimentally verified. A method for SOE estimation based on SOC estimation with extended Kalman filter upgraded with current, voltage and temperature response prediction is presented in [52]. The presented method accounts for the full life cycle of the battery. Additionally, the authors presented a method for estimation of the entire battery pack state-of-energy. A dual forgetting factor-based adaptive extended Kalman filter for SOC estimation is presented in [53]. The authors combined the existing extended Kalman filter for online SOC estimation [44], [54], [55], [56] with SOE estimation method [43] to get the reliable SOC and SOE estimations.

Methods with prediction algorithms are often limited to capacity estimation under given conditions. Authors in [57] developed a prediction technique for estimation of the remaining driving range of an electric vehicle. The proposed method considers operational dynamics, but neglects temperature variability. On the other hand, the authors in [58] presented the predictive algorithm that predicts both future operation and temperature conditions. Model for operation

conditions is based on an equivalent circuit model, and temperature prediction is based on historical data.

Methods with neural networks that use historical data may consider environmental and operational impact on capacity, but they highly depend on the quantity and choice of historical data and used methods for training of the models [32], [59]. Similarly, fuzzy logic models are able to provide highly precise estimations based on historical and experimental data at given operational and environmental conditions [60]. Machine learning model [61] has proven that the diversity of feasible data is critical for the estimation with high accuracy. The presented model uses multi-channel technique based on voltage, current, and temperature profiles, and the results outperforms the conventional method that uses only voltage profile.

As stated in [62], the disadvantages of complex models are accuracy dependence on training/historical data, computational costs and development complexity.

Chapter 3

Main Scientific Contribution

3.1 A methodology for experimental testing and evaluation of different types of lithium-ion batteries for the purpose of selecting the optimal battery for electric vehicles application

A proposed methodology for determining the optimal battery cell for usage in a special-purpose vehicle is divided in two parts. First, performance tests are conducted on different battery cells according to the European standard EN 15429-2 [63] and additional rigorous tests designed specifically according to performance requirements on the vehicle. Second, the Analytic Hierarchy Process (AHP) algorithm is used for evaluation and categorization of battery cells' characteristics and experimental testing results. It is shown that the evaluation of the battery cell characteristics based merely on technical characteristics given by the manufacturers can result in sub-optimal battery cell selection. However, the analysis of experimental results resolves that problem and identifies the optimal battery cell for a given purpose.

3.1.1 Battery cell types

LCO, LMO, NCA and NMC batery types are evaluated, with characteristics of the battery cells shown in Table 3.1.

LCO batteries and have low energy capacity compared to the other types, so the expectations of the energy tests for this cell are low. LCO batteries have rather high energy capacity, but the maximum discharging current is quite low, which could result in poor performance at high loads. NCA batteries have similar technical characteristics as the LCO battery. LMO Cells have the ability to withstand high discharge currents, while the cells themselves have high energy capacity. According to the technical characteristics, above-average results are expected in both

Table 3.1: Battery cells characteristics as declared by the manufacturers

Type	Nominal cell voltage (V)	Max charging current of the cell (A)	Max discharging current of the cell (A)	Capacity of the cell C_{cell} (Ah)	Energy of the cell E_{cell} (Wh)	Cell price ($/Wh)
LCO	3.65–3.7	2.17–4.00	6.4–25	2–3.2	7.30–11.83	0.26–0.60
NCA	3.6	1.45–1.60	20.48–29	2.9–3.2	10.73–12.24	0.40–0.43
LMO	3.6–3.7	4.00	10-25	2.6–3.13	9.36–11.27	0.45–0.54
LFP	3.2	1.50	10	1.5	4.80	0.86
NMC	3.6–3.7	2–4	10–20	2-3.5	7.2–12.72	0.33–0.69

energy and heating test results. LFP have high maximum allowed current and long cycle life, but low energy capacity. Thus, good heating characteristics and specific charging and discharging results, but poor energy test results, are expected. NMC cells with high energy capacity and high maximum allowed charging / discharging current should yield good results in both the heating and the energy tests. NMC cells with lower energy capacity are not expected to perform well in energy tests, but their heating characteristics are expected to be good.

3.1.2 Evaluation of the battery cell types

The evaluation of the batteries is conducted with two different approaches. First, the evaluation is based on analysis of technical data provided by the manufacturers, and secondly based on data obtained from proposed experimental tests (Figure 3.1).

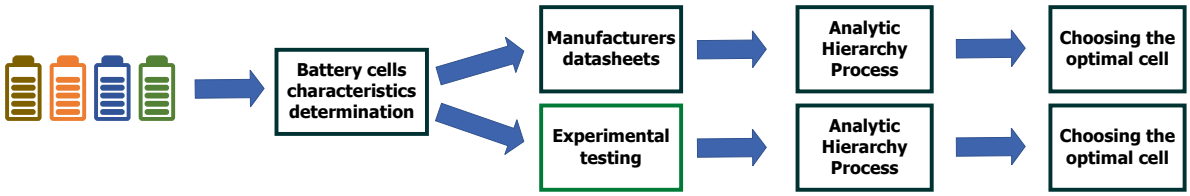

Figure 3.1: Methodology for selecting the optimal battery cell

Analytic Hierarchy Process (AHP) [64], [65], [66] is used to determine the optimal battery cell based on the following criteria:

- Based on manufacturers data: declared energy capacity, maximum discharge current, maximum charge current and price
- Based on data obtained from experimental tests (measured energy capacity and temperature increase) and price

The algorithm used to calculate AHP is shown in Algorithm 1, where:

•PWC is Pair-Wise Comparison,
•C is Criteria,
•A is Alternative,
•PCM is Pair-Wise comparison Matrix,
•CM is Comparison Matrix,
•SR is Sum of Rows of comparison matrix,
•CSR is Column vector containing the Sum of each Row of comparison matrix,
•SAE is Sum of All Elements of SR,
•PV is Priority Vector,
•CI is Consistency Index,
•RCI is Random Consistency Index,
•CR is Consistency Ratio,
•CV is Comparison Vector and
•CWAC is Composite Weight of each Alternative Choice.

The criteria pair-wise comparison matrix and the priority vector of AHP analysis of the experimental results according to the relative importance's of pairwise comparisons Relative pair-wise comparisons are defined on scale 1 to 9 according to criteria such as the number of hours of vehicle operation per day, the proportion of days in the year with low temperatures, etc.

Not all the proposed tests are equally important for application in an electric vehicle, where the Energy Test and Adjusted Consumption Test play a key input in deciding on the optimal battery cell. On the other hand, the charging tests at 0.2C and 0.4C are used as control tests where a cell can fail only if the achieved results are well below an average. Therefore, the AHP is used to compare the results of the conducted tests and to choose the optimal battery cell for a vehicle. The criteria used for comparison are measured energy capacity and temperature increase in the four conducted tests, i.e. the Energy Test, Adjusted Consumption Test, and two charging tests.

The optimal lithium-ion battery cell selected with the proposed methodology is different than the battery cell selected solely on analysis of the manufacturers' datasheets. So, although the manufacturers' datasheets contain many useful information, it is shown that an analysis based exclusively on such data may result in sub-optimal battery cell selection.

Algorithm 1 Analytic Hierarchy Process

Input: C1, C2, ..., Cn ⇒enter Criteria
Input: A1, A2, ..., Am ⇒enter Alternatives (battery cells)

for $i \leftarrow 1$ to $length(C)$ **do** ⇒create Relative Importance Pair-wise Comparisons Matrix

  for $j \leftarrow 1$ to $length(C)$ **do Input:** $PWC_{i,j}$

  end for

end for

$CM \leftarrow PCM$

$i \leftarrow 1$ ⇒initialize counter for while loop

while $tolerance > acceptable\_value$ **do** ⇒calculate Normalized Eigen Vector of the Criteria Matrix

  $i \leftarrow i+1$

  $CM \leftarrow CM \times PCM$

  $CSR \leftarrow sum\_of\_each\_row\_of\_CM$

  $SAE \leftarrow the\_sum\_of\_all\_elements\_of\_SR$

  $tolerance \leftarrow SR(i) \div CSR(i) - SR(i-1) \div CSR(i-1)$

end while

$PV \leftarrow SR(i) \div CSR(i)$ ⇒calculate Priority Vector

for $i \leftarrow 1$ to $length(C)$ **do**

  $\lambda_{max} \leftarrow SAE + CM(i) + \lambda_{max}$

end for

$CI \leftarrow (\lambda_{max} - length(C)) \div (length(C) - 1)$ ⇒calculate Consistency Index

switch $length(A)$ **do** ⇒define Random Consistency Index

  case 2 $RCI \leftarrow 0$

  case 3 $RCI \leftarrow 0.58$

  case 4 $RCI \leftarrow 0.90$

  case 5 $RCI \leftarrow 1.12$

  case 6 $RCI \leftarrow 1.24$

  case 7 $RCI \leftarrow 1.32$

  case 8 $RCI \leftarrow 1.41$

  case 9 $RCI \leftarrow 1.45$

  case 10$RCI \leftarrow 1.49$

  case 11$RCI \leftarrow 1.51$

$CR \leftarrow (CI/RCI)$ ⇒calculate Random Consistency Ratio

if $CR \leq 10\%$ **then**

The inconsistency is acceptable ⇒evaluate Inconsistency

else

The inconsistency is not acceptable

end if

for $i \leftarrow 1$ to $length(CV)$ **do**

for $j \leftarrow 1$ to $length(A)$ **do Input:** CV(i,j) ⇒enter Comparison Vectors

end for

end for

$CWAC \leftarrow PV \times CV$ ⇒calculate Composite Weight of Alternative Choices

$The\_best\_result\_location \leftarrow location(max(CWAC))$ ⇒location of Best Alternative (Optimal Battery Cell)

3.2 Lithium-ion battery characteristics

3.2.1 A model of lithium-ion charge – discharge cycle efficiency in representative working conditions of electric vehicles based on laboratory testing

Whenever a battery is either charged or discharged, some energy is lost. These losses are associated with the battery's internal resistance of the electrodes and electrolyte, manifesting mostly as heat dissipation. Quantification of these losses is called battery efficiency (Figure 3.2).

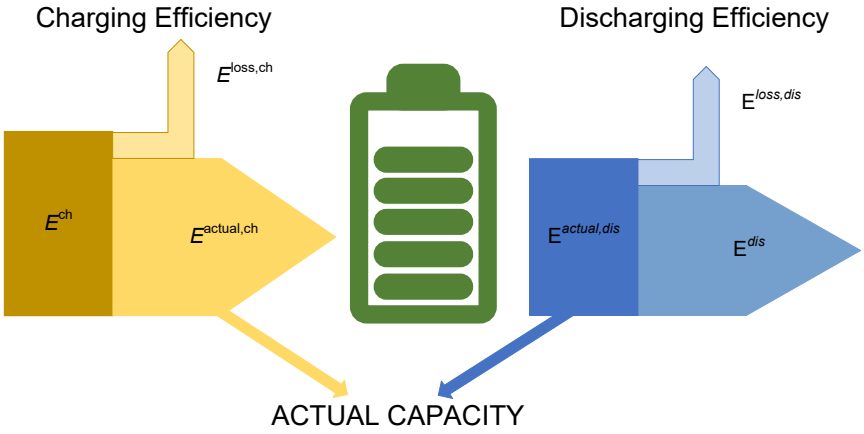

Figure 3.2: Battery charging/discharging efficiency

There are multiple battery efficiency types and they are all variable, since they depend on the charging/discharging conditions (C-rate, P-rate, environmental temperature etc.), as well as the battery's age and state-of-health (SOH) and state-of-charge (SOC) / state-of-energy (SOE).

C-rate is the speed at which a battery is charged or discharged. At 1C the battery (dis)charges with the current corresponding to its Ah-rating (e.g. 1C for a 10 Ah battery is 10 A, 0.5C is 5 A, etc.). P-rate is the percentage of nominal power of a battery at which it is charged or discharged. At 1P the battery (dis)charges at a rate corresponding to its nominal power (e.g. 1P for a 10 Ah battery 10 V nominal voltage is 100 W, 0.5P is 50 W, etc.). Battery SOC is a measure for the amount of charge stored in a battery with respect to the charge that the battery contains when fully charged. Battery SOE is a measure for the amount of energy stored in a battery with respect to the energy that the battery contains when fully charged. Battery SOH is a measure for the overall battery condition. A new, healthy battery has 100% SOH.

Battery efficiency can be divided by the measured electrical quantity used to determine the efficiency: coulombic (η^{I}), voltaic (η^{U}), and energy (η^{E}) efficiency. Battery efficiency can also be divided by the direction of energy flow: charging (η^{ch}), discharging (η^{dis}), and roundtrip (η^{cycle}) efficiency.

Battery charging and discharging C-rates and P-rates can differ greatly, so using separate charging and discharging efficiencies (instead of a single roundtrip efficiency) can allow for more accurate assessment of battery's SOE (and/or SOC) in real-time, as well as more accurate prediction of energy losses when scheduling battery energy storage operation or even when sizing a battery. However, determining the charging and discharging efficiencies (one-way efficiencies) is not straightforward.

Efficiencies can be experimentally obtained by subjecting a battery to a cycle or half-cycle. Cycle implies both charging and discharging over the same SOC range (energy flow in both directions) and is used to obtain the roundtrip efficiency. Half-cycle implies either charging or discharging (energy flow in one direction only) and is used to obtain the charging or discharging (one-way) efficiency. It can be either full or partial. Full (half-)cycle implies going from 0% to 100% SOC and/or back, while partial (half-)cycle implies covering some custom SOC range. When determining battery efficiencies, a full (half-)cycle should be started (and finished, in case of the roundtrip efficiency) with the battery either fully depleted (0% SOC) or fully charged (100% SOC). This methodology ensures a fixed starting (and finishing) point in terms of the measurable electrical quantities (terminal voltage and current). Still, SOC is normally used as a reference for determining the range of partial (half-)cycles (which can also be away from 0% and 100% SOC). For this purpose, SOC can be determined by the simplest form of coulomb counting:

$$soc(t) = soc(t-1) + \frac{100}{C} \cdot \int_{t-1}^{t} I(\tau) d\tau, \tag{3.1}$$

where $soc(t)$ is expressed in percentages, C is the cell capacity (Ah) and I is current (A), assumed positive for charging and negative for discharging. To avoid error accumulation associ-

ated with coulomb counting, it is advisable to first fully charge or discharge a battery and then go straight to the target SOC.

The existing methodologies for determining coulombic, voltaic and energy efficiencies are explained in the following subsections.

Coulombic Efficiency

This efficiency is associated with the charge (Ah) extracted from or injected into a battery.

•Charging coulombic efficiency is a ratio of the total charge stored in the battery (C^{batt}) and the total charge injected into the battery (C^{ch}) over a partial or full charging half-cycle:

$$\eta^{\text{ch,I}} = \frac{C^{\text{batt}}}{C^{\text{ch}}}. \tag{3.2}$$

•Discharging coulombic efficiency is a ratio of the total charge extracted from the battery (C^{dis}) and the total charge stored in the battery (C^{batt}) over a partial or full discharging half-cycle:

$$\eta^{\text{dis,I}} = \frac{C^{\text{dis}}}{C^{\text{batt}}}. \tag{3.3}$$

•Roundtrip coulombic efficiency is a ratio of the total charge extracted from the battery (C^{dis}) and the total charge injected in the battery (C^{ch}) over a partial or full cycle:

$$\eta^{\text{cycle,I}} = \eta^{\text{ch,I}} \cdot \eta^{\text{dis,I}} = \frac{C^{\text{dis}}}{C^{\text{ch}}}. \tag{3.4}$$

The injected/extracted charge (Ah) is easily calculated from the measured current, as follows:

$$C^{\text{ch}} = \int_0^{T^{\text{ch}}} I^{\text{ch}}(\tau) d\tau, \tag{3.5}$$

$$C^{\text{dis}} = \int_0^{T^{\text{dis}}} I^{\text{dis}}(\tau) d\tau, \tag{3.6}$$

where I^{ch} and I^{dis} are the charging and discharging currents, while T^{ch} and T^{dis} are the charging and discharging durations. On the other hand, C^{batt} is not straightforward to determine since the internal battery processes cannot be measured (at least not by tools available to us).

Voltaic Efficiency

Voltaic efficiency is associated with the average charging/discharging voltage. In this context, it is important to distinguish between the open-circuit voltage (U^{OC}) and the closed-circuit voltage (U^{ch}, U^{dis}). OCV is the voltage under the no load condition, while closed-circuit voltage is the voltage under the load condition, i.e. during charging or discharging. Closed-circuit voltage increases with the charging current and decreases with the discharging current, so voltaic efficiency is very dependent on the value of a battery's charging/discharging current.

•Charging voltaic efficiency is a ratio of the average open-circuit voltage ($\overline{U^{\mathrm{OC}}}$) and the average charging voltage ($\overline{U^{\mathrm{ch}}}$) over a partial or full charging half-cycle:

$$\eta^{\mathrm{ch,U}} = \frac{\overline{U^{\mathrm{OC}}}}{\overline{U^{\mathrm{ch}}}}. \tag{3.7}$$

•Discharging voltaic efficiency is a ratio of the average discharging voltage ($\overline{U^{\mathrm{dis}}}$) and the average open-circuit voltage ($\overline{U^{\mathrm{OC}}}$) over a partial or full discharging half-cycle:

$$\eta^{\mathrm{dis,U}} = \frac{\overline{U^{\mathrm{dis}}}}{\overline{U^{\mathrm{OC}}}}. \tag{3.8}$$

•Roundtrip voltaic efficiency is a ratio of the average discharging voltage ($\overline{U^{\mathrm{dis}}}$) and the average charging voltage ($\overline{U^{\mathrm{ch}}}$) over a partial or full cycle:

$$\eta^{\mathrm{cycle,U}} = \eta^{\mathrm{ch,U}} \cdot \eta^{\mathrm{dis,U}} = \frac{\overline{U^{\mathrm{dis}}}}{\overline{U^{\mathrm{ch}}}}. \tag{3.9}$$

To obtain one-way voltaic efficiency, an OCV-SOC characteristic ($U^{\mathrm{OC}} = f(soc)$) must be known, i.e. it needs to be determined experimentally.

Energy Efficiency

This efficiency is associated with the energy (Wh) extracted from or injected into a battery. Energy efficiencies are defined analogously to the coulombic efficiencies, with E denoting energy in Wh.

•Charging energy efficiency:

$$\eta^{\mathrm{ch,E}} = \frac{E^{\mathrm{batt}}}{E^{\mathrm{ch}}}. \tag{3.10}$$

•Discharging energy efficiency:

$$\eta^{\mathrm{dis,E}} = \frac{E^{\mathrm{dis}}}{E^{\mathrm{batt}}}. \tag{3.11}$$

•Roundtrip energy efficiency:

$$\eta^{\text{cycle,E}} = \eta^{\text{ch,E}} \cdot \eta^{\text{dis,E}} = \frac{E^{\text{dis}}}{E^{\text{ch}}}. \tag{3.12}$$

The injected energy E^{ch} (Wh) and the extracted energy E^{dis} (Wh) are easily calculated from the measured voltage and current as follows:

$$E^{\text{ch}} = \int_0^{T^{\text{ch}}} U^{\text{ch}}(\tau) I^{\text{ch}}(\tau) d\tau, \tag{3.13}$$

$$E^{\text{dis}} = \int_0^{T^{\text{dis}}} U^{\text{dis}}(\tau) I^{\text{dis}}(\tau) d\tau, \tag{3.14}$$

where U^{ch} and U^{dis} are charging and discharging closed-circuit voltages. Total energy stored in a battery E^{batt} cannot be determined directly from the measured voltage and current.

However, with the established method that employs the OCV-SOC characteristic (later in the paper referred to as *ocv* method), the following expressions that describe E^{batt} are obtained:

$$E^{\text{batt,ocv,ch}} = \int_0^{T^{\text{ch}}} U^{\text{OC}}(soc) I^{\text{ch}}(\tau) d\tau, \tag{3.15}$$

$$E^{\text{batt,ocv,dis}} = \int_0^{T^{\text{dis}}} U^{\text{OC}}(soc) I^{\text{dis}}(\tau) d\tau, \tag{3.16}$$

where U^{OC} is a function of the battery's state-of-charge. One-way energy efficiencies can now be calculated by including (3.15) in (3.10) and (3.16) in (3.11):

$$\eta^{\text{ch,E,ocv}} = \frac{E^{\text{batt,ocv,ch}}}{E^{\text{ch}}}, \tag{3.17}$$

$$\eta^{\text{dis,E,ocv}} = \frac{E^{\text{dis}}}{E^{\text{batt,ocv,dis}}}, \tag{3.18}$$

where *ocv* in superscript denotes that $E^{\text{batt,ocv,ch}} \neq E^{\text{batt}}$ and $E^{\text{batt,ocv,dis}} \neq E^{\text{batt}}$. The reason for this discrepancy is the omission of coulombic losses in (3.15) and (3.16). Consequently, the product of two one-way efficiencies in (3.30) and (3.31) results in an incorrect roundtrip efficiency:

$$\eta^{\text{cycle,E,ocv}} = \eta^{\text{ch,E,ocv}} \cdot \eta^{\text{dis,E,ocv}} > \eta^{\text{cycle,E}} = \frac{E^{\text{dis}}}{E^{\text{ch}}}, \tag{3.19}$$

since $C^{\text{ch}} > C^{\text{dis}}$ (see (3.5) and (3.6)) and $E^{\text{batt,ocv,ch}} > E^{\text{batt,ocv,dis}}$, which is the case whenever

a cycle is performed over the same SOC range. In other words, coulombic losses are neglected in (3.15)–(3.19).

Coulombic, Voltaic and Energy Efficiency Relations

Using the OCV-SOC characteristic to obtain one-way energy efficiencies, as described above, is reasonable since the voltaic losses are normally more dominant (higher) than the coulombic losses (especially for higher C-rates). Roundtrip coulombic efficiency for lithium-ion battery technology is typically 99% or higher, as reported in many papers, e.g. [21, 24, 25, 39], and confirmed by our own experimental results. Therefore, expressions $C^{\text{ch}} \approx C^{\text{dis}}$ and $E^{\text{batt,ocv,ch}} \approx E^{\text{batt,ocv,dis}}$ typically hold for lithium-ion battery cycles. Moreover, simple coulomb counting (3.1) can be used to cycle lithium-ion battery in the desired SOC range, in which case $C^{\text{ch}} = C^{\text{dis}}$ and $E^{\text{batt,ocv,ch}} = E^{\text{batt,ocv,dis}}$ is implied, while inequality (3.19) becomes equality. This approach to determining one-way energy efficiencies (i.e. neglecting coulombic losses) is commonly used in the literature, e.g. see [37, 38, 40].

Finally, it is worth noting that the energy efficiency is generally not a product of the coulombic and the voltaic efficiency. This is because energies are obtained by calculating Watt-hours, not Ampere-hours multiplied by the averaged voltages, i.e.:

$$\int_0^{T^{\text{ch}}} U^{\text{OC}}(soc) I^{\text{ch}}(\tau) d\tau \neq \overline{U^{\text{OC}}} \cdot \int_0^{T^{\text{ch}}} I^{\text{ch}}(\tau) d\tau. \tag{3.20}$$

Although the deviation is relatively small, energies obtained by the two calculus given in (3.20) are not the same, leading to the roundtrip energy efficiency being different as well:

$$\eta^{\text{cycle,E}} \neq \eta^{\text{cycle,U}} \cdot \eta^{\text{cycle,I}}. \tag{3.21}$$

However, not-equal marks in (3.20) and (3.21) can be replaced with equal marks in case $I^{\text{ch}} = \text{const.}$, since (see also [19, 22]):

$$\overline{U^{\text{OC}}} = \frac{\int_0^{T^{\text{ch}}} U^{\text{OC}}(soc) d\tau}{T^{\text{ch}}}. \tag{3.22}$$

Novel optimization-based Method for Obtaining One-way Efficiencies

This section describes the proposed algorithm for a novel optimization-based approach for determining one-way energy efficiencies is proposed. Moreover, this approach can also be used to determine one-way coulombic efficiencies, which none of the conventional approaches are capable of.

Steps of the algorithm are described in the following susections.

1.Step 1: Charging/discharging Cycles in the CP Mode

2.Step 2: Roundtrip Energy Efficiencies
3.Step 3: One-way Energy Efficiencies
4.Step 4: One-way Energy Efficiency Characteristics

Step 1: Charging/discharging Cycles in the CP Mode

In this experimental part of the algorithm, the battery is cycled as follows:

- •Each cycle is always started with a depleted battery, where depleted means that a non-depleted battery is discharged until the battery's low voltage limit has been reached with the provision that the discharging battery P-rate is equal to the cycle's discharging P-rate in point 3) below. This ensures the same starting and finishing point of the cycle in terms of currents and voltages.
- •Each charging is performed in the constant-power mode and is terminated as soon as the declared battery high voltage limit is reached.
- •Each discharging is performed in the constant-power mode and is terminated as soon as the declared battery low voltage limit is reached.
- •Each cycle is performed at room temperature.

A number of P-rates is chosen to cover the expected battery's charging (C) and discharging (D) operational ranges. Then, $C \times D$ partial cycles in the CP mode are conducted, for all possible combinations of the chosen charging/discharging P-rates. To increase accuracy and ensure consistency, cycling can be repeated J times.

Step 2: Roundtrip Energy Efficiencies

For every cycle from Step 1, charging and discharging energies are calculated by integrating the logged powers, see (3.13) and (3.14). Then, the roundtrip energy efficiency for every cycle is obtained according to (3.12). Finally, roundtrip efficiency for each combination of the charging/discharging P-rate is averaged as:

$$\eta_{c,d}^{\text{cycle,E}} = \frac{\sum_{j=1}^{J} \eta_{c,d,j}^{\text{cycle,E}}}{J}. \tag{3.23}$$

Step 3: One-way Energy Efficiencies

To obtain one-way efficiencies from the measured roundtrip efficiencies, we formulate and solve the following nonlinear optimization problem:

$$\underset{\Xi=\{s_{c,d},\eta_c^{\text{ch,E,opt}},\eta_d^{\text{dis,E,opt}}\}}{\text{Minimize}} \quad \sum_{c\in\Omega^{\text{C}}} \sum_{d\in\Omega^{\text{D}}} s_{c,d}^2 \tag{3.24}$$

subject to

$$\eta_c^{\mathrm{ch,E,opt}} \cdot \eta_d^{\mathrm{dis,E,opt}} = \eta_{c,d}^{\mathrm{cycle,E}} + s_{c,d}, \quad \forall c \in \Omega^{\mathrm{C}}, \forall d \in \Omega^{\mathrm{D}}, \tag{3.25}$$

$$0 \leq \eta_c^{\mathrm{ch,E,opt}} \leq 1, \quad \forall c \in \Omega^{\mathrm{C}}, \tag{3.26}$$

$$0 \leq \eta_d^{\mathrm{dis,E,opt}} \leq 1, \quad \forall d \in \Omega^{\mathrm{D}}. \tag{3.27}$$

Objective function (3.24) minimizes the squares of slack variable $s_{c,d}$ summed over all charging (c) and discharging (d) rates. Slack variable $s_{c,d}$ appears in constraint (3.25) to offset the inequality of the left- and right-hand sides of the equation. Note that (3.25) is a set of equations containing $C+D$ unknowns ($\eta_c^{\mathrm{ch,E,opt}}$ and $\eta_d^{\mathrm{dis,E,opt}}$) and $C \times D$ equations. However, this set of equations, assuming $s_{c,d} = 0$, cannot be solved analytically, as it is ill-posed, i.e. it either does not have a solution or it has infinitely many solutions. In other words, there is no combination of $\eta_c^{\mathrm{ch,E,opt}}$ and $\eta_d^{\mathrm{dis,E,opt}}$ that satisfies all $C \times D$ equations. Thus, the goal of this optimization problem is to find the values of $\eta_c^{\mathrm{ch,E,opt}}$ and $\eta_d^{\mathrm{dis,E,opt}}$, whose multiplication diverges from the measured efficiency $\eta_{c,d}^{\mathrm{cycle,E}}$ the least. Since constraint (3.25) is nonlinear, additional constraints (3.26) and (3.27) are imposed to avoid possible physically meaningless solutions.

The strength of the proposed method, as mentioned in Section **??**, lies in the fact that it can also be used to obtain one-way coulombic efficiencies (based on the measured roundtrip coulombic efficiencies), in which case superscript I can be used instead of E in (3.24)–(3.27). In this context, it is also worth noting that the obtained one-way energy efficiencies $\eta^{\mathrm{ch,E,opt}}$ and $\eta^{\mathrm{dis,E,opt}}$ account for both the voltaic and the coulombic losses and are thus potentially more accurate than $\eta^{\mathrm{ch,E,ocv}}$ and $\eta^{\mathrm{dis,E,ocv}}$. This may not be as important for lithium-ion batteries which have high coulombic efficiency (cca. 99% roundtrip), but it may be beneficial for application to other technologies that have lower coulombic efficiency, e.g. Ni-MH batteries or some emerging technologies. Furthermore, obtaining OCV-SOC characteristics takes time (cca. 48 hours typically) and requires relatively precise instrumentation, as cycling is performed with very low currents. Another strength of the proposed method, compared to the OCV-based method, is the possibility of obtaining one-way efficiencies quicker (e.g. for $C = D = 2$) and with less precise instrumentation, as low currents are avoided.

Step 4: One-way Energy Efficiency Characteristics

The output of Step 3 are C charging and D discharging energy efficiencies that correspond to the charging/discharging P-rates chosen in Step 1 of the algorithm. Linear interpolation between these values can be used to assess one-way energy efficiency characteristics (functions) over the entire range of battery's operational power: $\eta^{\mathrm{CH,E,opt}} = f(P^{\mathrm{ch}})$ and $\eta^{\mathrm{DIS,E,opt}} = f(P^{\mathrm{dis}})$ (see Fig. **??** for the specific characteristics). These characteristics can now be used to calculate the energy injected into the battery $E^{\mathrm{batt,opt,ch}}$ (Wh) and the energy extracted from the battery

$E^{\text{batt,opt,dis}}$ (Wh) with variable one-way energy efficiencies accounted for, as follows:

$$E^{\text{batt,opt,ch}} = \int_0^{T^{\text{ch}}} P^{\text{ch}}(\tau) \cdot \eta^{\text{CH,E,opt}}(P^{\text{ch}}) d\tau, \tag{3.28}$$

$$E^{\text{batt,opt,dis}} = \int_0^{T^{\text{dis}}} \frac{P^{\text{dis}}(\tau)}{\eta^{\text{DIS,E,opt}}(P^{\text{dis}})} d\tau, \tag{3.29}$$

where $P^{\text{ch}}(\tau) = U^{\text{ch}}(\tau) \cdot I^{\text{ch}}(\tau)$ and $P^{\text{dis}}(\tau) = U^{\text{dis}}(\tau) \cdot I^{\text{dis}}(\tau)$.

Remark: The method described in this section ignores the nonlinearity and the one-way efficiency dependence on the SOC level. This is justified by the findings from [23], where it is shown that voltaic efficiency curves can be considered constant in a wide SOC range. Thus, the errors due to this neglection are insignificant, especially if the edge parts of the SOC – one-way efficiency characteristic are not used.

Proposed Method for Determination of Average Battery Energy Capacity and State-of-Energy

This section describes the proposed method for battery energy capacity determination step-by-step.

In the first step, the battery is cycled with the aim of obtaining the charging and discharging energies for a number of full cycles. Cycles are always started at a fully depleted battery a fully depleted battery means that a non-depleted battery is discharged until the battery's low-voltage limit has been reached and the current has dropped below the specified cut-off value) (0% SOE), while each charging and discharging process is terminated when the current drops below the low cut-off threshold an end-of-charge current specified by the manufacturer). Full cycles in the constant power–constant voltage (CPCV) mode are conducted, always using the same charging/discharging P-rate within a cycle. In CPCV mode, the battery is charged and discharged at constant power until the effect of voltage saturation, where the battery voltage reaches the high (for charging) or the low (for discharging) voltage limit. In that moment, the constant voltage mode begins and the power consequently decreases. The set of K full cycles is repeated at each considered ambient temperature, in order to obtain the efficiency–power characteristics for different ambient temperature conditions.

The second step is the one-way efficiency determination. As Coulombic losses for the observed lithium-ion battery cell are less than 1% [21], their effect is neglected in this research. Thus, one-way efficiencies are determined from the open-circuit voltage vs. state-of-charge (OCV-SOC) characteristic in this work, the OCV-SOC characteristic is also determined for each considered ambient temperature), according to [23]:

$$\eta_{\mathrm{k}}^{\mathrm{Prop,ch,E}} = \frac{\int_0^{T^{\mathrm{ch}}} U^{\mathrm{OC}}(soc) \cdot I_{\mathrm{k}}^{\mathrm{ch}}(\tau) d\tau}{\int_0^{T^{\mathrm{ch}}} U_{\mathrm{k}}^{\mathrm{ch}}(\tau) \cdot I_{\mathrm{k}}^{\mathrm{ch}}(\tau) d\tau}, \tag{3.30}$$

where $k \in [1 \ldots K]$, $U^{\mathrm{OC}}(soc)$ is an OCV-SOC characteristic and $I_{\mathrm{k}}^{\mathrm{ch}}(\tau)$ is the charging current, and

$$\eta_{\mathrm{k}}^{\mathrm{Prop,dis,E}} = \frac{\int_0^{T^{\mathrm{dis}}} U_{\mathrm{k}}^{\mathrm{dis}}(\tau) \cdot I_{\mathrm{k}}^{\mathrm{dis}}(\tau) d\tau}{\int_0^{T^{\mathrm{dis}}} U^{\mathrm{OC}}(soc) \cdot I_{\mathrm{k}}^{\mathrm{dis}}(\tau) d\tau}, \tag{3.31}$$

where $I_{\mathrm{k}}^{\mathrm{dis}}(\tau)$ is the discharging current. In this way, it is possible to determine one-way charging and discharging efficiencies $\eta_{\mathrm{k}}^{\mathrm{Prop,ch,E}}$ and $\eta_{\mathrm{k}}^{\mathrm{Prop,dis,E}}$ for all K P-rates. Here, only the CP mode of each cycle (for both charge and discharge) is used to determine the efficiencies, so that the one-way efficiencies correlate with the P-rates.

Battery efficiency is a nonlinear function depending on operating conditions (power rate). To approximate this nonlinearity, an efficiency–power curve is introduced in the third step based on linear interpolation between K determined one-way efficiencies in the whole range of the operating powers. .

In the fourth step, for every full cycle (out of K full cycles in the CPCV mode), the logged powers ($P_{\mathrm{k}}^{\mathrm{ch}}(t)$ and $P_{\mathrm{k}}^{\mathrm{dis}}(t)$) are corrected for one-way energy efficiencies by using the determined efficiency–power curves:

$$P_{\mathrm{k}}^{\mathrm{Prop,ch}}(t) = \eta^{\mathrm{Prop,ch,E}}(P^{\mathrm{ch}}) \cdot P_{\mathrm{k}}^{\mathrm{ch}}(t), \tag{3.32}$$

$$P_{\mathrm{k}}^{\mathrm{Prop,dis}}(t) = \frac{P_{\mathrm{k}}^{\mathrm{dis}}(t)}{\eta^{\mathrm{Prop,dis,E}}(P^{\mathrm{dis}})}, \tag{3.33}$$

where $\eta^{\mathrm{Prop,ch,E}}(P^{\mathrm{ch}})$ and $\eta^{\mathrm{Prop,dis,E}}(P^{\mathrm{dis}})$ are charging and discharging efficiency–power curves.

Finally, in the fifth step, by integrating the corrected powers, K values of $E_{\mathrm{k}}^{\mathrm{Prop,ch}} = \int_0^{T^{\mathrm{ch}}} P_{\mathrm{k}}^{\mathrm{Prop,ch}}(\tau) d\tau$ and K values of $E_{\mathrm{k}}^{\mathrm{Prop,dis}} = \int_0^{T^{\mathrm{dis}}} P_{\mathrm{k}}^{\mathrm{Prop,dis}}(\tau) d\tau$ are obtained, representing the energy stored in a battery during charging and energy extracted from a battery during discharging, respectively. In an ideal case, values of the corrected energies $E_k^{\mathrm{Prop,ch}}$ and $E_k^{\mathrm{Prop,dis}}$ are all the same, representing the energy that can be stored in a battery. In reality, due to various effects and uncertainties (various electrochemical phenomena, e.g., loss of lithium ions due to lithium plating, as well as measurement uncertainties), these values slightly vary, and the battery energy capacity is declared to be the mean of all the corrected energies:

$$E_{\mathrm{av}}^{\mathrm{Prop}} = \frac{\sum_{k=1}^{K} E_{\mathrm{k}}^{\mathrm{Prop,ch}} + \sum_{k=1}^{K} E_{\mathrm{k}}^{\mathrm{Prop,dis}}}{2 \cdot K}. \tag{3.34}$$

Expression (3.34) represents the fifth and last step of the *Proposed* method, where state-of-

energy is defined as

$$SOE(t) = SOE(t-1) + \frac{1}{E_{\text{av}}^{\text{Prop}}} \cdot \left(\int_{\text{t}-1}^{\text{t}} P^{\text{Prop,ch}}(\tau) d\tau - \int_{\text{t}-1}^{\text{t}} P^{\text{Prop,dis}}(\tau) d\tau \right), \tag{3.35}$$

where $P^{\text{Prop,ch}}(t)$ and $P^{\text{Prop,dis}}(t)$ are corrected powers, given by (3.32) and (3.33), for the time frame $\langle t-1, t]$.

Chapter 4

List of Publications

The publications published within this thesis and considered as the main contribution are divided into two sections: journal papers and conference papers. Other published papers can be found under biography Chapter 6.2.

4.1 Journal Papers

Published

[P_1]H. Baši ć, V. Bobanac and H. Pandžić, "Determination of Lithium-ion Battery Capacity for Practical Applications," *Batteries* (ISSN 2313-0105), 2023, DOI: https://doi.org/10.3390/batteries9090459

[P_2]V. Bobanac, H. Baši ć and H. Pandžić, "A Method for Deriving Battery One-way Efficiencies," *Journal of Energy Storage*, 2023, DOI: https://doi.org/10.1016/j.est.2023.108815

[P_3]H. Baši ć, H. Pandžić, M. Miletić and I. Pavić, "Experimental Testing and Evaluation of Lithium-Ion Battery Cells for a Special-Purpose Electric Vacuum Sweeper Vehicle," *IEEE Access*, vol. 8, pp. 216308-216319, 2020, DOI: 10.1109/ACCESS.2020.3040206

4.2 Conference Papers

Published and Presented

[C_5]V. Bobanac, H. Baši ć, H. Pandžić, "One-way voltaic and energy efficiency analysis for lithium-ion batteries" in *13th Mediterranean Conference on Power Generation, Transmission, Distribution and Energy Conversion (MEDPOWER 2022)*, 2022, pp. 261–266, DOI: 10.1049/icp.2023.0003

[C_6]V. Bobanac, H. Baši ć, H. Pandžić, "Determining Lithium-ion Battery One-way Energy Efficiencies: Influence of C-rate and Coulombic Losses", in *IEEE EUROCON 2021 - 19th*

International Conference on Smart Technologies, 2021, pp. 385–389, DOI: 10.1109/EUROCON52738.2021.9535542

[C_7]H. Baši ć, T. Dragičević, H. Pandžić, F. Blaabjerg, "DC microgrids with energy storage systems and demand response for providing support to frequency regulation of electrical power systems", in *2017 19th European Conference on Power Electronics and Applications (EPE'17 ECCE Europe)*, 2017, pp. P.1-P.10, DOI: 10.23919/EPE17ECCEEurope.2017.8099000

[C_8]H. Baši ć, T. Dragičević, H. Pandžić, F. Blaabjerg, "DC microgrids providing frequency regulation in electrical power system - imperfect communication issues", in *2017 IEEE Second International Conference on DC Microgrids (ICDCM)*, 2017, pp. 434–439, DOI: 10.1109/ICDCM.2017.8001081

Chapter 5

Author's Contribution to the Publications

The contribution of this thesis was achieved during the period of 2016–2023 at the University of Zagreb Faculty of Electrical Engineering and Computing, Unska 3, HR-10000 Zagreb, Croatia. The research was conducted under under the projects listed below:

- Project *Smart Integration of RENewables* (SIREN), funded by the Croatian TSO - HOPS and Croatian Science Foundation
- Project *Development of a new generation of numeric protection devices* (KONPRO 2), funded by European Regional Development Fund
- Project *Electric Compact Urban Vacuum Sweeper with an ICT System Project*, funded by European Regional Development Fund
- Project *Connected Stationary Battery Energy Storage* (USBSE), funded by European Regional Development Fund
- Project *microGRId Positioning* (uGRIP), funded by the Environmental Protection and Energy Efficiency Fund through the ERA Net Smart Grid +
- Project *Development of a digital platform for building Critical Infrastructure Protection Systems in Smart Industries* (CIP 4 SI), funded by European Regional Development Fund

The author's main contribution to each paper is listed below:

[P_1] In the journal paper *"Determination of Lithium-ion Battery Capacity for Practical Applications"*: literature review, development of a method for determining battery capacity that considers charging/discharging (one-way) efficiencies and different ambient temperatures, verification of the proposed method and an experimental comparison of the proposed method with the baseline methods, paper writing and results elaboration.

[P_2] In the journal paper *"A Method for Deriving Battery One-way Efficiencies"*: literature review, development of optimization algorithm for obtaining one-way efficiencies, design of an experimental setup and measurement procedures, paper writing and results elaboration proposal and implementation of a bilevel market participation model, proposal of the solution algorithm and paper writing.

[P_3]In the journal paper *"Experimental Testing and Evaluation of Lithium-Ion Battery Cells for a Special-Purpose Electric Vacuum Sweeper Vehicle"*: literature review, design of a methodology for evaluation of battery cells for an electric compact urban vacuum sweeper, experimental testing and categorization of different lithium-ion battery cells using the Analytic Hierarchy Process, paper writing and results elaboration.

[P_4]In the conference paper *"One-way voltaic and energy efficiency analysis for lithium-ion batteries"*: literature review, design of an experimental setup and measurement procedures and paper writing.

[P_5]In the conference paper *"Determining Lithium-ion Battery One-way Energy Efficiencies: Influence of C-rate and Coulombic Losses"*: literature review, design of an experimental setup and measurement procedures and paper writing.

[P_6]In the conference paper *"DC microgrids with energy storage systems and demand response for providing support to frequency regulation of electrical power systems"*: literature review, development of the model of frequency regulation of electric power system with support from aggregated DC microgrids, verification of the simulation models implemented by OPAL-RT real time Model-in-Loop system, paper writing and results elaboration.

[P_7]In the conference paper *"DC microgrids providing frequency regulation in electrical power system - imperfect communication issues"*: literature review, development of DC microgrids and communication network model, paper writing and results elaboration.

Chapter 6

Conclusions and Future Work

6.1 Main Conclusions of the Thesis

The research conducted in this thesis is divided into two parts. In the first part, the methodology for selecting an optimal lithium-ion battery cell for a specific purpose electric vehicle in specific ambient conditions presented is based on analysis of the laboratory test results using the Analytic Hierarchy Process. It is shomn that the optimal lithium-ion battery cell selected with the proposed methodology is different than the battery cell selected solely on analysis of the manufacturers' datasheets. So, although the manufacturers' datasheets contain many useful information, it is shown that an analysis based exclusively on such data may result in sub-optimal battery cell selection.

In the second part, battery characteristics are analyzed, modelled and verified. An overview of different battery efficiency types and relations between them is given. An optimization-based method for obtaining one-way efficiencies is proposed and used to formulate a variable efficiency model. The obtained model is compared to two conventional models: one using fixed one-way efficiencies and the other, OCV-based, using variable one-way efficiencies. The proposed optimization-based method is potentially less time consuming than the established OCV-based method and can be used with relatively cheap (less precise) instrumentation, as very low currents, necessary for obtaining the OCV characteristics, can be avoided. The two methods show comparable results, which indicates that the proposed approach is valid and that it should be further tested in applications where the OCV-based method is inapplicable. One such application is determination of one-way coulombic efficiencies, which in case of lithium-ion batteries must be performed on expensive, highly precise instrumentation. The other such application is precise one-way energy efficiency determination (accounting for coulombic losses) of lithium-ion and other battery technologies.

The dependence of battery capacity and state-of-energy estimation to the operational and ambient conditions are analyzed, respectively. The operational conditions are related to the

charging and discharging current/power rates, while the ambient conditions are related to the ambient temperatures at which the batteries are used. Both operational and ambient conditions affect the efficiency and the health of the batteries to a different extent, depending on the range of observed conditions. The established (baseline) methods for estimation of battery capacity and state-of-energy either consider only nominal values given by the manufacturer, or neglect the variable operational and/or ambient conditions. Our work presents a novel method that considers both the variable operational and ambient conditions. It is based on experimental determination of one-way (charging and discharging) efficiencies for different current/power rates under different ambient conditions.

6.2 Future Work

The focus of the future research will be in expanding the developed methodologies with different battery types and more complex operational and ambient conditions for development of an algorithm for evaluation of a larger scope of the battery cell characteristics.

Future work will encompass the applications of the proposed model of battery efficiency and battery capacity, as well as reformulation of the presented variable efficiency models for inclusion in higher-level linear optimization models.

Bibliography

[1]V. Bobanac, H. Pandži ć, T. Capuder, "Survey on electric vehicles and battery swapping stations: Expectations of existing and future EV owners," 2018 IEEE International Energy Conference, ENERGYCON 2018, pp. 1–6, 2018., doi: 10.1109/ENERGYCON.2018.8398793

[2]S. M. Lukic, J. Cao, R. C. Bansal, F. Rodriguez, A. Emadi, "Energy storage systems for automotive applications," *IEEE Transactions on Industrial Electronics*, vol. 55, no. 6, pp. 2258–2267, 2008., doi:10.1109/TIE.2008.918390

[3]A. F. Burke, "Batteries and ultracapacitors for electric, hybrid, and fuel cell vehicles," *Proceedings of the IEEE*, vol. 95, no. 4, pp. 806–820, doi: 10.1109/JPROC.2007.892490

[4]D. Linden, T. B. Reddy, "Handbook of batteries," McGraw-Hill, 2002.

[5]X. Chen, W. Shen, T. T. Vo, Z. Cao, A. Kapoor, "An overview of lithium-ion batteries for electric vehicles," 10th International Power and Energy Conference, IPEC 2012, pp. 230–235, doi:10.1109/ASSCC.2012.6523269

[6]N. Omar, B. Verbrugge, G. Mulder, P. Van Den Bossche, J. Van Mierlo, M. Daowd, M. Dhaens, S. Pauwels, "Evaluation of performance characteristics of various lithium-ion batteries for use in BEV application," 2010 IEEE Vehicle Power and Propulsion Conference, 2010.

[7]R. Benato, S. D. Sessa, M. Musio, F. Palone, R. M. Polito, "Italian experience on electrical storage ageing for primary frequency regulation," *Energies*, vol. 11, no. 8, 2018., doi: 10.3390/en11082087

[8]L. Zhang, Z. Mu, X. Gao, "Coupling analysis and performance study of commercial 18650 lithium-ion batteries under conditions of temperature and vibration," *Energies*, vol. 11, no. 10, 2018., doi: 10.3390/en11102856

[9]X. Gong, R. Xiong, C. C. Mi, "Study of the Characteristics of Battery Packs in Electric Vehicles with Parallel-Connected Lithium-Ion Battery Cells," *IEEE Transactions on Industry Applications*, vol. 51, no. 2, pp. 1872–1879, doi: 10.1109/TIA.2014.2345951

[10]D. Anseán, M. González, V. M. García, J. C. Viera, J. C. Antón, C. Blanco, "Evaluation of LiFePO4 Batteries for Electric Vehicle Applications," *IEEE Transactions on Industry Applications*, vol. 51, no. 2, pp. 1855–1863, 2015., doi: 10.1109/TIA.2014.2344446

[11]"Electric Vehicle Battery Test Procedures Manual, rev. 2" U.S. Advanced Battery Consortium and U.S. Dept. Energy, Idaho Nat. Lab., Idaho Falls, ID, USA, Jan. 1996.

[12]F. P. Tredeau, Z. M. Salameh, "Evaluation of Lithium iron phosphate batteries for electric vehicles application," 2009 IEEE Vehicle Power and Propulsion Conference, 2009.

[13]A. Marongiu, A. Damiano, M. Heuer, "Experimental analysis of lithium iron phosphate battery performances," IEEE International Symposium on Industrial Electronics, pp. 3420–3424, 2010., doi: 10.1109/ISIE.2010.5637749

[14]J. Wang, Z. Sun, X. Wei, "Performance and characteristic research in LiFePO4 battery for electric vehicle applications," 5th IEEE Vehicle Power and Propulsion Conference, VPPC '09, pp. 1657–1661, 2009, doi: 10.1109/VPPC.2009.5289664

[15]F. P. Tredeau, B. G. Kim, Z. M. Salameh, "Performance evaluation of Lithium Cobalt cells and the suitability for use in electric vehicles," 2008 IEEE Vehicle Power and Propulsion Conference, 2008.

[16]B. G. Kim, F. P. Tredeau, Z. M. Salameh, "Performance evaluation of lithium polymer batteries for use in electric vehicles," IEEE Vehicle Power and Propulsion Conference, 2008., doi: 10.1109/VPPC.2008.4677513

[17]J. Tang, Q. Liu, S, Liu, X. Xie, J. Zhou, Z. Li, "A Health Monitoring Method Based on Multiple Indicators to Eliminate Influences of Estimation Dispersion for Lithium-Ion Batteries," *IEEE Access*, vol. 7, pp. 122302–122314, 2019., doi: 10.1109/ACCESS.2019.2936213

[18]A. Shafiei, A. Momeni, S. S. Williamson, "Battery modeling approaches and management techniques for plug-in hybrid electric vehicles," 2011 IEEE Vehicle Power and Propulsion Conference, VPPC 2011, 2011., doi: 10.1109/VPPC.2011.6043191

[19]P. Meister, H. Jia, J. Li, R. Kloepsch, M. Winter and T. Placke, "Best Practice: Performance and Cost Evaluation of Lithium Ion Battery Active Materials with Special Emphasis on Energy Efficiency," *Chemistry of Materials*, vol. 28(20), pp. 7203–7217, 2016.

[20]A. Eftekhari, "Energy efficiency: a critically important but neglected factor in battery research," *Sustainable Energy & Fuels*, vol. 1(10), 2017.

[21]J. Xiao, Q. Li, Y. Bi, M. Cai, B. Dunn, T. Glossmann, J. Liu, T. Osaka, R. Sugiura, B. Wu, J. Yang, J. Zhang and M. S. Whittingham, "Understanding and applying coulombic efficiency in lithium metal batteries," *Nature Energy*, vol. 5, pp. 561–568, 2020.

[22]R. Lu, A. Yang, Y. Xue, L. Xu and C. Zhu, "Analysis of the key factors affecting the energy efficiency of batteries in electric vehicle," *World Electric Vehicle Journal*, vol. 4, pp. 9–13, 2010.

[23]V. Bobanac, H. Baši ć, H. Pandžić, "One-way voltaic and energy efficiency analysis for lithium-ion batteries," *Medpower2022, The 13th Mediterranean Conference on Power Generation, Transmission, Distribution and Energy Conversion*, pp 53, 2022.

[24]A. J. Smith, J. C. Burns and J. R. Dahn, "A High Precision Study of the Coulombic Efficiency of Li-Ion Batteries," *Electrochemical and Solid-State Letters*, vol. 13 (12), pp. 177–179, 2010.

[25]A. J. Smith, J. C. Burns, D. Xiong and J. R. Dahn, "Interpreting High Precision Coulometry Results on Li-ion Cells," *Journal of The Electrochemical Society*, vol. 158 (10), pp. 1136–1142, 2011.

[26]W. H. Zhu, Y. Zhu, Z. Davis, B. J. Tatarchuk, "Energy efficiency and capacity retention of Ni–MH batteries for storage applications," *Applied Energy*, vol. 106, pp. 307–313, 2013.

[27]S. U. Jeon, J.-W. Park, B.-K. Kang and H.-J. Lee, "Study on Battery Charging Strategy of Electric Vehicles Considering Battery Capacity," *IEEE Access*, vol. 9, pp. 89757–89767, 2021, doi: 10.1109/ACCESS.2021.3090763

[28]S. Farhad, A. Nazari, "Introducing the energy efficiency map of lithium-ion batteries," *Int. J. Energy Res.*, 2018, vol. 43, 931–944

[29]K. Mamadou, A. Delaille, "Method for calibrating an electrochemical battery," *European patent*, nr. EP2449392B1, *US patent*, nr. US 9,075,117 B2, 2010.

[30]K. Mamadou, E. Lemaire, A. Delaille, D. Riu, S. Hing, Y. Bultel, "Definition of a State-of-Energy Indicator (SoE) for Electrochemical Storage Devices: Application for Energetic Availability Forecasting," *Journal of the Electrochemical Society*, vol. 159, pp. A1298–A1307, 2012.

[31]E. Fernandez, T. Delaplagne, R. Franchi, k. Mamadou, "Method for determining a state-of-energy of the basis of data originating from the processing method," *European patent*, nr. EP2856187B1, 2013.

[32]X. Liu, J. Wu, C. Zhang, Z. Chen, "A method for state of energy estimation of lithium-ion batteries at dynamic currents and temperatures," *Journal of Power Sources*, vol. 270, pp. 151–157, 2014.

[33]W. Zhang, W. Shi, Z. Ma, "Adaptive unscented Kalman filter based state of energy and power capability estimation approach for lithium-ion battery," *Journal of Power Sources*, vol. 289, pp. 50–62, 2015.

[34]X. Shen, L. Zhang, Q. Chen, P. Xiao and R. Long, "Energy management strategy for model predictive control of hybrid electric vehicle considering battery life and efficiency," 2021 5th CAA International Conference on Vehicular Control and Intelligence (CVCI), Tianjin, China, 2021, pp. 1–6, doi: 10.1109/CVCI54083.2021.9661238.

[35]G. L. Plett, "Extended Kalman filtering for battery management systems of LiPB-based HEV battery packs, Part 2. Modeling and identification," *Journal of Power Sources*, vol. 134, pp. 262–276, 2004.

[36]S. Abu-Sharkh and D. Doerffel, "Rapid test and non-linear model characterisation of solid-state lithium-ion batteries," *Journal of Power Sources*, vol. 130, pp. 266–274, 2004.

[37]M. Safoutin, J. Cherry, J. McDonald and S. Lee, "Effect of Current and SOC on Round-Trip Energy Efficiency of a Lithium-Iron Phosphate (LiFePO4) Battery Pack," SAE Technical Paper 2015-01-1186, 2015.

[38]J. Kang, F. Yan, P. Zhang and C. Du, "A novel way to calculate energy efficiency for rechargeable batteries," *Journal of Power Sources*, vol. 206, pp. 310–314, 2012.

[39]F. Yang, D. Wang, Y. Zhao, K. Tsui and S. J. Bae, "A study of the relationship between coulombic efficiency and capacity degradation of commercial lithium-ion batteries," *Energy*, vol. 145, pp. 486–495, 2018.

[40]E. Redondo-Iglesias, P. Venet and S. Pelissier, "Efficiency Degradation Model of Lithium-Ion Batteries for Electric Vehicles," *IEEE Transactions on Industry Applications*, vol. 55, no. 2, pp. 1932–1940, 2018.

[41]R. Xiong, J. Cao, Q. Yu, H. He, F. Sun, "Critical Review on the Battery State of Charge Estimation Methods for Electric Vehicles," *IEEE Access*, 2018, vol. 6, 1832–1843, doi: 10.1109/ACCESS.2017.2780258

[42]K. Li, K. J. Tseng,, "An equivalent circuit model for state of energy estimation of lithium-ion battery," in Proceedings of the 2016 IEEE Applied Power Electronics Conference and Exposition (APEC), Long Beach, CA, USA, 20–24 March, 2016; pp. 3422–3430, doi: 10.1109/APEC.2016.7468359

[43]L. Zheng, J. Zhu, G. Wang, T. He, Y. Wei, "Novel methods for estimating lithium-ion battery state of energy and maximum available energy," *Appl. Energy*, 2016, vol. 178, 1–8.

[44]W. Zhang, W. Shi, Z. Ma, "Adaptive unscented Kalman filter based state of energy and power capability estimation approach for lithium-ion battery," *J. Power Sources*, 2015, vol. 289, 50–62

[45]Y. Wang, C. Zhang, Z. Chen, "Model-based state-of-energy estimation of lithium-ion batteries in electric vehicles," *Energy Procedia*, 2016, vol. 88, 998–1004.

[46]G. Dong, Z. Chen, J. Wei, C. Zhang, P. Wang, "An online model-based method for state of energy estimation of lithium-ion batteries using dual filters," *J. Power Sources*, 2016, vol. 301, 277–286

[47]K. Li, K. J. Tseng, "Energy efficiency of lithium-ion battery used as energy storage devices in micro-grid," in Proceedings of the IECON 2015-41st Annual Conference of the IEEE Industrial Electronics Society, Yokohama, Japan, 9–12 November, 2015, pp. 005235–005240, doi: 10.1109/IECON.2015.7392923

[48]C. Bhat, J. Channegowda, K. Naraharisetti, "Electrolyte based Equivalent Circuit Model of Lithium ion Batteries for Intermittent Load Applications," in Proceedings of the 2022 IEEE International Conference on Power Electronics, Smart Grid, and Renewable Energy (PESGRE), Trivandrum, India, 2–5 January 2022, pp. 1–3, doi: 10.1109/PESGRE52268.2022.9715891

[49]P. Bhagyasree, V. A. Shah, "A Simplified Method to Evaluate Equivalent Circuit Model and State of Charge of Li-ion Battery," in Proceedings of the 2019 IEEE 1st International Conference on Energy, Systems and Information Processing (ICESIP), Chennai, India, 4–6 July 2019, pp. 1–6, doi: 10.1109/ICESIP46348.2019.8938242

[50]J. M. L. Fonseca, G. Sambandam Kulothungan, K. Raj, K. A. Rajashekara, "Novel State of Charge Dependent Equivalent Circuit Model Parameter Offline Estimation for Lithium-ion Batteries in Grid Energy Storage Applications," in Proceedings of the 2020 IEEE Industry Applications Society Annual Meeting, Detroit, MI, USA, 10–16 October, 2020, pp. 1–8, doi: 10.1109/IAS44978.2020.9334862

[51]Y. Ko, K. Cho, M. Kim, W. Choi, "A Novel Capacity Estimation Method for the Lithium Batteries Using the Enhanced Coulomb Counting Method With Kalman Filtering," *IEEE Access*, 2022., 10, 38793–38801, doi: 10.1109/ACCESS.2022.3165639

[52]F. An, J. Jiang, W. Zhang, C. Zhang, X. Fan, "State of Energy Estimation for Lithium-Ion Battery Pack via Prediction in Electric Vehicle Applications," *IEEE Trans. Veh. Technol.*, 2022, vol. 71, 184–195, Jan. 2022, doi: 10.1109/TVT.2021.3125194.

[53]P. Shrivastava, T. Kok Soon, M. Y. I. Bin Idris, S. Mekhilef, S. B. R. S. Adnan, "Combined State of Charge and state-of-energy Estimation of Lithium-Ion Battery Using Dual Forgetting Factor-Based Adaptive Extended Kalman Filter for Electric Vehicle Applications," *IEEE Trans. Veh. Technol.*, 2022, vol. 70, 1200–1215, Feb. 2021, doi: 10.1109/TVT.2021.3051655.

[54]G. L. Plett, "Extended Kalman filtering for battery management systems of LiPB-based HEV battery packs: Part 3. State and parameter estimation," *J. Power Sources*, 2004, vol. 134, 277–292

[55]M. Mastali, J. Vazquez-Arenas, R. Fraser, M. Fowler, S. Afshar, M. Stevens, "Battery state of the charge estimation using Kalman filtering" *J. Power Sources*, 2013, vol. 239, 294–307

[56]Z. Chen, Y. Fu, C. C. Mi, "State of charge estimation of lithium-ion batteries in electric drive vehicles using extended Kalman filtering," *IEEE Trans. Veh. Technol.*, 2013, vol. 62, 1020–1030

[57]G. Liu, M. Ouyang, L. Lu, J. Li, J. Hua, "A highly accurate predictive-adaptive method for lithium-ion battery remaining discharge energy prediction in electric vehicle applications," *Appl. Energy*, 2015, vol. 149, 297–314

[58]D. Ren, L. Lu, P. Shen, X. Feng, X. Han, M. Ouyang, "Battery remaining discharge energy estimation based on prediction of future operating conditions," *J. Energy Storage*, 2019, vol. 25, 100836

[59]G. Dong, X. Zhang, C. Zhang, Z. Chen, "A method for state of energy estimation of lithium-ion batteries based on neural network model," *Energy*, 2015, vol. 90, 879–888

[60]P. Singh, C. Fennie, D. Reisner, "Fuzzy logic modelling of state-of-charge and available capacity of nickel/metal hydride batteries," *J. Power Sources*, 2004, vol. 136, 322–333

[61]Y. Choi, S. Ryu, K. Park, H. Kim, "Machine Learning-Based Lithium-Ion Battery Capacity Estimation Exploiting Multi-Channel Charging Profiles," *IEEE Access*, 2019, vol. 7, 75143–75152

[62]M. Lucu, E. Martinez-Laserna, I. Gandiaga, H. Camblong, "A critical review on self-adaptive Li-ion battery ageing models," *J. Power Sources*, 2018., vol. 401, 85–101

[63]"European standard EN 15429-2, Sweepers Part 2: Performance requirements and test methods," 2012.

[64]T. L. Saaty, "The Analytic Hierarchy Process: Planning, Priority Setting, Resource Allocation," McGraw-Hill International Book Company, 1980.

[65]H. H. M. H. Alababi, "A New AHP Model for Selecting the Best Battery for a Firefighting and Rescue Boat," http://iraj.in

[66]F. B. Ammar, H. Hafsa, F. Hammami, "Analytic Hierarchy Process Selection for Batteries Storage Technologies," International Conference on Electrical Engineering and Software Applications, 2013., doi: 10.1109/ICEESA.2013.6578374

List of Figures

List of Tables

Abbreviation

CCConstant Current

CPConstant Power

CVConstant Voltage

EVElectric Vehicle

LCOLithium-Cobalt-Oxide

LFPLithium-Iron-Phosphate

LTOLithium-Titanium-Oxide

NMCLithium-Nickel-Manganese-Cobalt-Oxide

OCVOpen-Circuit Voltage

SOCState-of-Charge

SOEState-of-Energy

SOHState-of-Health

Publications

There are in total 3 journal papers and 4 presented conference paper under this thesis. All journal and conference papers are attached bellow.

Journal Papers

[J_1]H. Baši ć, V. Bobanac and H. Pandžić, "Determination of Lithium-ion Battery Capacity for Practical Applications," *Batteries* (ISSN 2313-0105), 2023, DOI: https://doi.org/10.3390/batteries9090459

[J_2]V. Bobanac, H. Baši ć and H. Pandžić, "A Method for Deriving Battery One-way Efficiencies," *Journal of Energy Storage*, 2023, DOI: https://doi.org/10.1016/j.est.2023.108815

[J_3]H. Baši ć, H. Pandžić, M. Miletić and I. Pavić, "Experimental Testing and Evaluation of Lithium-Ion Battery Cells for a Special-Purpose Electric Vacuum Sweeper Vehicle," *IEEE Access*, vol. 8, pp. 216308-216319, 2020, DOI: 10.1109/ACCESS.2020.3040206

Published and Presented

[C_5]V. Bobanac, H. Baši ć, H. Pandžić, "One-way voltaic and energy efficiency analysis for lithium-ion batteries" in *13th Mediterranean Conference on Power Generation, Transmission, Distribution and Energy Conversion (MEDPOWER 2022)*, 2022, pp. 261–266, DOI: 10.1049/icp.2023.0003

[C_6]V. Bobanac, H. Baši ć, H. Pandžić, "Determining Lithium-ion Battery One-way Energy Efficiencies: Influence of C-rate and Coulombic Losses", in *IEEE EUROCON 2021 - 19th International Conference on Smart Technologies*, 2021, pp. 385–389, DOI: 10.1109/EUROCON52738.2021.9535542

[C_7]H. Baši ć, T. Dragičević, H. Pandžić, F. Blaabjerg, "DC microgrids with energy storage systems and demand response for providing support to frequency regulation of electrical power systems", in *2017 19th European Conference on Power Electronics and Applications (EPE'17 ECCE Europe)*, 2017, pp. P.1-P.10, DOI: 10.23919/EPE17ECCEEurope.2017.8099000

[C_8]H. Baši ć, T. Dragičević, H. Pandžić, F. Blaabjerg, "DC microgrids providing frequency

regulation in electrical power system - imperfect communication issues", *2017 IEEE Second International Conference on DC Microgrids (ICDCM)*, 2017, pp. 434–439, DOI: 10.1109/ICDCM.2017.8001081

IEEE Access
Multidisciplinary ⋮ Rapid Review ⋮ Open Access Journal

Received October 7, 2020, accepted November 19, 2020, date of publication November 24, 2020,
date of current version December 11, 2020.

Digital Object Identifier 10.1109/ACCESS.2020.3040206

Experimental Testing and Evaluation of Lithium-Ion Battery Cells for a Special-Purpose Electric Vacuum Sweeper Vehicle

HRVOJE BAŠIĆ, (Graduate Student Member, IEEE), HRVOJE PANDŽIĆ, (Senior Member, IEEE), MARIJA MILETIĆ, (Graduate Student Member, IEEE), AND IVAN PAVIĆ, (Graduate Student Member, IEEE)
University of Zagreb, Faculty of Electrical Engineering and Computing, 10000 Zagreb, Croatia

Corresponding author: Hrvoje Bašić (hrvoje.basic@fer.hr)

This work was supported by the European Regional Development Fund and company RASCO, Ltd., through the Next Generation Municipal Equipment: Electric Compact Urban Vacuum Sweeper with an ICT System Project under Grant KK.01.2.1.01.0020.

ABSTRACT Battery-powered electric vehicles are gradually expanding their market outside of the typical public and private transportation sector. A good example is a growing demand for electrification of special-purpose vehicles such as compact urban vacuum sweeper trucks. These vehicles are characterized by low production numbers and specific limitations such as restricted volume for battery placement, specific working conditions, requirement to supply electro-hydraulic systems, etc. Therefore, the selection of optimal battery cell and identification of its required characteristics is not a straightforward task. This article addresses this by presenting a methodology for selecting optimal battery cell for compact urban vacuum sweepers. A laboratory testing procedure is established to measure electric and heating characteristics of candidate battery types and battery producers. After evaluation of the experimental test results using the Analytic Hierarchy Process (AHP), the most appropriate battery cell is selected. The experimental tests and the presented AHP methodology prove that battery cell selection for a specific purpose based solely on manufacturers' datasheet can result in a sub-optimal decision.

INDEX TERMS Lithium-ion batteries, experimental testing, compact urban vacuum sweeper, special-purpose electric vehicle, analytic hierarchy process.

I. ABBREVIATIONS

ACT	Adjusted Consumption Test
AHP	Analytic Hierarchy Process
DEC	Declared Energy Capacity (Wh)
EC	Energy Capacity (Wh)
ET	Energy Test
FCT	Fast Charge Test
LCO	Lithium Cobalt Oxide
LMO	Lithium Manganese Oxide
LFP	Lithium Iron Phosphate
MCC	Max Charge Current (A)
MDC	Max Discharge Currrent (A)
MTI	Maximum Temperature Increase (°C)
NCA	Lithium Nickel Cobalt Aluminum Oxide
NMC	Lithium Nickel Manganese Cobalt Oxide
SCT	Slow Charge Test
P	Price ($/Wh)

The associate editor coordinating the review of this manuscript and approving it for publication was Yongquan Sun.

II. INTRODUCTION

Electric vehicles are one of the main pillars of reducing our ecological footprint [1]. However, fully electric vehicles still have drawbacks that slow down their rollout. According to [2], the main reason for not buying an electric vehicle are high investment cost, lack of public infrastructure and lower driving range as compared to the gasoline-powered vehicles.

Research on different batteries for electric vehicles studied in [3] and [4] highlights energy density characteristics of lithium-ion batteries as a significant drawback for their application in the vehicle industry. Thus, an improvement in battery performance can greatly improve utilization characteristics and economy of electric vehicles. Battery advancements, e.g. increased energy density and decreased sensitivity to environmental temperature, make them an

attractive alternative to the existing internal combustion engine-powered vehicles.

This work focuses on electric compact urban vacuum sweeper trucks, traditionally powered by 62–75 kW Diesel engines. Electric compact municipal vacuum sweepers are characterized by a multipurpose design that enables their usage during all seasons. They can be used for cleaning and washing public municipal surfaces, spreading deicing materials and even snow ploughing. In order to meet the functionality requirements, two essential criteria must be met. First, it is necessary to provide sufficient volume for connecting the equipment and installing the necessary waste tanks, severely limiting the size of the battery. Second, the battery needs to provide enough power not only to the motor drive and the common systems in the vehicles (cooling, ventilation, air conditioning, auxiliary systems), but also to drive the electro-hydraulic systems used for cleaning the streets. A commercial example of an electric municipal vacuum cleaner can be found in [5].

A. LITERATURE REVIEW

A detailed technical and theoretical description as well as a general overview of batteries is available in [6]. Currently dominant batteries are based on lithium and this research thus focuses on lithium-based batteries. An overview of lithium-ion batteries used specifically for electric vehicles is presented in [7]. LCO, LMO, LFP and NMC battery types are presented and compared as the most promising batteries for electric vehicles. An evaluation of performance of various lithium-ion batteries for use in electric vehicle applications is presented in [8]. The authors compare and evaluate capacity and efficiency performance, charging capabilities, Butler-Volmer phenomenon (electrical current dependence on the electrode potential), thermal characteristics, cycle life and cost of NCA, LFP and NMC batteries. The study shows that NMC batteries have the highest energy density, NCA and NMC batteries have the best charging and discharging capabilities in terms of ampere-hours and the highest energy efficiency, while LFP batteries demonstrate the highest thermal stability.

Technological development and battery research is important both in the industry and the research community due to increasing applications of lithium-ion batteries in home appliances, consumer electronics, transportation, and power system industry. Technology readiness level generally starts with computer modelling and simulations, moves to hardware-in-the-loop simulations and, finally, results in experimental testing.

1) MODELING AND SIMULATION

Categorization of battery models focused on vehicular applications presented in [9] divides and summarizes them into electrochemical, stochastic, analytical and electrical-circuit models. A model suitable for simulating the behaviour of dynamic battery characteristics in Cadence-compatible simulators with the ability of predicting runtime, steady-state and transient response is presented in [10]. In [11] an accurate model of a lithium-ion battery operation in the day-ahead electricity market is presented and an impact of using a widely accepted inaccurate battery charging model on balancing costs is demonstrated. The presented model is based on laboratory testing and utilizes the state-of-energy vs. maximum energy charging capacity in one time period curve.

As information on the main battery parameters are very important, the authors in [12] present a method for establishing the available capacity, the state-of-charge and the state-of-health of a battery with unknown charging history using a two-pulse current method. The presented method applies two current pulses to a battery to stabilize its voltage and accurately estimates the main parameters of a battery within 30 seconds. A state-of-charge estimator for lithium-ion batteries based on the square-root recursive least-squares algorithm for online battery model parameter estimation extended with Kalman-Bucy filter is presented in [13]. The model alleviates problems of the ampere-hour integration (an unknown initial value of the state-of-charge) and the voltage-based (an accuracy problem of the open circuit voltage to state-of-charge relation) state-of-charge estimation methods. Accuracy of the model is demonstrated using Matlab Simulink and the presented model showed better performance compared to the traditional Coulomb counting methods. The authors in [14] present a method for state-of-health estimation with the standardized 10-second discharge resistance test. Battery's internal resistance is estimated directly using the system identification techniques based on operating data collected under normal electric vehicle operation. The method provides precise and accurate estimates of the internal resistance.

A state-of-health estimation method based on integration of the estimation effects of different health indicators and calculation of the weight coefficient of each indicator using the analytic hierarchy process is presented in [15]. The experimental life cycle tests on an NMC battery cells are performed to verify the presented method. An initial performance of the battery cells is determined using the static capacity test, resistance test, hybrid pulse test and three representative simulated driving schedule tests (federal urban driving schedule, inspection and maintenance driving schedule and dynamic stress test). The aging cycles consists of two patterns, the charging (constant current mode) and the discharging (several discharge steps with the same current excitation) pattern.

2) EXPERIMENTAL TESTING

A step toward real-life battery performance assessment is achieved by laboratory testing. The authors of [16] share a valuable experience on usage and ageing testing of lithium-based and sodium-nickel-chloride-based batteries used for providing ancillary services to the power system. The experimental results show a significant difference in degradation of batteries depending on the types of test cycles for different types of batteries. An interesting research from the vehicular technology standpoint tests lithium-ion batteries under

different temperature conditions, vibration frequencies and vibration directions [17]. NCA batteries were used in the tests and the results indicate that battery characteristics are significantly more affected by the ambient temperature than the road vibrations. Importance of an adequate and reliable management of parallel-connected lithium-ion battery cells is noted in [18], as the experimental tests showed that the management of parallel-connected lithium-ion battery cells with different levels of degradation causes further degradation of the whole battery pack. It is shown that the degraded cells in the parallel connection force the healthier cells to discharge at a higher current. The increased current and power lead to a higher polarization voltage drop and generation of more heat, which causes accelerated cell degradation.

Evaluation of LFP batteries for electric vehicle applications is presented in [19]. Five different commercial LFP batteries with different power and energy ratings were tested according to the recommendations from [20]. The following experimental procedures were conducted: commissioning (identification and weighting of the batteries), energy efficiency, specific energy (Wh/kg) and specific power (W/kg) capabilities tests at various C-rates,[1] thermodynamic tests, fast-charging tests and aging tests. The results indicate that all of the tested batteries met the short-term U.S. Advanced Consortium goals [20], while the long-term results were achieved only for energy efficiency and cycle life under standard conditions. Specific power and fast charging capability test results did not meet the goals for most of the tested cells.

Additional experimental analyses of LFP battery for electric vehicle applications are presented in [22], [23] and [24]. In [22], the results of 50 moderate charging and discharging cycle tests of an LFP battery cell at the ambient temperature of 20°C are presented and analysed. The results demonstrate less than 0.5% loss of capacity, which can be used to extrapolate to the supplyer's claimed 1000 cycles before the capacity falls to 80%. The realistic road tests were conducted at ambient temperatures of −20°C, 0°C, +20°C and +40°C. The results reveal increased capacity and power degradation at low temperatures.

Two different test benches are used in the experiments described in [23], one for the tests in the steady state, and the other one under the dynamic operation conditions. Battery electrical characteristics, capacity-temperature dependence, ageing effects and energy storage efficiency under different currents and the dynamic performance are evaluated. It is shown that the charging / discharging efficiency at 1C rate is higher than charging / discharging efficiency at currents much lower than 1C rate. Even though the value of the lost power in the internal resistance of the battery is low for lower C-rates, chemical reactions inside the battery are slower because of the material deterioration inside the cell.

Results of the capacity test, power capability test, open-circuit voltage test and voltage hysteresis test of an LFP battery are presented and evaluated for the hybrid electric vehicle application in [24]. Evaluation of the capacity tests and power capability tests at various states of charge and temperatures indicate degradation of cell performance at low ambient temperatures. Open-circuit voltage tests reveal only small variation at different ambient temperatures.

Electric vehicle application of LCO cells is evaluated in [25], where the results of cycling and loading tests are presented. The results demonstrate that cells perform well according to the manufacturer's specifications at ambient temperatures above 0°C in both Ah and Wh capacity, but a depression of capacity is revealed at temperatures lower than 0°C.

In [26], the authors conduct an experimental performance analysis of the lithium-polymer battery cell. Battery cell capacity, battery energy efficiency, temperature effects on performance of batteries, self-discharge, fast charging ability and realistic load tests were all conducted and analysed. It is determined that the resulting battery efficiency is over 96% at temperatures between +20°C and +40°C. The temperature test shows that the battery performs well at temperatures between 0°C and +40°C, but its efficiency and capacity decrease at temperatures below 0°C. The battery self-discharge is less than 5% per month. Results from the fast charging ability and realistic load tests are close to the values of the long-term United States Advanced Battery Consortium goals [20].

A concise overview of the performed literature review is provided in Table 1 for a quick reference. It indicates that a comprehensive comparison of the testing results of different lithium-ion batteries has not yet been performed in the literature.

TABLE 1. Literature overview.

Review	[6], [7], [8]
Modelling and simulation	[9], [10], [13]
Modelling based on experimental testing	[11], [12], [14], [15]
Experimental testing and evaluation of one batteries	[16], [17], [18], [19], [22], [23], [24], [25], [26]

B. SCOPE OF WORK AND CONTRIBUTION

In this work, we conduct performance tests on different battery cells with the aim of determining the optimal battery cell for usage in a special-purpose vehicle, i.e. electric compact urban vacuum sweeper. The tests are conducted according to the European standard EN 15429-2 [27] and additional rigorous tests are designed according to the specific performance requirements on the sweeper. Hence, the contribution of this article is twofold:

- First, the design of a methodology for evaluation of battery cells for an electric compact urban vacuum sweeper.

[1] Battery capacity rated at 1C means that a fully charged battery rated at 1 Ah should provide 1 A for one hour [21].

TABLE 2. Battery cells characteristics as declared by the manufacturers.

Internal mark of the cell	Type	Nominal cell voltage (V)	Max charging current of the cell (A)	Max discharging current of the cell (A)	Capacity of the cell C_{cell} (mAh)	Energy of the cell E_{cell} (Wh)	Cell price ($/Wh)
Cell 01	LCO	3.65	4.00	25.00	2000	7.30	0.60
Cell 02	LCO	3.75	2.17	4.65	3100	11.63	0.26
Cell 03	LCO	3.7	3.20	6.40	3200	11.84	0.33
Cell 04	NCA	3.6	1.60	20.48	3200	12.24	0.40
Cell 05	NCA	3.6	1.45	29.00	2900	10.73	0.43
Cell 06	LMO	3.7	3.99	25.00	3000	11.10	0.54
Cell 07	LMO	3.6	4.00	20.00	2600	9.36	0.45
Cell 08	LMO	3.6	4.00	10.00	3130	11.27	0.53
Cell 09	LFP	3.2	1.50	10.00	1500	4.80	0.86
Cell 10	NMC	3.7	3.40	10.00	3500	12.72	0.33
Cell 11	NMC	3.6	4.00	20.00	2500	9.00	0.44
Cell 12	NMC	3.6	4.00	22.00	2000	7.20	0.69
Cell 13	NMC	3.6	4.00	20.00	3000	10.80	0.55
Cell 14	NMC	3.6	2.45	5.00	3500	12.60	0.48
Cell 15	NMC	3.6	2.00	8.00	3350	12.06	0.41
Cell 16	NMC	3.7	3.10	10.00	3200	11.84	0.42

- Second, the experimental testing and categorization of different lithium-ion battery cells using the Analytic Hierarchy Process.

It is important to note that, as will be shown in this work, evaluation of the battery cell characteristics based merely on technical characteristics given by the manufacturers can result in sub-optimal battery cell selection. However, the analysis of experimental results resolves that problem and identifies the optimal battery cell for a given purpose.

The rest of this article is structured as follows. Section III describes the experimental equipment used in this research and the battery cells that were tested and evaluated. This section also elaborates the AHP algorithm used for evaluation of battery cells' characteristics and experimental testing results. Four experimental tests conducted on each battery cell are described in Section IV. Presentation and analysis of the results of experimental tests is presented in Section V. In Section VI the tested battery cells were evaluated and the optimal battery cell was identified using the AHP. Finally, a brief overview of this article and most relevant conclusions are provided in Section VII.

III. DESCRIPTION OF THE EXPERIMENTAL TESTBED

A. TESTED BATTERY CELLS

Table 2 lists the tested lithium-ion battery cells and presents their basic characteristics (nominal voltage, maximum charge and discharge current, capacity and energy). All tested cells are 18650-type, i.e. cylindrical with 18 mm diameter and 65 mm height, and they are shown in Figure 1. Energy capacity is measured on five battery cells of each type to ensure a valid representation of each type of the battery cell. They are all available for purchase in bulk quantities, which is essential for their installation in commercial vehicles. However, producers' names and cell models are intentionally not disclosed.

Cell 01 is based on LCO and has low energy capacity compared to the other tested cells, so the expectations of the energy tests for this cell are low. On the positive side,

FIGURE 1. Tested lithium-ion cells.

it has an above-average maximum discharging current, 25 A. As opposed to Cell 01, Cells 02 and 03 have rather high energy capacity, 11.84 Wh, but the maximum discharging current is quite low, which could result in poor performance at high loads. NCA Cells 04 and 05 have similar technical characteristics as the LCO battery. LMO Cells 06, 07 and 08 have the ability to withstand high discharge currents, while the cells themselves have high energy capacity. According to the technical characteristics, above-average results are expected in both energy and heating test results. LFP Cell 09, according to technical documentation of the manufacturer, have high maximum allowed current and long cycle life, but low energy capacity. Thus, good heating characteristics and specific charging and discharging results, but poor energy test results, are expected. NMC cells (Cells 10, 14, 15 and 16) with high energy capacity and high maximum allowed charging/discharging current should yield good results in both the heating and the energy tests. Cells 11, 12 and 13 with lower energy capacity are not expected to perform well in energy tests, but their heating characteristics should be good.

B. PRELIMINARY EVALUATION OF THE TESTED BATTERIES

The preliminary evaluation of the tested batteries is based on analysis of technical data provided by the manufacturers. Analytic Hierarchy Process (AHP) [28]–[30] is used to

determine the optimal battery cell based on the criteria available in all manufacturers' data: declared energy capacity, maximum discharge current, maximum charge current and price.

The algorithm used to calculate AHP is shown in Algorithm1, where:

- PWC is Pair-Wise Comparison,
- C is Criteria,
- A is Alternative,
- PCM is Pair-Wise comparison Matrix,
- CM is Comparison Matrix,
- SR is Sum of Rows of comparison matrix,
- CSR is Column vector containing the Sum of each Row of comparison matrix,
- SAE is Sum of All Elements of SR,
- PV is Priority Vector,
- CI is Consistency Index,
- RCI is Random Consistency Index,
- CR is Consistency Ratio,
- CV is Comparison Vector and
- CWAC is Composite Weight of each Alternative Choice.

Relative pair-wise comparisons on scale 1 to 9 are:

- Maximum Discharge Current (MDC) is 2 time as important as Maximum Charge Current (MCC),
- Declared Energy Capacity (DEC) is 6 time as important as maximum charge current (MCC),
- Declared Energy Capacity (DEC) is 4 time as important as maximum discharge current (MDC),
- Price (P) is 2 time as important as maximum discharge current (MDC),
- Price (P) is 3 time as important as maximum charge current (MCC),
- Declared Energy Capacity (DEC) is 2 time as important as price (P).

TABLE 3. Criteria pair-wise comparison matrix and priority vector based on technical data.

	DEC	MCC	MDC	P	The priority vector
DEC	1.00	6.00	4.00	2.00	**0.51**
MCC	0.17	1.00	0.50	0.33	**0.09**
MDC	0.25	2.00	1.00	0.50	**0.13**
P	0.50	3.00	2.00	1.00	**0.27**

The criteria pair-wise comparison matrix and the priority vector (normalized eigen vector of the criteria matrix) are shown in Table3. According to the procedure described in Algorithm1, the consistency index is 0.0344 and the random consistency is 0.9. Thus, the consistency ratio is 0.0382, which is lower than 10%, indicating acceptable inconsistency [28]. Comparison vectors, i.e. normalized values from the technical data from Table 2, and overall results (CWAC column) are shown in Table 4. The overall results of the AHP presented in Table 4 are shown in Figure 2, where Cell 10 is chosen as the optimal battery cell according to the declared technical data.

TABLE 4. Comparison vectors and overall results (CWAC column) based on technical data.

Internal mark of the cell	DEC	MCC	MDC	P	CWAC
Cell 01	0.044	0.082	0.083	0.0655	**0.058**
Cell 02	0.070	0.044	0.019	0.0955	**0.068**
Cell 03	0.071	0.065	0.027	0.0734	**0.066**
Cell 04	0.070	0.033	0.085	0.0622	**0.066**
Cell 05	0.063	0.030	0.121	0.0638	**0.068**
Cell 06	0.067	0.082	0.104	0.0477	**0.068**
Cell 07	0.056	0.082	0.083	0.0678	**0.065**
Cell 08	0.068	0.082	0.042	0.0478	**0.061**
Cell 09	0.029	0.031	0.042	0.0694	**0.042**
Cell 10	0.078	0.070	0.042	0.0678	**0.070**
Cell 11	0.054	0.082	0.083	0.0716	**0.065**
Cell 12	0.043	0.082	0.091	0.0573	**0.057**
Cell 13	0.065	0.082	0.083	0.0478	**0.064**
Cell 14	0.076	0.050	0.021	0.0477	**0.059**
Cell 15	0.073	0.041	0.033	0.0573	**0.061**
Cell 16	0.071	0.063	0.042	0.0573	**0.063**

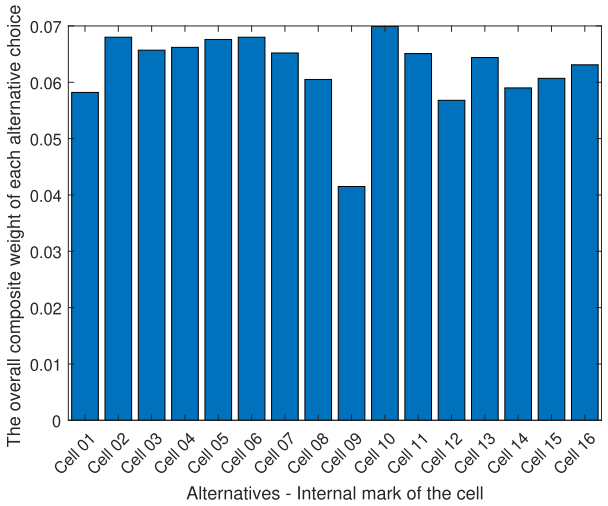

FIGURE 2. Overall results of the AHP based on technical data.

C. DESCRIPTION OF THE LABORATORY TESTING EQUIPMENT

An advanced custom-made grid-tied bidirectional AC-DC converter (description available in [11]) is used for testing the batteries and measuring of input / output currents and voltages. Nominal output power of the converter is 1 kW, output DC voltage range is from 0 to 20 V, and the output DC current is limited to 50 A in both directions. The converter is controlled over a supervisory control and data acquisition system developed in National Instruments LabVIEW and controlled over a National Instruments cRIO. The testbed also contains a temperature sensor PT100-1020 with temperature range from −70°C to +500°C and temperature coefficient 3850 ppm/°C, which is used for measurement of temperature on the surface of the battery cells. Temperature chamber KMH-408, with temperature range −40°C to +150°C,

Algorithm 1 Analytic Hierarchy Process

Input: C1, C2, . . . , Cn ⇒enter Criteria
Input: A1, A2, . . . , Am ⇒enter Alternatives (battery cells)
for $i \leftarrow 1$ to $length(C)$ **do** ⇒create Relative Importance Pair-wise Comparisons Matrix
  for $j \leftarrow 1$ to $length(C)$ **do Input:** $PWC_{i,j}$
  end for
end for
$CM \leftarrow PCM$
$i \leftarrow 1$ ⇒initialize counter for while loop
while $tolerance > acceptable\_value$ **do** ⇒calculate Normalized Eigen Vector of the Criteria Matrix
  $i \leftarrow i + 1$
  $CM \leftarrow CM \times PCM$
  $CSR \leftarrow sum\_of\_each\_row\_of\_CM$
  $SAE \leftarrow the\_sum\_of\_all\_elements\_of\_SR$
  $tolerance \leftarrow SR(i) \div CSR(i) - SR(i-1) \div CSR(i-1)$
end while
  $PV \leftarrow SR(i) \div CSR(i)$ ⇒calculate Priority Vector
for $i \leftarrow 1$ to $length(C)$ **do**
  $\lambda_{max} \leftarrow SAE + CM(i) + \lambda_{max}$
end for
$CI \leftarrow (\lambda_{max} - length(C)) \div (length(C) - 1)$ ⇒calculate Consistency Index
switch $length(A)$ **do** ⇒define Random Consistency Index
  cases 2 $RCI \leftarrow 0$
  cases 3 $RCI \leftarrow 0.58$
  cases 4 $RCI \leftarrow 0.90$
  cases 5 $RCI \leftarrow 1.12$
  cases 6 $RCI \leftarrow 1.24$
  cases 7 $RCI \leftarrow 1.32$
  cases 8 $RCI \leftarrow 1.41$
  cases 9 $RCI \leftarrow 1.45$
  cases 10 $RCI \leftarrow 1.49$
  cases 11 $RCI \leftarrow 1.51$
  $CR \leftarrow (CI/RCI)$ ⇒calculate Random Consistency Ratio
if $CR \leq 10\%$ **then**
  The inconsistency is acceptable ⇒evaluate Inconsistency
else
  The inconsistency is not acceptable
end if
for $i \leftarrow 1$ to $length(CV)$ **do**
  for $j \leftarrow 1$ to $length(A)$ **do Input:** CV(i,j) ⇒enter Comparison Vectors
  end for
end for
$CWAC \leftarrow PV \times CV$ ⇒calculate Composite Weight of Alternative Choices
$The\_best\_result\_location \leftarrow location(max(CWAC))$ ⇒location of Best Alternative (Optimal Battery Cell)

temperature uniformity ±2°C, humidity range from 20% to 98% relative humidity (RH) and humidity uniformity +/−3% RH, is used for creating specific testing environment. The laboratory testing equipment is shown in Figures 3 and 4.

IV. DESCRIPTION OF EXPERIMENTAL TESTS

The designed battery pack to power a compact urban vacuum sweeper consist of a series of four identical segments, each made of a series of six modules (60 parallels of 4 cells in series). Overall, 5760 cells are connected in the battery pack. Nominal voltage of the pack is around 350 V, while the energy capacity ranges between 42 and 73 kWh, depending on the chosen battery cell.

All tests are conducted with the uniform initial nominal characteristics of the battery cells (charged to 100% state-of-charge with the same charging power and the same ambient conditions), and on the identical testbed (efficiency of the system and the measurement accuracy are consistent) in order

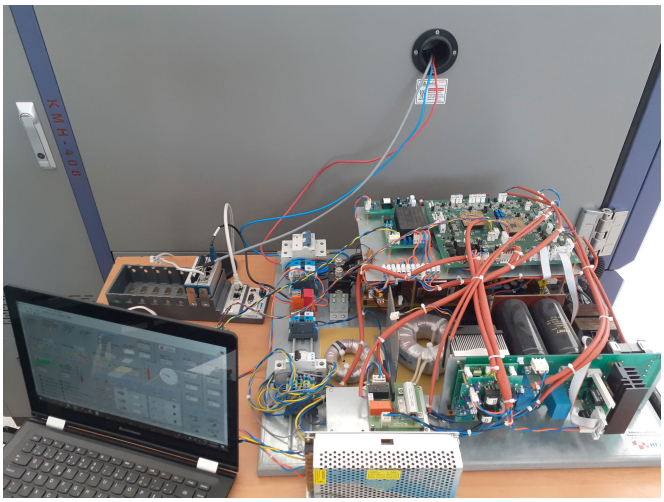

FIGURE 3. Bidirectional converter used for battery cell testing.

FIGURE 4. Temperature chamber used to set the environmental conditions.

to make the results comparable. Prior to the tests, each cell had been inactive for at least five hours.

Charging/discharging current of one cell depends on the relation of the required power for one cell and its nominal power:

$$I_{cell} = \frac{P_{bp}}{5760} \cdot \frac{C_{cell}}{E_{cell}} \tag{1}$$

where P_{bp} (W) is the charging / discharging power of the battery pack, E_{cell} (Wh) the nominal energy capacity of a cell, and C_{cell} (Ah) the capacity of a cell.

Since the energy capacity is one of the most important criteria for evaluation, an energy test is conducted to identify the capacity of each cell at high power conditions. Energy capacity in standard operating conditions of the compact urban vacuum sweeper is tested by performing the adjusted consumption test cycle. In order to evaluate the charging characteristics, two different charging tests (constant current/constant voltage mode) are conducted. One with low power, to represent slow charging during the night, and the other with higher power to resemble the charging between the shifts during the day. Therefore, each battery cell was subject to the four tests presented in the following subsections.

A. ENERGY TEST

This test discharges battery cells with constant high power at almost 1C rate, which is the highest expected current during the highest consumption of the compact urban vacuum sweeper. The test is conducted on fully charged battery cells according to the manufacturers' data sheets. The energy of a battery cell is measured simulating the sweeping mode at operating speed 5 km/h and 30% road slope. Calculated discharging power of one battery cell is $P_{cell} = 8.829$ W (discharging power of the battery pack $P_{bp} = 50.86$ kW).

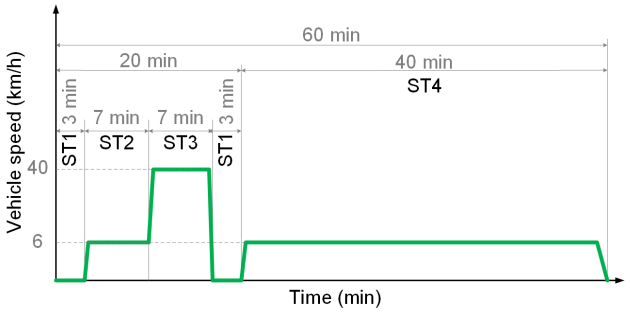

FIGURE 5. Adjusted consumption test.

B. ADJUSTED CONSUMPTION TEST

This experiment is conducted according to the sub-tests defined in standard EN 15249 with few adjustments, as shown in Figure5. The test is repeated until the battery cell voltage reaches the discharge limit normalized for the tested battery cells. Battery cells remain inactive for 10 minutes between test cycles to reduce possible unrested battery effects [31]. The following sub-tests are conducted:

- Sub-test 1 (ST1): Propulsion prime mover at idle speed. Calculated power of one battery cell P_{cell}=0 W (power of the battery pack P_{bp}=0 kW).
- Sub-test 2 (ST2): 50% of the maximum operating speed, not exceeding 6 km/h. Calculated discharge power P_{cell}=4.78 W (discharge power P_{bp}=27.52 kW).
- Sub-test 3 (ST3): Maximum travel speed, not exceeding 40 km/h. Calculated discharging power P_{cell}=7.31 W (discharge power P_{bp}=42.09 kW).
- Sub-test 4 (ST4): 50% of the maximum operating speed, not exceeding 6 km/h. Calculated discharge power P_{cell}=4.78 W (discharge power P_{bp}=27.52 kW).

C. CHARGING AT 0.4C

Charging test at 0.4C is conducted after a full discharge in the Energy Test or Adjusted Consumption Test. The calculated charging power is P_{cell}=3.82 W, which is close to 0.4C (battery pack charging at constant power P_{bp}=22 kW).

D. CHARGING AT 0.2C

This charging test is also conducted after a full discharge in the Energy Test or Adjusted Consumption Test. The calculated charging power is P_{cell}=1.91 W or approximately 0.2C (battery pack charging at constant power P_{bp}=11 kW).

V. ANALYSIS OF THE EXPERIMENTAL RESULTS

Measurements of current, voltage, temperature on the cell surface and time were conducted in all experimental tests, and the results were logged with a 1-second resolution. Based on the measured results, energy in Wh and energy capacity in Ah (Coulomb counting method) were calculated. As a result, state-of-charge and state-of-energy [11] can be expressed in percentages for every second of the conducted tests. In the electric vehicle industry, energy expressed in Wh is more convenient as the power of vehicles is expressed in W. Therefore, in this work the results related to energy are expressed in Wh and calculations of state-of-energy are used. Based on the measured temperature at the battery cell surface and the controlled temperature in the temperature chamber, a specific maximum temperature increase on the surface of a battery cell is calculated and expressed in °C/Wh in all tests.

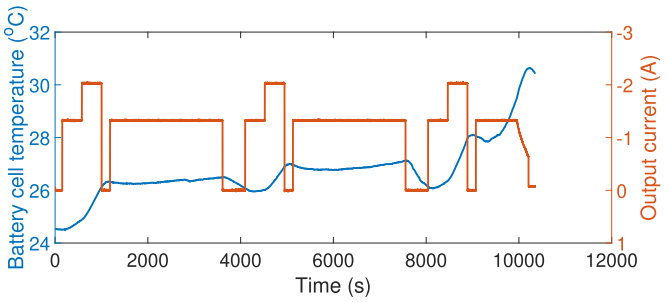

FIGURE 6. Thermal characteristic during the Adjusted Consumption Test of Cell 04.

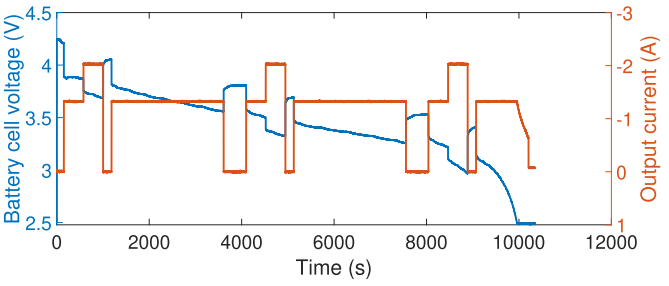

FIGURE 7. Discharging current-voltage characteristic during the Adjusted Consumption Test of Cell 04.

Examples of logged measurements for Cell 04 tests are presented in Figures6and7to visualize the conducted tests. Thermal characteristic in the Adjusted Consumption Test shown in Figure 6 illustrates a temperature increase at low values of state-of-energy, i.e. high depth-of-discharge, of the tested cell (right-hand side of the cell discharge curve). This is due to higher stress levels induced in the electrodes because of a high mechanical expansion and contraction at high depth-of-discharge. The effects of battery resting can be noticed in Figure7, which shows the discharging current-voltage characteristic of the Adjusted Consumption Test. Every interval with zero output current results in increased battery cell voltage. The magnitude of this phenomenon depends on the cell voltage at the end of the discharging period and the battery state-of-charge.

TABLE 5. Results of the Energy Test.

Internal mark of the cell	Discharging time (h)	Energy (Wh)	Specific discharged energy (Wh/h)	Maximum temperature increase (°C)	Specific maximum temperature increase (°C/Wh)
Cell 01	0.70	5.58	7.97	7.80	1.40
Cell 02	1.37	10.61	7.75	16.37	1.54
Cell 03	1.16	9.19	7.92	17.52	1.91
Cell 04	1.35	11.14	8.25	12.44	1.12
Cell 05	1.13	8.79	7.78	11.27	1.28
Cell 06	0.82	4.48	5.46	8.19	1.83
Cell 07	1.05	8.64	8.23	7.69	0.89
Cell 08	1.26	10.43	8.28	9.43	0.90
Cell 09	0.54	4.21	7.80	9.43	2.24
Cell 10	1.24	9.96	8.03	10.86	1.09
Cell 11	0.98	8.21	**8.40**	**7.41**	0.90
Cell 12	0.80	6.38	7.98	10.70	1.68
Cell 13	1.11	8.92	8.04	10.16	1.14
Cell 14	1.42	**11.40**	8.03	7.61	**0.67**
Cell 15	**1.47**	10.65	7.24	11.26	1.06
Cell 16	1.41	10.35	7.34	11.58	1.12

TABLE 6. Results of the adjusted consumption test.

Internal mark of the cell	Discharging time (h)	Energy (Wh)	Specific discharged energy (Wh/h)	Number of test cycles	Maximum temperature increase (°C)	Specific maximum temperature increase (°C/Wh)
Cell 01	1.58	6.31	4.01	1.35	3.50	0.55
Cell 02	2.85	10.82	3.80	2.44	3.50	**0.32**
Cell 03	2.62	10.16	3.88	2.25	10.43	1.03
Cell 04	2.80	11.72	**4.19**	2.40	5.53	0.47
Cell 05	2.47	9.72	3.94	2.12	5.20	0.53
Cell 06	1.92	7.15	3.73	1.64	**2.85**	0.40
Cell 07	2.34	8.86	3.79	2.01	3.34	0.38
Cell 08	2.64	10.80	4.09	2.26	4.47	0.41
Cell 09	1.06	4.29	4.05	0.91	3.47	0.81
Cell 10	2.74	10.69	3.90	2.35	7.12	0.67
Cell 11	1.96	8.13	4.15	1.68	4.39	0.54
Cell 12	1.66	6.58	3.96	1.42	6.62	1.01
Cell 13	2.54	9.99	3.93	2.18	5.68	0.57
Cell 14	2.97	**11.80**	3.97	2.55	4.80	0.41
Cell 15	**2.99**	11.56	3.87	**2.56**	6.43	0.56
Cell 16	2.90	10.63	3.67	2.49	5.55	0.52

Tables5–8show the results of each of the four experimental tests. To make them easier to read, the results above average are highlighted with grey background, while the best result is also in bold font. The results in the tables cover time, energy, specific energy, maximum increase in the temperature during the test and specific increase in the temperature during the test. Due to the nature of the tests, Tables5and 6 show cell discharging time and discharged

TABLE 7. Charging at 0.2C test results.

Internal mark of the cell	Charging time (h)	Energy (Wh)	Specific charged energy (Wh/h)	Maximum temperature increase (°C)	Specific maximum temperature increase (°C/Wh)
Cell 01	3.49	5.22	1.50	1.84	0.35
Cell 02	5.26	9.17	1.74	1.54	0.17
Cell 03	4.06	6.32	1.56	2.21	0.35
Cell 04	5.16	9.68	**1.88**	1.24	0.13
Cell 05	5.09	7.93	1.56	1.42	0.18
Cell 06	4.27	6.34	1.48	1.05	0.17
Cell 07	4.38	7.5	1.71	**0.52**	**0.07**
Cell 08	5.88	8.91	1.52	0.86	0.10
Cell 09	**2.36**	4.04	1.71	1.58	0.39
Cell 10	5.72	8.96	1.57	2.13	0.24
Cell 11	4.42	7.43	1.68	1.91	0.26
Cell 12	4.06	6.02	1.48	0.93	0.15
Cell 13	6.48	9.39	1.45	2.49	0.27
Cell 14	6.11	9.82	1.61	1.08	0.11
Cell 15	6.62	**9.89**	1.49	1.66	0.17
Cell 16	5.06	8.1	1.60	2.24	0.28

TABLE 8. Charging at 0.4C test results.

Internal mark of the cell	Charging time (h)	Energy (Wh)	Specific charged energy (Wh/h)	Maximum temperature increase (°C)	Specific maximum temperature increase (°C/Wh)
Cell 01	2.33	5.24	2.25	3.77	0.72
Cell 02	3.75	9.74	2.60	3.13	0.32
Cell 03	3.76	9.52	2.53	4.92	0.52
Cell 04	3.77	10.5	2.79	3.09	0.29
Cell 05	3.12	8.07	2.59	3.51	0.43
Cell 06	2.84	6.49	2.29	1.96	0.30
Cell 07	2.39	7.53	**3.15**	2.99	0.40
Cell 08	3.70	9.37	2.53	2.98	0.32
Cell 09	**1.35**	4.08	3.02	3.29	0.81
Cell 10	5.47	**11.52**	2.11	4.11	0.36
Cell 11	2.49	7.81	3.14	**0.96**	**0.12**
Cell 12	2.66	6.37	2.39	4.44	0.70
Cell 13	3.85	9.09	2.36	3.86	0.42
Cell 14	3.97	10.26	2.58	2.96	0.29
Cell 15	3.36	8.50	2.53	4.5	0.53
Cell 16	4.47	9.42	2.11	4.49	0.48

energy, while Tables7and 8 contain data on the charging time and charged energy. Temperature measurement results are presented and evaluated because safety aspects [32] and preservation of state-of-health of a battery [33] highly depend on its heating characteristics.

Energy Test results in Table 5 indicate that the highest discharging times and discharged energy are achieved for the battery cells with highest capacity (see Table 2). Cell 15 takes the longest to discharge (1.47 h), followed by Cells 14, 16 and 04. These cells have the highest amount of discharged energy as well. Best score in the amount of discharged energy is achieved by Cell 14 (11.40 Wh). However, when this is scaled to the battery cell capacity from Table 2, the highest specific discharged energy is achieved by Cell 11 due to its lower cell capacity (2500 mAh). Cell 11 has the lowest temperature increase during the test as well. However, when scaled to the cell capacity, the lowest specific temperature increase is achieved by Cell 14. Based on the results of this test, the best performance is obtained by NMC Cells 11 and 14. Cell 11 is characterized by low capacity, but high specific discharged energy and low temperature increase, while Cell 14 is characterized by high capacity, high discharge time and energy and low specific temperature increase. However, it is important to note that the only cell, besides Cell 14, that has above-average results in all the categories is an LMO-based Cell 08.

To further examine the results of the Energy Test, output current and temperatures of Cells 01, 02, 10 and 14 are visualized in Figure 8. One can observe that the discharging time of Cell 01 is 50% shorter than the one of Cell 14. Cell 14 also has very low temperature increase compared to the other three cells in the graph. The highest temperature increase is observed for Cell 02.

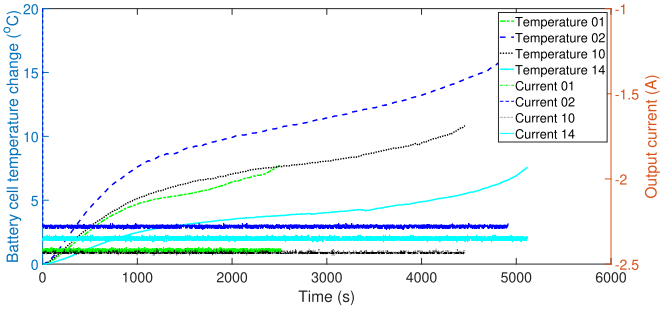

FIGURE 8. Output current and temperature increase during the Energy Test for Cells 01, 02, 10 and 14.

Results of the Adjusted Consumption Test in Table6are quite similar to the Energy Test results in Table 5. Again, the only two cells with above-average results in all categories are Cell 08 and Cell 14. Furthermore, the longest discharging time is again achieved by Cell 15 and the highest amount of discharged energy by Cell 14. However, the highest specific discharged energy is achieved for Cell 04, which performed extremely well in this category in the Energy Test as well. The highest number of cycles is achieved by Cell 15, which has the second highest nominal energy capacity (3350 mAh). The lowest temperature increase during the Adjusted Consumption Test is achieved by Cell 06, while the lowest specific temperature increase is gained by Cell 02. Overall, Cell 15 completed this test with the highest score in two categories, while performance of Cell 11 not as great as in the Energy Test.

To further evaluate the differences between specific cells, output current and temperature increase data during the Adjusted Consumption Test are presented in Figure 9. Discharging power in this test is lower than in the Energy Test so the resulting temperature increases in Figure 9 are much lower than those in Figure 8. Although at the beginning of the test the temperature of Cell 02 harshly increases, the worst result overall is achieved by Cell 10. Observing closely the temperature curve of Cell 02, and combining it with extremely poor results in the high-power

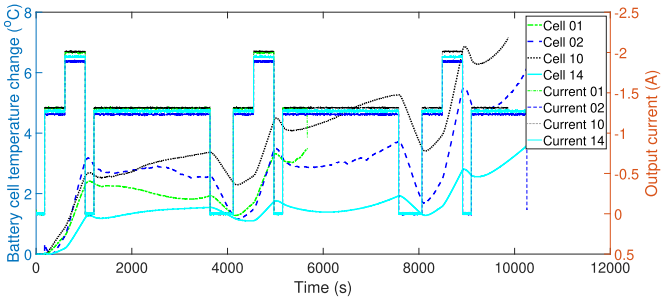

FIGURE 9. Output current and temperature increase during the Adjusted Consumption Test for Cells 01, 02, 10 and 14.

Energy Test, the conclusion is that Cell 02 suffers from extremely high temperature increase under high output currents (above 1.5 A), while at lower currents this increase is not as dramatic.

Tables7and 8 show the results for 0.2C and 0.4C charging tests. The shortest charging time is achieved for Cell 09 due to its very low nominal capacity (1500 mAh). The shortest charging time of high-capacity cells is achieved for Cell 03, whose nominal capacity is 3200 mAh and it charges at 0.2C within 4.06 hours. The highest amount of energy during the 0.2C charging test is injected in Cells 13, 14 and 15. However, this process takes over 6 hours. On the other hand, Cell 04 requires only 5.16 hours to charge 9.68 Wh. Cell 04 thus performs the best when observing specific charged energy. By far the lowest temperature increase is obtained for Cell 07.

Very similar results are achieved for the final test where cells are charged at 0.4C (Table 8). Cell 09 is again quickest to charge. However, the most energy is charged in Cell 10, but Cells 13, 14 and 15 perform above-average as well. The highest specific charged energy is achieved for Cell 07. As opposed to the 0.2C charging test, where it performs below-average, Cell 11 in the 0.4C charging test gains the lowest temperature increase.

VI. CHOOSING THE OPTIMAL CELL

Not all the conducted tests are equally important for application in compact urban vacuum sweepers, where the Energy Test and Adjusted Consumption Test play a key input in deciding on the optimal battery cell. On the other hand, the charging tests at 0.2C and 0.4C are used as control tests where a cell can fail only if the achieved results are well below an average. Therefore, the AHP is used to compare the results of the conducted tests and to choose the optimal battery cell for an urban compact vacuum sweeper. The criteria used for comparison are measured energy capacity and temperature increase in the four conducted tests, i.e. the Energy Test, Adjusted Consumption Test, and two charging tests. Relative importance's of pairwise comparisons are:

- adjusted consumption test (ACT) is 2 times as important as energy test (ET),
- energy test is 3 times as important as slow charge test (SCT),
- energy test is 4 times as important as fast charge test (FCT),

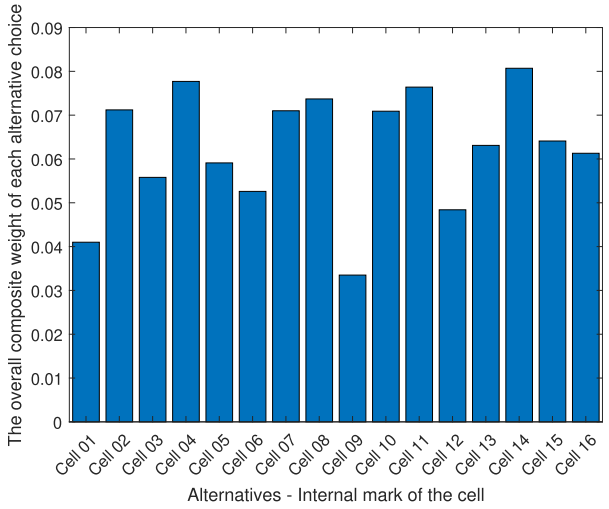

FIGURE 10. Overall results of AHP (Experimental Testing).

- adjusted consumption test is 3.5 times as important as slow charge test,
- adjusted consumption test is 4.5 times as important as fast charge test,
- slow charge test is 2 times as important as fast charge test,
- slow charge test is 2 times as important as fast charge test,
- measured energy capacity (MEC) is 2 times as important as measured temperature increase (MTI),
- energy test, measured energy capacity is 2 times as important as price (P),
- energy test, measured temperature increase is 1 times as important as price,
- adjusted consumption test, measured energy capacity is 3 times as important as price,
- adjusted consumption test, measured temperature increase is 1.5 times as important as price,
- slow charge, energy test is 1 times as important as price,
- price is 2 times as important as slow charge, measured temperature increase,
- fast charge, measured energy capacity is 1 times as important as price,
- price is 2 times as important as fast charge, measured temperature increase.

The criteria pair-wise comparison matrix and the priority vector of AHP analysis of the experimental results are shown in Table9. According to the procedure in Algorithm1, the consistency index is 0.0209 and the random consistency is 1.45, resulting in the consistency ratio 0.0144, which is lower than 10% (inconsistency is acceptable). Comparison vectors, i.e. normalized values from the experimental results presented in Tables5,6,7and8, are shown in Table10.

A. OUTCOMES OF THE AHP

The overall results of the AHP analysis of the tested battery cells are presented in Table 10 and shown in Figure 10.

TABLE 9. Criteria pair-wise comparison matrix and the priority vector based on experimental testing.

	ET,MEC	ET,MTI	ACT,MEC	ACT,MTI	SCT,MEC	SCT,MTI	FCT,MEC	FCT,MTI	P	The priority vector
ET,MEC	1.00	2.00	0.50	1.00	3.00	6.00	4.00	8.00	2.00	**0.191**
ET,MTI	0.50	1.00	0.25	0.50	1.50	3.00	2.00	4.00	1.00	**0.096**
ACT,MEC	2.00	4.00	1.00	2.00	3.50	7.00	4.50	9.00	3.00	**0.287**
ACT,MTI	1.00	2.00	0.50	1.00	1.75	3.50	2.25	4.50	1.50	**0.144**
SCT,MEC	0.33	0.67	0.29	0.57	1.00	2.00	2.00	4.00	1.00	**0.082**
SCT,MTI	0.17	0.33	0.14	0.29	0.50	1.00	1.00	2.00	0.50	**0.041**
FCT,MEC	0.25	0.50	0.22	0.44	0.50	1.00	1.00	2.00	1.00	**0.054**
FCT,MTI	0.13	0.25	0.11	0.22	0.25	0.50	0.50	1.00	0.50	**0.027**
P	0.50	1.00	0.33	0.67	1.00	2.00	1.00	2.00	1.00	**0.080**

TABLE 10. Comparison vectors and overall results based on experimental testing.

Internal mark of the cell	SCT,MEC	SCT,MTI	FCT,MEC	FCT,MTI	ET,MEC	ET,MTI	ACT,MEC	ACT,MTI	P	CWAC
Cell 01	0.042	0.030	0.039	0.031	0.040	0.053	0.042	0.061	0.0655	**0.041**
Cell 02	0.073	0.062	0.073	0.070	0.076	0.048	0.073	0.059	0.0955	**0.071**
Cell 03	0.051	0.030	0.071	0.043	0.066	0.039	0.068	0.033	0.0734	**0.056**
Cell 04	0.078	0.082	0.079	0.076	0.080	0.066	0.079	0.072	0.0622	**0.078**
Cell 05	0.064	0.059	0.060	0.052	0.063	0.057	0.065	0.063	0.0638	**0.059**
Cell 06	0.051	0.063	0.049	0.074	0.032	0.040	0.048	0.085	0.0477	**0.053**
Cell 07	0.060	0.151	0.056	0.057	0.062	0.082	0.059	0.090	0.0678	**0.071**
Cell 08	0.071	0.109	0.070	0.071	0.075	0.081	0.072	0.082	0.0478	**0.074**
Cell 09	0.032	0.027	0.031	0.028	0.030	0.033	0.029	0.042	0.0694	**0.034**
Cell 10	0.072	0.044	0.086	0.063	0.072	0.067	0.072	0.051	0.0678	**0.071**
Cell 11	0.060	0.041	0.058	0.183	0.059	0.081	0.054	0.063	0.0716	**0.076**
Cell 12	0.048	0.068	0.048	0.032	0.046	0.044	0.044	0.034	0.0573	**0.048**
Cell 13	0.075	0.040	0.068	0.053	0.064	0.064	0.067	0.059	0.0478	**0.063**
Cell 14	0.079	0.095	0.077	0.078	0.082	0.110	0.079	0.083	0.0477	**0.081**
Cell 15	0.079	0.062	0.064	0.042	0.077	0.069	0.077	0.061	0.0573	**0.064**
Cell 16	0.065	0.038	0.071	0.047	0.074	0.066	0.071	0.065	0.0573	**0.061**

The optimal cell for the compact urban sweeper considering the results of the experimental testing is Cell 14. The main reason for this is the highest amount of discharged energy in both the Energy Test and the Adjusted Consumption Test. Also this cell exhibits very good thermal characteristics. The only below-average categories for this cell are charging times in the charging tests. However, these results have lower weight in the AHP method. Long charging times are caused by this cell's high capacity (3500 mAh). Cell 10, which was considered optimal based on the manufacturers' technical data, is only fifth best cell after the experimental testing. The main reason is that its high declared energy capacity was proven much lower in both the Energy Test and the Adjusted Consumption Test. In the Energy Test, the measured energy capacity is only 9.96 Wh, which is 13% lower than 11,40 Wh drained from Cell 14. In the Adjusted Consumption Test, Cell 10 performed slightly better, but again its 10.69 Wh capacity is significantly lower than 11.80 Wh of Cell 14. Cells 04, 08 and 11 also surpassed Cell 10 when experimental tests and AHP method is used. The main reasons for Cells 04 and 08 placing ahead of Cell 10 is their high measured energy capacity. However, Cell 11 has lower energy capacity, but shows very good thermal characteristics (it excels in the maximum temperature increase), which is sufficient for the third place in the AHP scores.

While some results are expected, e.g. charging time of Cell 09, which has the lowest capacity among the tested cells, is the shortest, some results are not as expected. For instance, the longest charging time is not achieved for cells with the highest energy capacity (Cells 10 and 14 have 3500 mAh capacity), but for Cell 15 (3350 mAh) in the 0.2C charging test and Cell 16 (3200 mAh) in the 0.4C charging test. The conducted tests also indicate that LCO battery cells have the worst characteristics when it comes to thermal ratings.

VII. CONCLUSION

The methodology for selecting an optimal lithium-ion battery cell for a compact urban vacuum sweeper presented in this article is based on analysis of the laboratory test results using the Analytic Hierarchy Process. Four experimental tests are conducted on sixteen different lithium-ion battery cells in the same ambient conditions. The proposed experimental tests were conducted under simulated real-world conditions, which is essential to verify and assess the suitability of a battery cell for a specific purpose. The conducted laboratory tests follow the European standard EN 15429-2, while the additional tests are designed according to the specific performance requirements on the sweeper. Results of the tests are evaluated and compared using the Analytic Hierarchy Process with the following criteria: measured energy capacity

in all the tests, temperature increase in all the tests and price of the battery cell. The optimal lithium-ion battery cell selected with the proposed methodology is different than the battery cell selected solely on analysis of the manufacturers' datasheets. So, although the manufacturers' datasheets contain many useful information, it is shown that an analysis based exclusively on such data may result in sub-optimal battery cell selection.

In future work, the focus of the research will be in expanding the experimental tests with different ambient testing conditions, and in developing a more complex algorithm for evaluation of a larger scope of the battery cell characteristics.

REFERENCES

[1] C. C. Chan and Y. S. Wong, "Electric vehicles charge forward," *IEEE Power Energy Mag.*, vol. 2, no. 6, pp. 24–33, Nov. 2004.
[2] V. Bobanac, H. Pandzic, and T. Capuder, "Survey on electric vehicles and battery swapping stations: Expectations of existing and future EV owners," in *Proc. IEEE Int. Energy Conf. (ENERGYCON)*. Piscataway, NJ, USA: Institute Electrical Electronics Engineers, Jun. 2018, pp. 1–6.
[3] S. M. Lukic, J. Cao, R. C. Bansal, F. Rodriguez, and A. Emadi, "Energy storage systems for automotive applications," *IEEE Trans. Ind. Electron.*, vol. 55, no. 6, pp. 2258–2267, Jun. 2008.
[4] A. F. Burke, "Batteries and ultracapacitors for electric, hybrid, and fuel cell vehicles," *Proc. IEEE*, vol. 95, no. 4, pp. 806–820, Apr. 2007.
[5] *Dulevo International*. Accessed: Nov. 20, 2020. [Online]. Available: https://www.dulevo.com/en/p/Dulevo_D.zero%C2%B2.xhtml
[6] D. Linden and T. B. Reddy, *Handbook of Batteries*. New York, NY, USA: McGraw-Hill, 2002.
[7] X. Chen, W. Shen, T. T. Vo, Z. Cao, and A. Kapoor, "An overview of lithium-ion batteries for electric vehicles," in *Proc. 10th Int. Power Energy Conf. (IPEC)*, Nov. 2012, pp. 230–235.
[8] N. Omar, B. Verbrugge, G. Mulder, P. Van den Bossche, J. Van Mierlo, M. Daowd, M. Dhaens, and S. Pauwels, "Evaluation of performance characteristics of various lithium-ion batteries for use in BEV application," in *Proc. IEEE Vehicle Power Propuls. Conf.* Lille, France: IEEE, Sep. 2010, pp. 1–6.
[9] A. Shafiei, A. Momeni, and S. S. Williamson, "Battery modeling approaches and management techniques for plug-in hybrid electric vehicles," in *Proc. IEEE Vehicle Power Propuls. Conf.*, Sep. 2011, pp. 1–5.
[10] M. Chen and G. A. Rincon-Mora, "Accurate electrical battery model capable of predicting runtime and I–V performance," *IEEE Trans. Energy Convers.*, vol. 21, no. 2, pp. 504–511, Jun. 2006.
[11] H. Pandzic and V. Bobanac, "An accurate charging model of battery energy storage," *IEEE Trans. Power Syst.*, vol. 34, no. 2, pp. 1416–1426, Mar. 2019.
[12] M. Coleman, W. G. Hurley, and C. Kwan Lee, "An improved battery characterization method using a two-pulse load test," *IEEE Trans. Energy Convers.*, vol. 23, no. 2, pp. 708–713, Jun. 2008.
[13] I. Arasaratnam, J. Tjong, and R. Ahmed, "Battery management system in the Bayesian paradigm: Part I: SOC estimation," in *Proc. IEEE Transp. Electrific. Conf. Expo (ITEC)*. Piscataway, NJ, USA: Institute Electrical Electronics Engineers, Jun. 2014, pp. 1–5.
[14] G. Giordano, V. Klass, M. Behm, G. Lindbergh, and J. Sjöberg, "Model-based lithium-ion battery resistance estimation from electric vehicle operating data," *IEEE Trans. Veh. Technol.*, vol. 67, no. 5, pp. 3720–3728, May 2018.
[15] J. Tang, Q. Liu, S. Liu, X. Xie, J. Zhou, and Z. Li, "A health monitoring method based on multiple indicators to eliminate influences of estimation dispersion for lithium-ion batteries," *IEEE Access*, vol. 7, pp. 122302–122314, 2019. [Online]. Available: https://ieeexplore.ieee.org/document/8805385/
[16] R. Benato, S. Dambone Sessa, M. Musio, F. Palone, and R. Polito, "Italian experience on electrical storage ageing for primary frequency regulation," *Energies*, vol. 11, no. 8, p. 2087, Aug. 2018.
[17] L. Zhang, Z. Mu, and X. Gao, "Coupling analysis and performance study of commercial 18650 lithium-ion batteries under conditions of temperature and vibration," *Energies*, vol. 11, no. 10, p. 2856, Oct. 2018.
[18] X. Gong, R. Xiong, and C. C. Mi, "Study of the characteristics of battery packs in electric vehicles with parallel-connected lithium-ion battery cells," *IEEE Trans. Ind. Appl.*, vol. 51, no. 2, pp. 1872–1879, Mar. 2015.
[19] D. Anseán, M. González, V. M. García, J. C. Viera, J. C. Antón, and C. Blanco, "Evaluation of $LiFePO_4$ batteries for electric vehicle applications," *IEEE Trans. Ind. Appl.*, vol. 51, no. 2, pp. 1855–1863, Mar. 2015.
[20] *Electric Vehicle Battery Test Procedures Manual, Revsion 2*, United States Adv. Battery Consortium, Southfield, MI, USA, 1996.
[21] *Battery University*. Accessed: Nov. 20, 2020. [Online]. Available: https://batteryuniversity.com
[22] F. P. Tredeau and Z. M. Salameh, "Evaluation of lithium iron phosphate batteries for electric vehicles application," in *Proc. IEEE Vehicle Power Propuls. Conf.* Dearborn, MI, USA: IEEE, Sep. 2009.
[23] A. Marongiu, A. Damiano, and M. Heuer, "Experimental analysis of lithium iron phosphate battery performances," in *Proc. IEEE Int. Symp. Ind. Electron.*, Jul. 2010, pp. 3420–3424.
[24] J. Wang, Z. Sun, and X. Wei, "Performance and characteristic research in $LiFePO_4$ battery for electric vehicle applications," in *Proc. 5th IEEE Vehicle Power Propuls. Conf. (VPPC)*, Sep. 2009, pp. 1657–1661.
[25] F. P. Tredeau, B. G. Kim, and Z. M. Salameh, "Performance evaluation of lithium cobalt cells and the suitability for use in electric vehicles," in *Proc. IEEE Vehicle Power Propuls. Conf.* Harbin, China: IEEE, Sep. 2008, pp. 1–5.
[26] B. G. Kim, F. P. Tredeau, and Z. M. Salameh, "Performance evaluation of lithium polymer batteries for use in electric vehicles," in *Proc. IEEE Vehicle Power Propuls. Conf.*, Sep. 2008, pp. 1–5.
[27] *Sweepers Part 2: Performance Requirements and Test Methods*, European Standard EN 15429-2, 2012.
[28] T. L. Saaty, *The Analytic Hierarchy Process: Planning, Priority Setting, Resource Allocation*. New York, NY, USA: McGraw-Hill, 1980.
[29] H. H. M. H. Alhababi. *A New AHP Model for Selecting the Best Battery for a Firefighting and Rescue Boat*. Accessed: Nov. 20, 2020. [Online]. Available: http://iraj.in
[30] F. Ben Ammar, I. H. Hafsa, and F. Hammami, "Analytic hierarchy process selection for batteries storage technologies," in *Proc. Int. Conf. Electr. Eng. Softw. Appl.*, Mar. 2013, pp. 1–6.
[31] S. Mischie. *Behavior of the Lead Acid Battery After the Rest Period*. Accessed: Nov. 20, 2020. [Online]. Available: http://www.etc.upt.ro
[32] C. J. Govar and J. A. Banner, "Safety testing of lithium ion batteries for navy devices," *IEEE Aerosp. Electron. Syst. Mag.*, vol. 18, no. 1, pp. 17–20, Jan. 2003.
[33] M. Jafari, A. Gauchia, S. Zhao, K. Zhang, and L. Gauchia, "Electric vehicle battery cycle aging evaluation in real-world daily driving and vehicle-to-grid services," *IEEE Trans. Transport. Electrific.*, vol. 4, no. 1, pp. 122–134, Mar. 2018.

HRVOJE BAŠIĆ (Graduate Student Member, IEEE) received the M.E.E. degree from the University of Zagreb, Faculty of Electrical Engineering and Computing, Croatia, in 2008, where he is currently pursuing the Ph.D. degree. His research interests include testing, evaluation, and modeling of lithium-based batteries for application in energy systems and electric vehicles.

HRVOJE PANDŽIĆ (Senior Member, IEEE) received the M.E.E. and Ph.D. degrees from the University of Zagreb, Faculty of Electrical Engineering and Computing, Zagreb, Croatia, in 2007 and 2011, respectively. From 2012 to 2014, he was a Postdoctoral Researcher with the University of Washington, Seattle, WA, USA. He is currently an Associate Professor and the Head of the Department of Energy and Power Systems at the University of Zagreb, Faculty of Electrical Engineering and Computing. His research interests include planning, operation, control, and economics of power and energy systems.

MARIJA MILETIĆ (Graduate Student Member, IEEE) received the M.E.E. degree from the University of Zagreb, Faculty of Electrical Engineering and Computing, Croatia, in 2018, where she is currently pursuing the Ph.D. degree. Her research interests include planning, operation, control, and economics of power and energy systems.

IVAN PAVIĆ (Graduate Student Member, IEEE) received the M.E.E. degree from the University of Zagreb, Faculty of Electrical Engineering and Computing, Croatia, in 2014. He is currently a Senior Researcher with the University of Zagreb, Faculty of Electrical Engineering and Computing. His research interests include planning, operation, control, and economics of power and energy systems.

Journal of Energy Storage 73 (2023) 108815

Contents lists available at ScienceDirect

Journal of Energy Storage

journal homepage: www.elsevier.com/locate/est

Research papers

A method for deriving battery one-way efficiencies

V. Bobanac, H. Bašić *, H. Pandžić

University of Zagreb Faculty of Electrical Engineering and Computing, Croatia

ARTICLE INFO

Keywords:
One-way battery efficiency
Variable battery efficiency
Lithium-ion batteries
Experimental testing
Electric vehicles

ABSTRACT

Batteries are becoming an important decarbonization technology because they can act as convenient energy storage in various applications. They are often part of larger, complex systems and, in order to preserve computational tractability, battery models are usually oversimplified. Majority of such battery models ignore dependency of the charging/discharging efficiency on the charging/discharging power rate and instead use a constant efficiency over the entire range of power rates.

This paper presents a method for obtaining individual one-way charging and discharging efficiencies dependent on the charging/discharging power. The method consists of two parts. First, the roundtrip cycle efficiency is experimentally obtained for different pairs of charging and discharging power rates. Second, an optimization problem is solved to decompose the roundtrip efficiency into the charging and the discharging efficiency for different power rates, resulting in one-way (charging/discharging) efficiency characteristics. As a demonstration, we apply the obtained efficiency characteristics to an electric vehicle driving profile consisting of both charging and discharging stages under different power rates and experimentally validate the accuracy of the proposed method.

1. Introduction

1.1. Motivation

Battery storage systems are becoming an established technology in many industries, e.g. transportation and power. Although highly accurate electrochemical battery models exist in the literature, we focus on high-level models which are appropriate for integration in large-scale problems. In literature, such models almost exclusively rely on constant efficiencies, i.e. efficiency dependence on the charging and discharging power is ignored. In this paper, we utilize a laboratory testbed to measure roundtrip efficiencies of different lithium-ion battery types at different charging and discharging power rates. Next, we develop an optimization model to derive one-way charging and discharging efficiency values from the measured roundtrip efficiencies. Optimization results are used to derive one-way charging and discharging efficiency characteristics, which can be used in high-level battery models.

1.2. Literature review

Battery efficiency is an important characteristic in battery storage system modeling and simulation, as well as in real-time applications. As stated in [1], from the electrochemical point of view, it is important to account for energy efficiency already during the development of new electrode materials. An analysis at the chemistry-material level is performed in [2]. Dependence of the coulombic and voltaic efficiencies on different electrode material properties is discussed, emphasizing the importance of accounting for energy efficiency in battery materials research. Coulombic efficiency of lithium-metal batteries is explained and analyzed in [3] at a structural and material levels. This work develops a coulombic efficiency measuring protocol for both lithium-metal and lithium-ion batteries.

A large number of papers analyze batteries based on electrical measurements. A relationship between the coulombic, the voltaic and the energy efficiency is studied in [4], with findings experimentally verified on nickel–metal hydride (Ni-MH) batteries. However, only roundtrip efficiencies with constant charging/discharging currents are considered. An analysis of one-way voltaic and energy efficiency is presented in [5], where the obtained characteristics are based on experimentally determined battery open-circuit voltage (OCV) characteristics. Contribution of parasitic reactions to the coulombic inefficiency is analyzed in [6], based on high-precision experimental testing on three commercial lithium-ion technologies. The results demonstrate that parasitic reactions cause coulombic inefficiency at a reaction rate independent of the cell cycling rate. Electrochemical reactions affecting coulombic efficiency and capacity fade are analyzed in [7] using high-precision experiments. The paper focuses on identification and evaluation of various parasitic coulombic losses. In [8], roundtrip coulombic and energy

* Corresponding author.
E-mail addresses: vedran.bobanac@fer.hr (V. Bobanac), hrvoje.basic@fer.hr (H. Bašić), hrvoje.pandzic@ieee.org (H. Pandžić).

https://doi.org/10.1016/j.est.2023.108815
Received 28 February 2023; Received in revised form 11 July 2023; Accepted 22 August 2023
Available online 11 September 2023

Abbreviations

CCConstant Current
CPConstant Power
CVConstant Voltage
EVElectric Vehicle
LCOLithium-Cobalt-Oxide
LFPLithium-Iron-Phosphate
LTOLithium-Titanium-Oxide
NMCLithium-Nickel-Manganese-Cobalt-Oxide
OCVOpen-Circuit Voltage
SOCState-of-Charge
SOEState-of-Energy
SOHState-of-Health

efficiencies, as well as capacity retention are analyzed for Ni-MH batteries, based on experimental measurements of the roundtrip efficiency. What is studied in this paper is the dependence of battery efficiency on the power rate, state-of-charge and battery operation duration. Differences in the electric vehicles' battery efficiency for constant-current (CC) and constant-power (CP) modes of operation are studied in [9]. Battery capacity efficiency in this study is defined as a roundtrip efficiency dependent on the charging power rate. An interesting research with experimental measurements of physical battery characteristics is presented in [10], where the concept of energy efficiency maps is introduced. The authors calculate one-way energy efficiencies based on measurements of the irreversible heat generated during charging and discharging, with these thermodynamic quantities determined from a detailed low-level multiphysics model of lithium-ion batteries. One-way charging and discharging characteristics are obtained by measuring irreversible heat using highly expensive equipment.

Besides the publications focused on electrical measurement analyses of batteries, another stream of research relevant for our work aims at developing battery models. Invention [11] claims a time-consuming method for calibration of a battery based on roundtrip charge/discharge cycles and power/energy measurements, resulting in a map of available discharge energy which is dependent on the discharging power and state-of-energy. This method does not determine one-way charging/discharging efficiencies.

Paper [12] is an extension of the invention [11] where the environmental temperature is accounted for. However, one-way efficiencies are still not considered. Invention [13] claims the method for obtaining the remaining energy in a battery, by utilizing the normalized state-of-energy dependence on power and temperature. Again, one-way efficiencies are not determined. A state-of-energy estimation method based on the back-propagation neural network model is presented in [14]. The model is trained using a large number of the measured voltage, current, temperature and state-of-energy samples. Additionally, it is combined with a particle filter for suppression of the measurement noise. An experimental verification of the model proved its high reliability and accuracy. As the model accounts for power states with dynamic discharge currents, only the roundtrip energy efficiency is indirectly accounted for, while the one-way charging and discharging efficiency is neglected. Furthermore, the energy efficiency characteristics are not evaluated in the review of the experimental results.

A model-based joint state estimator based on an adaptive unscented Kalman filter is developed in [15] for battery state-of-energy and power capability prediction. The model considers environmental temperature and aging of the battery, while it does not evaluate efficiency.

In [16], an equivalent circuit model and a life-cycle model of a lithium-ion battery are used to develop an energy management strategy for model predictive control of hybrid electric vehicles. These models account for the effect of the power rate on the efficiency and try to minimize high-power discharges that result in high energy losses. However, the models do not distinguish between the one-way charging and discharging efficiencies. The main drawback of relying only to the roundtrip efficiency is the inability to assess the amount of energy stored in the battery and the amount of energy that can be effectively discharged, which is especially relevant when charging and discharging at various P-rates,[1] which directly affect the one-way charging and discharging efficiencies.

Battery one-way energy efficiencies can be determined from an open-circuit voltage characteristics. The OCV characteristic provides information about terminal voltage that a battery exhibits after being at rest for some time (typically few hours). OCV is state-of-charge or state-of-energy dependant so researchers typically consider OCV–SOC or OCV–SOE characteristics. In [17], the OCV-SOC characteristic is determined by subjecting a battery to a full cycle at low C-rates and then averaging the measured charging and discharging voltages. Two other, less time-consuming methods are described in [18]. They are based on periodical pausing of the charging and discharging processes. In the first method, the voltages reached during 1-minute pauses are measured and averaged over the charging and discharging processes. In the second method, exponential best-fit curves of the voltages measured during pauses are fitted and used to extrapolate the voltage steady-state values, which are again averaged over the charging and discharging processes to construct the OCV-SOC characteristic. Another, less time-consuming method, is presented in [19], where one-way energy efficiencies are determined for a pulse charging/discharging half-cycles, with reference to the OCV estimated from the voltage levels measured after 10-minute rests following each pulse. An OCV-based method for determining battery one-way energy efficiency characteristics is presented in [20], where the OCV-SOC curve is determined as described in [17], while the mathematical OCV(SOC) function is obtained by a nonlinear fit. Experiments to evaluate battery aging parameters are conducted in [21], where the authors found that a loss of active material contributes to the coulombic inefficiency. The authors established the relationship between the coulombic efficiency and the capacity degradation based on incremental capacity analysis. Lithium-ion battery efficiency degradation is evaluated in [22] based on the OCV characteristic and accelerated calendar aging tests. Optimal SOC in terms of the efficiency is determined, while two efficiency degradation models are developed and evaluated. High correlation between the capacity fade and the energy efficiency degradation is reported.

The downside of using OCV characteristics to estimate one-way energy efficiencies is the fact that only voltaic efficiency is taken into account, while the effect of coulombic efficiency is neglected, as reported in [5]. This might not pose a big problem when talking about lithium-ion batteries which have high coulombic efficiency of 99% or more [3,7,21]. However, this renders the OCV-based method inappropriate for high-precision one-way energy efficiency measurements (as the current losses are neglected), while it is not possible to use it for one-way coulombic efficiency determination.

1.3. Contribution and paper structure

The conducted literature review is summarized in Table1 for easier comparison and better understanding of this paper's claimed contribution, which is formulated as follows:

(1) Design of an experimental setup and measurement procedure to obtain battery roundtrip energy efficiencies, by using constant-power mode exclusively.

[1] P-rate is the percentage of nominal power of a battery at which it is charged or discharged. At 1P the battery (dis)charges at a rate corresponding to its nominal power (e.g. 1P for a 10 Ah battery 10 V nominal voltage is 100 W, 0.5P is 50 W, etc.).

Table 1
Overview of the related literature.

Ref.	Efficiency	Primary contribution
[1]	/	Importance of accounting for efficiency in development of battery systems
[2]	Roundtrip	Evaluation of battery characteristics for different anode and cathode materials
[3]	/	Development of the coulombic efficiency measuring protocol for lithium metal and lithium-ion batteries
[4]	Roundtrip	Relationship between coulombic, voltaic and energy efficiency for EV batteries
[5]	OCV one-way	An in-depth analysis of batteries' open-circuit voltage characteristics
[6]	Roundtrip coulombic	Identification of parasitic reactions as the dominant contributor to the coulombic inefficiency of lithium-ion batteries
[7]	/	Identification and evaluation of various parasitic coulombic losses
[8]	Roundtrip	Evaluation of battery roundtrip efficiency dependence on power rate, state-of-charge and different storage times
[9]	Roundtrip	Differences in battery efficiencies for constant current and constant power modes of operation
[10]	One-way	Determination of battery one-way energy efficiencies based on measurements of irreversible heat losses
[11]	Roundtrip	Determination of available energy with respect to discharging power and state-of-charge
[12]	Roundtrip	Determination of available energy with respect to discharging power, state-of-charge and environmental temperature
[13]	Roundtrip	Development of a method for mapping state-of-energy dependence on power and temperature
[14]	/	State-of-energy estimation based on neural network algorithm
[15]	/	Development of a model for battery state-of-energy and power capability prediction
[16]	Roundtrip	Development of an energy management strategy for model predictive control of hybrid electric vehicles' lithium-ion batteries
[17]	OCV one-way	Determination of the OCV-SOC characteristic
[18]	OCV one-way	Development of two methods for the estimation of the OCV-SOC characteristic with 1-minute rest pauses
[19]	OCV one-way	Development of a method for the estimation of the OCV-SOC characteristic with 10-minute rest pauses
[20]	OCV one-way	Determination of a nonlinear OCV(SOC) function which is used to calculate battery one-way energy efficiency characteristics
[21]	Roundtrip	Findings that loss of active material contributes to the coulombic inefficiency and formulation of the relationship between the coulombic efficiency and the capacity degradation.
[22]	OCV one-way	Development of efficiency degradation model for electric vehicles' lithium-ion batteries

(2)An optimization algorithm for obtaining one-way efficiencies based on the roundtrip efficiencies from the previous point. One-way energy efficiencies determined in this fashion account for both the voltaic and the coulombic losses, which is novel and improved as compared to the existing OCV method that neglects coulombic losses.

(3)The method consisting of the previous two points is experimentally validated using a standardized electric vehicle (EV) driving cycle. Obtained one-way energy efficiencies are used to calculate state-of-energy while accounting for variable charging/discharging power rates. A comparison is made to two other methods predominantly used in the literature: (i) the one using constant one-way energy efficiencies, and (ii) the one using OCV-based variable one-way energy efficiencies.

(4)The proposed method can also be used to obtain one-way coulombic efficiencies. To the best of the authors' knowledge, this is the first method that can be used for determining one-way coulombic efficiencies, using only the measured current as an input.

The rest of the paper is organized as follows. Section2provides a deep insight into battery efficiency, distinguishing the quantities that can be measured from the ones that can only be calculated. Section3 proposes a method for derivation of individual one-way battery efficiencies, as well as their interconnection to the one-way efficiency characteristics. In Section4the proposed method is applied to four different lithium-ion battery types, in order to obtain experimental one-way efficiency characteristics. Accuracy of the proposed method is verified by using an EV driving cycle case study in Section5. Finally, the conclusions and further work plans are summarized in Section6.

2. Lithium-ion battery efficiency

2.1. Efficiency definition

Whenever a battery is either charged or discharged, some energy is lost. These losses are associated with the battery's internal resistance of the electrodes and electrolyte, manifesting mostly as heat dissipation. Quantification of these losses is called battery efficiency. There are multiple battery efficiency types and they are all variable, since they depend on the charging/discharging conditions (C-rate,[2] P-rate,

[2] C-rate is the speed at which a battery is charged or discharged. At 1C the battery (dis)charges with the current corresponding to its Ah-rating (e.g. 1C for a 10 Ah battery is 10 A, 0.5C is 5 A, etc.).

environmental temperature etc.), as well as the battery's age, state-of-health[3] and state-of-charge[4]/state-of-energy.[5] Efficiency characteristics are different for different lithium-ion chemistries. Despite being a critical parameter, efficiency is normally not specified by the battery manufacturer, most likely because of its variability [23].

2.2. Types of efficiencies

Battery efficiency can be divided by the measured electrical quantity used to determine the efficiency: coulombic (η^{I}), voltaic (η^{U}), and energy (η^{E}) efficiency. Battery efficiency can also be divided by the direction of energy flow: charging (η^{ch}), discharging (η^{dis}), and roundtrip (η^{cycle}) efficiency.

Battery charging and discharging C-rates and P-rates can differ greatly, so using separate charging and discharging efficiencies (instead of a single roundtrip efficiency) can allow for more accurate assessment of battery's SOE (and/or SOC) in real-time, as well as more accurate prediction of energy losses when scheduling battery energy storage operation or even when sizing a battery. However, determining the charging and discharging efficiencies (one-way efficiencies) is not straightforward.

Efficiencies can be experimentally obtained by subjecting a battery to a cycle or half-cycle[6] which can be either full or partial.[7] When determining battery efficiencies, a full (half-)cycle should be started (and finished, in case of the roundtrip efficiency) with the battery either fully depleted (0% SOC) or fully charged (100% SOC). This methodology ensures a fixed starting (and finishing) point in terms of the measurable electrical quantities (terminal voltage and current). Still, SOC is normally used as a reference for determining the range of partial (half-)cycles (which can also be away from 0% and 100% SOC). For this purpose, SOC can be determined by the simplest form of coulomb counting:

$$soc(t) = soc(t-1) + \frac{100}{C} \cdot \int_{t-1}^{t} I(\tau) d\tau, \tag{2.1}$$

where $soc(t)$ is expressed in percentages, C is the cell capacity (Ah) and I is current (A), assumed positive for charging and negative for discharging. To avoid error accumulation associated with coulomb counting, it is advisable to first fully charge or discharge a battery and then go straight to the target SOC.

The existing methodologies for determining coulombic, voltaic and energy efficiencies are explained in the following subsections.

2.2.1. Coulombic efficiency

This efficiency is associated with the charge (Ah) extracted from or injected into a battery.

- Charging coulombic efficiency is a ratio of the total charge stored in the battery (C^{batt}) and the total charge injected into the battery (C^{ch}) over a partial or full charging half-cycle:

$$\eta^{ch,I} = \frac{C^{batt}}{C^{ch}}. \tag{2.2}$$

- Discharging coulombic efficiency is a ratio of the total charge extracted from the battery (C^{dis}) and the total charge stored in the battery (C^{batt}) over a partial or full discharging half-cycle:

$$\eta^{dis,I} = \frac{C^{dis}}{C^{batt}}. \tag{2.3}$$

- Roundtrip coulombic efficiency is a ratio of the total charge extracted from the battery (C^{dis}) and the total charge injected in the battery (C^{ch}) over a partial or full cycle:

$$\eta^{cycle,I} = \eta^{ch,I} \cdot \eta^{dis,I} = \frac{C^{dis}}{C^{ch}}. \tag{2.4}$$

The injected/extracted charge (Ah) is easily calculated from the measured current, as follows:

$$C^{ch} = \int_{0}^{T^{ch}} I^{ch}(\tau) d\tau, \tag{2.5}$$

$$C^{dis} = \int_{0}^{T^{dis}} I^{dis}(\tau) d\tau, \tag{2.6}$$

where I^{ch} and I^{dis} are the charging and discharging currents, while T^{ch} and T^{dis} are the charging and discharging durations. On the other hand, C^{batt} is not straightforward to determine since the internal battery processes cannot be measured (at least not by tools available to us).

2.2.2. Voltaic efficiency

Voltaic efficiency is associated with the average charging/discharging voltage. In this context, it is important to distinguish between the open-circuit voltage (U^{OC}) and the closed-circuit voltage (U^{ch}, U^{dis}). OCV is the voltage under the no load condition, while closed-circuit voltage is the voltage under the load condition, i.e. during charging or discharging. Closed-circuit voltage increases with the charging current and decreases with the discharging current, so voltaic efficiency is very dependent on the value of a battery's charging/discharging current.

- Charging voltaic efficiency is a ratio of the average open-circuit voltage ($\overline{U^{OC}}$) and the average charging voltage ($\overline{U^{ch}}$) over a partial or full charging half-cycle:

$$\eta^{ch,U} = \frac{\overline{U^{OC}}}{\overline{U^{ch}}}. \tag{2.7}$$

- Discharging voltaic efficiency is a ratio of the average discharging voltage ($\overline{U^{dis}}$) and the average open-circuit voltage ($\overline{U^{OC}}$) over a partial or full discharging half-cycle:

$$\eta^{dis,U} = \frac{\overline{U^{dis}}}{\overline{U^{OC}}}. \tag{2.8}$$

- Roundtrip voltaic efficiency is a ratio of the average discharging voltage ($\overline{U^{dis}}$) and the average charging voltage ($\overline{U^{ch}}$) over a partial or full cycle:

$$\eta^{cycle,U} = \eta^{ch,U} \cdot \eta^{dis,U} = \frac{\overline{U^{dis}}}{\overline{U^{ch}}}. \tag{2.9}$$

To obtain one-way voltaic efficiency, an OCV-SOC characteristic ($U^{OC} = f(soc)$) must be known, i.e. it needs to be determined experimentally.

2.2.3. Energy efficiency

This efficiency is associated with the energy (Wh) extracted from or injected into a battery. Energy efficiencies are defined analogously to the coulombic efficiencies, with E denoting energy in Wh.

- Charging energy efficiency:

$$\eta^{ch,E} = \frac{E^{batt}}{E^{ch}}. \tag{2.10}$$

[3] Battery SOH is a measure for the overall battery condition. A new, healthy battery has 100% SOH.

[4] Battery SOC is a measure for the amount of charge stored in a battery with respect to the charge that the battery contains when fully charged.

[5] Battery SOE is a measure for the amount of energy stored in a battery with respect to the energy that the battery contains when fully charged.

[6] Cycle implies both charging and discharging over the same SOC range (energy flow in both directions) and is used to obtain the roundtrip efficiency. Half-cycle implies either charging or discharging (energy flow in one direction only) and is used to obtain the charging or discharging (one-way) efficiency.

[7] Full (half-)cycle implies going from 0% to 100% SOC and/or back, while partial (half-)cycle implies covering some custom SOC range.

- Discharging energy efficiency:

$$\eta^{\mathrm{dis,E}} = \frac{E^{\mathrm{dis}}}{E^{\mathrm{batt}}}. \tag{2.11}$$

- Roundtrip energy efficiency:

$$\eta^{\mathrm{cycle,E}} = \eta^{\mathrm{ch,E}} \cdot \eta^{\mathrm{dis,E}} = \frac{E^{\mathrm{dis}}}{E^{\mathrm{ch}}}. \tag{2.12}$$

The injected energy E^{ch} (Wh) and the extracted energy E^{dis} (Wh) are easily calculated from the measured voltage and current as follows:

$$E^{\mathrm{ch}} = \int_0^{T^{\mathrm{ch}}} U^{\mathrm{ch}}(\tau) I^{\mathrm{ch}}(\tau) d\tau, \tag{2.13}$$

$$E^{\mathrm{dis}} = \int_0^{T^{\mathrm{dis}}} U^{\mathrm{dis}}(\tau) I^{\mathrm{dis}}(\tau) d\tau, \tag{2.14}$$

where U^{ch} and U^{dis} are charging and discharging closed-circuit voltages. Total energy stored in a battery E^{batt} cannot be determined directly from the measured voltage and current.

However, with the established method that employs the OCV-SOC characteristic (later in the paper referred to as *ocv* method), the following expressions that describe E^{batt} are obtained:

$$E^{\mathrm{batt,ocv,ch}} = \int_0^{T^{\mathrm{ch}}} U^{\mathrm{OC}}(soc) I^{\mathrm{ch}}(\tau) d\tau, \tag{2.15}$$

$$E^{\mathrm{batt,ocv,dis}} = \int_0^{T^{\mathrm{dis}}} U^{\mathrm{OC}}(soc) I^{\mathrm{dis}}(\tau) d\tau, \tag{2.16}$$

where U^{OC} is a function of the battery's state-of-charge. One-way energy efficiencies can now be calculated by including(2.15)in(2.10) and(2.16)in(2.11):

$$\eta^{\mathrm{ch,E,ocv}} = \frac{E^{\mathrm{batt,ocv,ch}}}{E^{\mathrm{ch}}}, \tag{2.17}$$

$$\eta^{\mathrm{dis,E,ocv}} = \frac{E^{\mathrm{dis}}}{E^{\mathrm{batt,ocv,dis}}}, \tag{2.18}$$

where *ocv* in superscript denotes that $E^{\mathrm{batt,ocv,ch}} \neq E^{\mathrm{batt}}$ and $E^{\mathrm{batt,ocv,dis}} \neq E^{\mathrm{batt}}$. The reason for this discrepancy is the omission of coulombic losses in(2.15)and(2.16). Consequently, the product of two one-way efficiencies in(2.17)and(2.18)results in an incorrect roundtrip efficiency:

$$\eta^{\mathrm{cycle,E,ocv}} = \eta^{\mathrm{ch,E,ocv}} \cdot \eta^{\mathrm{dis,E,ocv}} > \eta^{\mathrm{cycle,E}} = \frac{E^{\mathrm{dis}}}{E^{\mathrm{ch}}}, \tag{2.19}$$

since $C^{\mathrm{ch}} > C^{\mathrm{dis}}$ (see(2.5)and(2.6)) and $E^{\mathrm{batt,ocv,ch}} > E^{\mathrm{batt,ocv,dis}}$, which is the case whenever a cycle is performed over the same SOC range. In other words, coulombic losses are neglected in(2.15)–(2.19).

2.2.4. Coulombic, voltaic and energy efficiency relations

Using the OCV-SOC characteristic to obtain one-way energy efficiencies, as described above, is reasonable since the voltaic losses are normally more dominant (higher) than the coulombic losses (especially for higher C-rates). Roundtrip coulombic efficiency for lithium-ion battery technology is typically 99% or higher, as reported in many papers, e.g. [3,6,7,21], and confirmed by our own experimental results. Therefore, expressions $C^{\mathrm{ch}} \approx C^{\mathrm{dis}}$ and $E^{\mathrm{batt,ocv,ch}} \approx E^{\mathrm{batt,ocv,dis}}$ typically hold for lithium-ion battery cycles. Moreover, simple coulomb counting (2.1)can be used to cycle lithium-ion battery in the desired SOC range, in which case $C^{\mathrm{ch}} = C^{\mathrm{dis}}$ and $E^{\mathrm{batt,ocv,ch}} = E^{\mathrm{batt,ocv,dis}}$ is implied, while inequality(2.19)becomes equality. This approach to determining one-way energy efficiencies (i.e. neglecting coulombic losses) is commonly used in the literature, e.g. see [19,20,22].

Finally, it is worth noting that the energy efficiency is generally not a product of the coulombic and the voltaic efficiency. This is because energies are obtained by calculating Watt-hours, not Ampere-hours multiplied by the averaged voltages, i.e.:

$$\int_0^{T^{\mathrm{ch}}} U^{\mathrm{OC}}(soc) I^{\mathrm{ch}}(\tau) d\tau \neq \overline{U^{\mathrm{OC}}} \cdot \int_0^{T^{\mathrm{ch}}} I^{\mathrm{ch}}(\tau) d\tau. \tag{2.20}$$

Although the deviation is relatively small, energies obtained by the two calculus given in(2.20)are not the same, leading to the roundtrip energy efficiency being different as well:

$$\eta^{\mathrm{cycle,E}} \neq \eta^{\mathrm{cycle,U}} \cdot \eta^{\mathrm{cycle,I}}. \tag{2.21}$$

However, not-equal marks in(2.20)and(2.21)can be replaced with equal marks in case $I^{\mathrm{ch}} = \mathrm{const.}$, since (see also [2,4]):

$$\overline{U^{\mathrm{OC}}} = \frac{\int_0^{T^{\mathrm{ch}}} U^{\mathrm{OC}}(soc) d\tau}{T^{\mathrm{ch}}}. \tag{2.22}$$

Table 2
Battery efficiency — classification and possibilities of experimental determination.

Energy flow	Meas. quantity		
	Coulombic	Voltaic	Energy
Roundtrip	Directly	Directly	Directly
One-way OCV-based (*ocv* method, Section2.2.3)	No	Indirectly	Partially
One-way optimization-based (*opt* method, Section3)	Indirectly	Indirectly	Indirectly

2.3. Efficiency classification

Table2provides an overview of possibilities to experimentally determine different battery efficiencies, with an assumption that only standard electrical quantities (terminal voltage and current) are measured. In this context, *directly* means that an efficiency can be determined by a simple calculus from the voltage and current that are logged at a sufficiently high sample rate (order of seconds or higher). *No* means that an efficiency cannot be determined from the logged voltage and current. *Partially* means that an efficiency can be obtained, but it will not be completely accurate (because of the inability to measure one-way coulombic losses). Finally, *indirectly* means that an efficiency can be determined, but only with additional experimentally obtained information (the OCV-SOC characteristic) or by conducting additional calculations (as described in the following section).

Methods compared in Section5are placed in theTable2as follows: method *fix* in the first row, method *ocv* in the second row and method *opt*, proposed in this work, in the third row.

Due to considered issues regarding the assessment of one-way efficiencies, as well as the fact that experiments for obtaining OCV-SOC characteristics are time consuming, we adopt a novel, optimization-based approach for determining one-way energy efficiencies, as discussed in Section3(later in the paper referred to as *opt* method). Moreover, this approach can also be used to determine one-way coulombic efficiencies, which none of the conventional approaches are capable of.

3. Optimization-based method for obtaining one-way efficiencies

This section describes the proposed algorithm for obtaining battery one-way efficiencies. Steps of the algorithm are displayed inFig.1.

3.1. Step 1: Charging/discharging cycles in the CP mode

In this experimental part of the algorithm, the battery is cycled as follows:

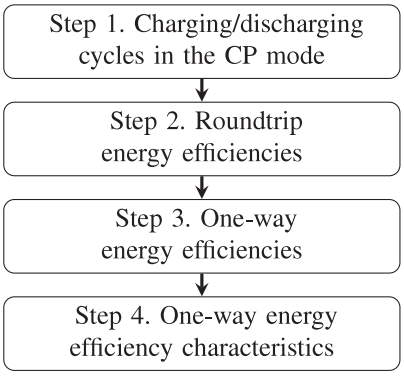

Fig. 1. Algorithm for obtaining battery one-way efficiencies (*opt* method).

(1)Each cycle is always started with a depleted battery, where depleted means that a non-depleted battery is discharged until the battery's low voltage limit has been reached with the provision that the discharging battery P-rate is equal to the cycle's discharging P-rate in point (3) below. This ensures the same starting and finishing point of the cycle in terms of currents and voltages.
(2)Each charging is performed in the constant-power mode and is terminated as soon as the declared battery high voltage limit is reached.
(3)Each discharging is performed in the constant-power mode and is terminated as soon as the declared battery low voltage limit is reached.
(4)Each cycle is performed at room temperature.

A number of P-rates is chosen to cover the expected battery's charging (C) and discharging (D) operational ranges. Then, $C \times D$ partial cycles in the CP mode are conducted, for all possible combinations of the chosen charging/discharging P-rates. To increase accuracy and ensure consistency, cycling can be repeated J times.

Remark 1. In this work the main focus is on energy and power characteristics, so the batteries are cycled in the CP mode, which means that the obtained one-way efficiencies will be correlated with constant power rates (P-rates). One-way efficiencies could also be correlated with C-rates, in which case cycling should be performed in the CC mode. Nevertheless, as far as one-way efficiencies go, there is no significant difference between the CC and the CP mode, since the currents adopt similar values when charging/discharging at the same C-rates and P-rates [5].

Remark 2. It is important to emphasize that one-way efficiency determination is based on experiments which are conducted in the CP (or CC) mode exclusively. Therefore, the effect of voltage saturation present in the CV charging mode is evaded.

3.2. Step 2: Roundtrip energy efficiencies

For every cycle from Step 1, charging and discharging energies are calculated by integrating the logged powers, see(2.13)and(2.14). Then, the roundtrip energy efficiency for every cycle is obtained according to(2.12). Finally, roundtrip efficiency for each combination of the charging/discharging P-rate is averaged as:

$$\eta_{c,d}^{\text{cycle,E}} = \frac{\sum_{j=1}^{J} \eta_{c,d,j}^{\text{cycle,E}}}{J}. \tag{3.1}$$

3.3. Step 3: One-way energy efficiencies

To obtain one-way efficiencies from the measured roundtrip efficiencies, we formulate and solve the following nonlinear optimization problem:

$$\underset{\Xi=\{s_{c,d},\eta_c^{\text{ch,E,opt}},\eta_d^{\text{dis,E,opt}}\}}{\text{Minimize}} \quad \sum_{c\in\Omega^{\text{C}}}\sum_{d\in\Omega^{\text{D}}} s_{c,d}^2 \tag{3.2}$$

subject to

$$\eta_c^{\text{ch,E,opt}} \cdot \eta_d^{\text{dis,E,opt}} = \eta_{c,d}^{\text{cycle,E}} + s_{c,d}, \quad \forall c \in \Omega^{\text{C}}, \forall d \in \Omega^{\text{D}}, \tag{3.3}$$

$$0 \le \eta_c^{\text{ch,E,opt}} \le 1, \quad \forall c \in \Omega^{\text{C}}, \tag{3.4}$$

$$0 \le \eta_d^{\text{dis,E,opt}} \le 1, \quad \forall d \in \Omega^{\text{D}}. \tag{3.5}$$

Objective function(3.2)minimizes the squares of slack variable $s_{c,d}$ summed over all charging (c) and discharging (d) rates. Slack variable $s_{c,d}$ appears in constraint(3.3)to offset the inequality of the left- and right-hand sides of the equation. Note that(3.3)is a set of equations containing $C+D$ unknowns ($\eta_c^{\text{ch,E,opt}}$ and $\eta_d^{\text{dis,E,opt}}$) and $C \times D$ equations. However, this set of equations, assuming $s_{c,d} = 0$, cannot be solved analytically, as it is ill-posed, i.e. it either does not have a solution or it has infinitely many solutions. In other words, there is no combination of $\eta_c^{\text{ch,E,opt}}$ and $\eta_d^{\text{dis,E,opt}}$ that satisfies all $C \times D$ equations. Thus, the goal of this optimization problem is to find the values of $\eta_c^{\text{ch,E,opt}}$ and $\eta_d^{\text{dis,E,opt}}$, whose multiplication diverges from the measured efficiency $\eta_{c,d}^{\text{cycle,E}}$ the least. Since constraint(3.3)is nonlinear, additional constraints (3.4)and(3.5)are imposed to avoid possible physically meaningless solutions.

The strength of the proposed method, as mentioned in Section1.3, lies in the fact that it can also be used to obtain one-way coulombic efficiencies (based on the measured roundtrip coulombic efficiencies), in which case superscript I can be used instead of E in(3.2)–(3.5). In this context, it is also worth noting that the obtained one-way energy efficiencies $\eta^{\text{ch,E,opt}}$ and $\eta^{\text{dis,E,opt}}$ account for both the voltaic and the coulombic losses and are thus potentially more accurate than $\eta^{\text{ch,E,ocv}}$ and $\eta^{\text{dis,E,ocv}}$. This may not be as important for lithium-ion batteries which have high coulombic efficiency (cca. 99% roundtrip), but it may be beneficial for application to other technologies that have lower coulombic efficiency, e.g. Ni-MH batteries or some emerging technologies. Furthermore, obtaining OCV-SOC characteristics takes time (cca. 48 h typically) and requires relatively precise instrumentation, as cycling is performed with very low currents. Another strength of the proposed method, compared to the OCV-based method, is the possibility of obtaining one-way efficiencies quicker (e.g. for $C = D = 2$) and with less precise instrumentation, as low currents are avoided.

3.4. Step 4: One-way energy efficiency characteristics

The output of Step 3 are C charging and D discharging energy efficiencies that correspond to the charging/discharging P-rates chosen in Step 1 of the algorithm. Linear interpolation between these values can be used to assess one-way energy efficiency characteristics (functions) over the entire range of battery's operational power: $\eta^{\text{CH,E,opt}} = f(P^{\text{ch}})$ and $\eta^{\text{DIS,E,opt}} = f(P^{\text{dis}})$ (seeFig.3for the specific characteristics). These characteristics can now be used to calculate the energy injected into the battery $E^{\text{batt,opt,ch}}$ (Wh) and the energy extracted from the battery $E^{\text{batt,opt,dis}}$ (Wh) with variable one-way energy efficiencies accounted for, as follows:

$$E^{\text{batt,opt,ch}} = \int_0^{T^{\text{ch}}} P^{\text{ch}}(\tau) \cdot \eta^{\text{CH,E,opt}}(P^{\text{ch}}) d\tau, \tag{3.6}$$

$$E^{\text{batt,opt,dis}} = \int_0^{T^{\text{dis}}} \frac{P^{\text{dis}}(\tau)}{\eta^{\text{DIS,E,opt}}(P^{\text{dis}})} d\tau, \tag{3.7}$$

where $P^{\text{ch}}(\tau) = U^{\text{ch}}(\tau) \cdot I^{\text{ch}}(\tau)$ and $P^{\text{dis}}(\tau) = U^{\text{dis}}(\tau) \cdot I^{\text{dis}}(\tau)$.

Table 3
Bi-directional DC power supplies.

Parameter	Power supply	
	Itech IT-M3413	Itech IT-M3622
Output voltage	0 ~ 150 V	0 ~ 60 V
Setup resolution	1 mV	
Accuracy	$< 0.1\% \cdot U_{max}$	
Output current	−12 A ~ 12 A	−30 A ~ 30 A
Setup resolution	1 mA	10 mA
Accuracy	$< 0.1\% \cdot I_{max} + 0.1\% \cdot I_{current}$	
Output power	−200 W ~ 200 W	−400 W ~ 400 W
Setup resolution	0.1 W	
Accuracy	$< 0.1\% \cdot P_{max}$	

Table 4
Specifications of the tested battery cells.

Parameter	Battery cells			
	LFP	NMC	LCO	LTO
Type	18 650	18 650	18 650	18 650
Nominal capacity	1.5 Ah	3.0 Ah	3.2 Ah	1.3 Ah
Nominal energy capacity	4.8 Wh	10.8 Wh	12.0 Wh	3.12 Wh
Nominal voltage	3.2 V	3.6 V	3.75 V	2.4 V
Charging voltage	3.65 V	4.2 V	4.35 V	2.75 V
Discharge cut-off voltage	2.0 V	2.5 V	2.75 V	1.6 V
Cut-off current	0.03 A	0.05 A	0.16 A	0.10 A
Max. charge current	1C	1.33C	1C	10C
Max. discharge current	3.6C	6.67C	2C	10C

Remark. The method described in this section ignores the nonlinearity and the one-way efficiency dependence on the SOC level. This is justified by the findings from [5], where it is shown that voltaic efficiency curves can be considered constant in a wide SOC range. Thus, the errors due to this neglection are insignificant, especially if the edge parts of the SOC – one-way efficiency characteristic are not used.

4. Experimental application of the proposed method

4.1. Experimental setup

The experiments are conducted on the professional bi-directional DC power supplies (inverters), controlled by the proprietary NI LabVIEW software. Four most commonly used battery chemistries are tested: lithium-ferro-phosphate (LFP), lithium-nickel-manganese-cobalt-oxide (NMC), lithium-cobalt-oxide (LCO) and lithium-titanium-oxide (LTO). Technical specifications of the bi-directional power supplies are provided in Table 3 , while the manufacturer's specifications of the tested battery cells are listed in Table4 . Depending on the desired P-rates and specifications of a particular battery cell, one of the two power supplies is used to conduct the experiments, as displayed in Fig. 2 .

4.2. Derivation of one-way efficiency characteristics

The four battery cells are subjected to the cycling process described in Section3.1 (Step 1 in Fig. 1) with $C = D = J = 3$. The roundtrip efficiencies are calculated as described in Section3.2 (Step 2 in Fig. 1), for the following permutations of charging/discharging P-rates: (i) 0.2P, 0.5P and 1.0P for LFP, NMC and LCO cells, and (ii) 0.33P, 0.66P and 1.0P for the LTO cell. Cycling P-rates for the LTO cell had to be adjusted due to the limitations of the used power supplies at low voltages and low powers (LTO has the lowest voltage among the tested chemistries). The obtained, averaged roundtrip efficiencies are provided in Table 5 . As expected, higher efficiencies are achieved for lower P-rates. The NMC cell has the highest roundtrip efficiencies, followed by the LFP and LTO cells, while the LCO cell has by far the lowest roundtrip efficiencies, below 80% for the 1P charge/discharge cycle.

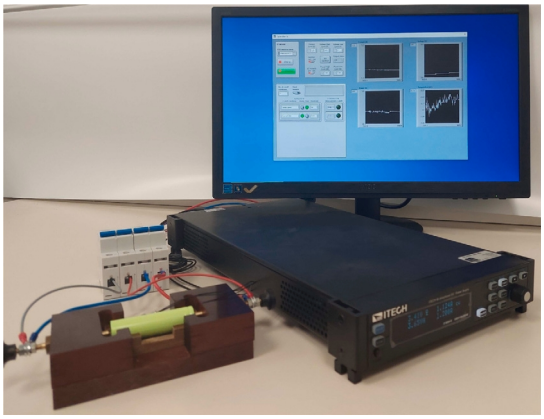

Fig. 2. Experimental setup.

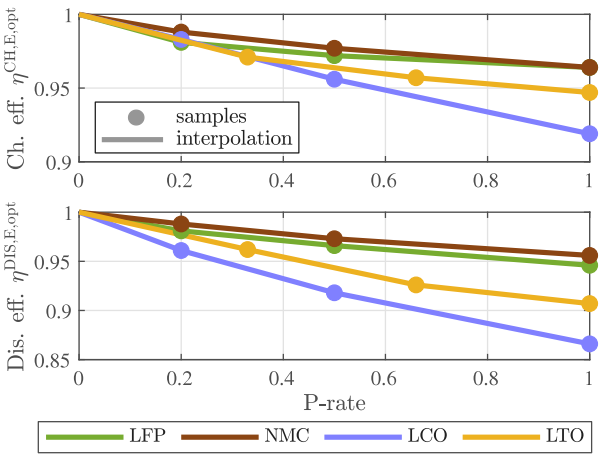

Fig. 3. Battery one-way efficiencies depending on the charging/discharging P-rate.

The obtained roundtrip efficiencies are inputs to the nonlinear optimization problem(3.2)–(3.5), which is used to determine one-way efficiencies as described in Section3.3 (Step 3 in Fig. 1). The obtained one-way energy efficiencies are provided in Table 6 , where it can be seen that their values are generally the highest for 0.2P and decrease as the P-rate increases. The efficiency reduction is more prominent for the discharging than for the charging process. For instance, the discharge efficiency of the LCO cell at 1P is 0.87, while the charging efficiency is 0.92 at the same P-rate. NMC is the most efficient cell at all P-rates, while LCO is the least efficient, with an exception of charging at 0.2P.

Samples from Table 6 and the point (0,1) [8] are connected by linear interpolation to form charging/discharging efficiency characteristics, as described in Section3.4 . The obtained characteristics are displayed in Fig.3 .

5. Experimental validation

5.1. Overview

The proposed method for deriving one-way energy efficiencies can be practically applied in industries where the battery state-of-energy is an important information. Such applications are battery management and monitoring systems in electric vehicles and stationary battery

[8] Efficiency is assumed 100% for 0 P-rate.

Table 5
Measured and averaged roundtrip efficiencies ($\eta_{c,d}^{\text{cycle,E}}$).

Ch.	Dis.									Ch.	Dis.		
	LFP			NMC			LCO				LTO		
	0.2P	0.5P	1.0P	0.2P	0.5P	1.0P	0.2P	0.5P	1.0P		0.33P	0.66P	1.0P
0.2P	0.963	0.947	0.927	0.977	0.962	0.945	0.940	0.903	0.852	0.33P	0.932	0.897	0.886
0.5P	0.953	0.939	0.919	0.9657	0.951	0.935	0.915	0.877	0.827	0.66P	0.923	0.889	0.863
1.0P	0.945	0.931	0.914	0.952	0.938	0.921	0.879	0.843	0.796	1.00P	0.911	0.876	0.859

Table 6
Battery one-way energy efficiencies ($\eta_c^{\text{ch,E,opt}}$ and $\eta_d^{\text{dis,E,opt}}$).

Cell	P-rate					
	0.2P		0.5P		1.0P	
	Ch.	Dis.	Ch.	Dis.	Ch.	Dis.
LFP	0.981	0.981	0.972	0.966	0.964	0.946
NMC	0.988	0.988	0.977	0.973	0.964	0.956
LCO	0.983	0.961	0.956	0.918	0.919	0.866
Cell	P-rate					
	0.33P		0.66P		1.0P	
	Ch.	Dis.	Ch.	Dis.	Ch.	Dis.
LTO	0.971	0.962	0.957	0.926	0.947	0.907

Table 7
Battery one-way energy efficiencies ($\eta_c^{\text{ch,E,ocv}}$ and $\eta_d^{\text{dis,E,ocv}}$).

Cell	P-rate					
	0.2P		0.5P		1.0P	
	Ch.	Dis.	Ch.	Dis.	Ch.	Dis.
LFP	0.984	0.985	0.973	0.970	0.965	0.956
NMC	0.990	0.982	0.974	0.964	0.960	0.947
LCO	0.968	0.975	0.933	0.929	0.907	0.894
Cell	P-rate					
	0.3P		0.6P		1.0P	
	Ch.	Dis.	Ch.	Dis.	Ch.	Dis.
LTO	0.974	0.960	0.956	0.941	0.942	0.918

storage systems [24]. Our experimental validation consists of subjecting four battery cells (seeTable4) to an EV charging/discharging profile and then comparing the state-of-energy calculation error at the end of the profile. Our method is compared to two other efficiency models.

Eq.(5.1)is used to calculate SOE in all the compared cases, with the expressions η^{CH} and η^{DIS} being different for each efficiency model.

$$soe(t) = soe(t-1) + \int_{t-1}^{t} P^{\text{ch}}(\tau)\eta^{\text{CH}}d\tau - \int_{t-1}^{t} P^{\text{dis}}(\tau)\eta^{\text{DIS}}d\tau \tag{5.1}$$

5.2. Compared efficiency models

This experimental validation is conducted under three efficiency models: *opt*, *ocv*, and *fix*.

The *opt* model is the one proposed in Section3and applied in Section4of this paper (see alsoTable6). It uses the one-way efficiency characteristics fromFig.3and interpolates efficiency values depending on the variable power rates. Thus, $\eta^{\text{CH}} = \eta^{\text{CH,E,opt}}(P^{\text{ch}})$ and $\eta^{\text{DIS}} = \eta^{\text{DIS,E,opt}}(P^{\text{dis}})$ for this model.

The *ocv* model uses an established method for one-way energy efficiency determination based on the OCV-SOC characteristics. This method is discussed in Section2.2.3and, in more detail, in [5]. One-way energy efficiency values experimentally obtained by this method are denoted $\eta_c^{\text{ch,E,ocv}}$ and $\eta_d^{\text{dis,E,ocv}}$ and presented inTable7(for the CP mode exclusively, see [5] for details). These one-way efficiency values are connected by linear interpolation to form one-way efficiency characteristics very similar to those shown inFig.3. The *ocv* model also interpolates efficiency values depending on the variable power rates, as in $\eta^{\text{CH}} = \eta^{\text{CH,E,ocv}}(P^{\text{ch}})$ and $\eta^{\text{DIS}} = \eta^{\text{DIS,E,ocv}}(P^{\text{dis}})$. One-way efficiency values used in the *opt* and *ocv* models are similar, as observed by a comparison ofTables6and7.

The *fix* model is baseline model, dominantly used in the current state-of-the-art. It uses constant one-way energy efficiencies, which are derived as square roots of the measured roundtrip efficiencies, resulting in the same charging and discharging efficiency values. So, the *fix* model does not account for the actual power rate variability, nor does it differentiate between the charging and the discharging processes. For each tested battery cell, one-way efficiencies are calculated from the three roundtrip efficiency values, i.e. 0.2P (0.33P for LTO), 0.5P (0.66P for LTO) and 1P, listed on the diagonal elements inTable5(cycles with the same charging/discharging P-rates). Thus, the *fix* model is applied three times: (i) $\eta^{\text{CH}} = \eta^{\text{DIS}} = \eta^{0.2\text{P,fix}}$ ($\eta^{0.33\text{P,fix}}$ for LTO), (ii) $\eta^{\text{CH}} = \eta^{\text{DIS}} = \eta^{0.5\text{P,fix}}$ ($\eta^{0.66\text{P,fix}}$ for LTO), and (iii) $\eta^{\text{CH}} = \eta^{\text{DIS}} = \eta^{1\text{P,fix}}$.

5.3. Experiment description

Battery cells are prepared for the test by performing full CP-CV,[9] low-power cycles: charge at 0.1P, rest for 60 min, discharge at 0.1P (for NMC and LCO cells) and 0.2P (for LFP and LTO cells), rest for 60 min.

The applied EV battery charging/discharging profile is based on the transient driving cycle *New European Driving Cycle* [25] with prolonged time sequences for a clearer interpretation and comparison of the results. The profile is presented with blue and red rectangles inFig.4 and consists of the following driving regimes: CP-CV charge at 0.1P until fully charged, discharge at 1.0P for 10 min, discharge at 0.75P for 20 min, discharge at 0.5P for 30 min, charge at 0.8P for 30 min, discharge at 0.5P for 10 min, discharge at 0.4P for 20 min, discharge at 0.3P for 30 min, and finally, charge at 0.4P for 30 min.

Fig.4also displays SOC of the LCO cell during the testing process. This particular SOC is displayed for illustrative purposes and it was calculated by virtue of Eq.(2.1). SOE characteristics, obtained by(5.1), for all the tested cells and for all the compared models are not displayed for brevity, however their shapes also generally resemble that of the SOC fromFig.4.

After finalizing the driving cycle charging/discharging profile, each battery cell is rested for 60 min and then fully depleted at low powers of 0.1P (for NMC and LCO cells) and 0.2P (for LFP and LTO cells), in order to measure the remaining energy of the cell, which is reported in Table8.

5.4. Results

Results of the experimental validation are displayed inTable8. The column *Remaining energy* represents energy measured during a controlled discharge (as described at the end of the previous sub-section) and acts as a baseline for comparing accuracy of the five efficiency models. Columns *Energy* represent the predicted energy as calculated from the SOE value at the end of the profile fromFig.4 and the assumed discharging efficiency (for 0.1P or 0.2P depending on the tested cell). Columns *Error* display the difference between the remaining (measured) and the predicted (calculated) energies, where

[9] Full CP-CV cycle implies constant-power-constant-voltage charging/discharging until the measured current drops below the cut-off value.

Table 8
Measured and calculated remaining energies.

Cell	Remaining energy	$fix^{0.2P}$		$fix^{0.5P}$		$fix^{1.0P}$		*ocv*		*opt*	
		Energy	Error	Energy	Error	Energy	Error	Energy	Error	Energy	Error
LFP	2.67 Wh	2.62 Wh	−0.14%	2.60 Wh	−4.01%	2.55 Wh	−8.32%	2.71 Wh	−0.66%	2.72 Wh	−1.96%
NMC	4.46 Wh	4.41 Wh	3.77%	4.35 Wh	−0.56%	4.28 Wh	−5.76%	4.52 Wh	0.32%	4.49 Wh	1.42%
LCO	4.03 Wh	3.91 Wh	6.80%	3.78 Wh	−4.06%	3.60 Wh	−19.40%	4.08 Wh	0.90%	4.11 Wh	−0.09%
Cell	Remaining energy	$fix^{0.33P}$		$fix^{0.66P}$		$fix^{1.0P}$		*ocv*		*opt*	
		Energy	Error	Energy	Error	Energy	Error	Energy	Error	Energy	Error
LTO	1.16 Wh	1.12 Wh	1.15%	1.09 Wh	−6.20%	1.07 Wh	−11.79%	1.20 Wh	0.13%	1.20 Wh	−0.19%

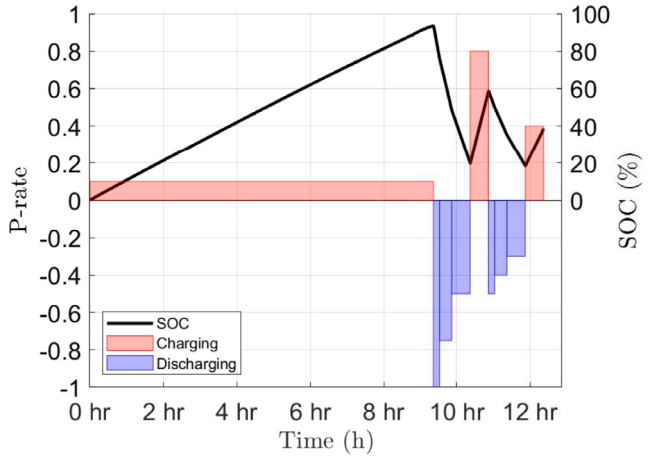

Fig. 4. Experimental electric vehicle charging/discharging profile. (For interpretation of the references to color in this figure legend, the reader is referred to the web version of this article.)

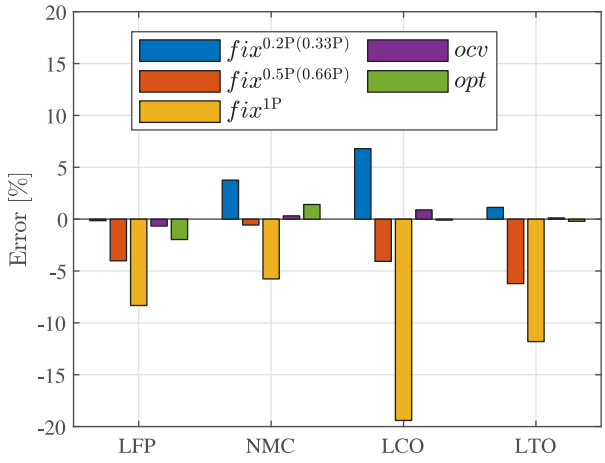

Fig. 5. Comparison of relative errors for calculations of the remaining energy with models *fix*, *ocv* and *opt*.

the percentage is determined with respect to the battery cell energy capacity (in Watt-hours). The error values are also displayed inFig. 5 .

The results indicate that the $fix^{0.2P}$ model generally underestimates energy losses (positive error value), while the $fix^{0.5P}$ and fix^{1P} models generally overestimate energy losses (negative error value), with fix^{1P} deviating more than $fix^{0.5P}$. This is because the average P-rate of the test profile amounts to 0.24, favoring the $fix^{0.2P}$ model. Thus, the models using fixed one-way efficiencies are inappropriate for variable power applications, despite having lower error than *ocv* and *opt* models in some very particular cases.

On the other hand, errors of the *ocv* and *opt* models are consistently low (under 2.0%), indicating the importance of accounting for one-way energy efficiency variability. The proposed *opt* model does not outperform the *ocv* model, since the *ocv* model has lower error for three out of four tested battery cells. However, these results indicate suitability of the proposed method as it is comparable to the OCV-based method which is well established for the tested lithium-ion batteries, having high coulombic efficiency.

Advantage of the *opt* over the *ocv* method lies in determining one-way coulombic efficiencies of lithium-ion batteries (using high-precision instrumentation), as well as in accurately determining one-way energy efficiencies of other battery technologies (having lower coulombic efficiency than the lithium-ion technology).

6. Conclusion

This paper focuses on battery efficiency and provides a thorough overview of different efficiency types and relations between them is given. An optimization-based method for obtaining one-way efficiencies is proposed and used to formulate a variable efficiency model. The obtained model is compared to two conventional models: one using fixed one-way efficiencies and the other, OCV-based, using variable one-way efficiencies. The three models are experimentally validated on four lithium-ion battery cells of different chemistries. The results clearly demonstrate the importance of accounting for variable battery energy efficiency, caused by the variable charging/discharging power rates. Ignoring variability of battery efficiencies might lead to significant errors, e.g. when determining state-of-energy in real time or when scheduling battery operation.

The proposed optimization-based method is potentially less time consuming than the established OCV-based method and can be used with relatively cheap (less precise) instrumentation, as very low currents, necessary for obtaining the OCV characteristics, can be avoided. Furthermore, the proposed method does not (always) outperform the OCV-based method, as the latter is fairly hard to beat for lithium-ion batteries, due to their high coulombic efficiency. However, the two methods show comparable results, which indicates that the proposed approach is valid and that it should be further tested in applications where the OCV-based method is inapplicable. One such application is determination of one-way coulombic efficiencies, which in case of lithium-ion batteries must be performed on expensive, highly precise instrumentation. The other such application is precise one-way energy efficiency determination (accounting for coulombic losses) of lithium-ion and other battery technologies.

Future work will encompass the mentioned applications, as well as reformulation of the presented variable efficiency models for inclusion in higher-level linear optimization models.

CRediT authorship contribution statement

V. Bobanac: Conceptualization, Methodology, Software, Formal analysis, Investigation, Data curation, Writing – original draft, Writing – review & editing, Visualization, Project administration. **H. Bašić:**

Conceptualization, Methodology, Validation, Formal analysis, Investigation, Writing – original draft, Writing – review & editing, Visualization, Project administration. **H. Pandžić:** Conceptualization, Methodology, Formal analysis, Resources, Writing – review & editing, Supervision, Funding acquisition.

Declaration of competing interest

The authors declare that they have no known competing financial interests or personal relationships that could have appeared to influence the work reported in this paper.

Data availability

The authors are unable or have chosen not to specify which data has been used

Acknowledgments

This work was funded by the European Union through the European Regional Development Fund for the Competitiveness and Cohesion Operational Programme 2014–2020 of the Republic of Croatia under project No. KK.01.1.1.07: "Universal Communication and Control System for Industrial Facilities".

References

[1] A. Eftekhari, Energy efficiency: a critically important but neglected factor in battery research, Sustain. Energy Fuels 1 (10) (2017).
[2] P. Meister, H. Jia, J. Li, R. Kloepsch, M. Winter, T. Placke, Best practice: Performance and cost evaluation of lithium ion battery active materials with special emphasis on energy efficiency, Chem. Mater. 28 (20) (2016) 7203–7217.
[3] J. Xiao, Q. Li, Y. Bi, M. Cai, B. Dunn, T. Glossmann, J. Liu, T. Osaka, R. Sugiura, B. Wu, J. Yang, J. Zhang, M.S. Whittingham, Understanding and applying coulombic efficiency in lithium metal batteries, Nat. Energy 5 (2020) 561–568.
[4] R. Lu, A. Yang, Y. Xue, L. Xu, C. Zhu, Analysis of the key factors affecting the energy efficiency of batteries in electric vehicle, World Electr. Veh. J. 4 (2010) 9–13.
[5] V. Bobanac, H. Bašić, H. Pandžić, One-way voltaic and energy efficiency analysis for lithium-ion batteries, in: Medpower2022, The 13th Mediterranean Conference on Power Generation, Transmission, Distribution and Energy Conversion, 2022, p. 53.
[6] A.J. Smith, J.C. Burns, J.R. Dahn, A high precision study of the Coulombic efficiency of Li-ion batteries, Electrochem. Solid-State Lett. 13 (12) (2010) 177–179.
[7] A.J. Smith, J.C. Burns, D. Xiong, J.R. Dahn, Interpreting high precision coulometry results on Li-ion cells, J. Electrochem. Soc. 158 (10) (2011) 1136–1142.
[8] W.H. Zhu, Y. Zhu, Z. Davis, B.J. Tatarchuk, Energy efficiency and capacity retention of Ni–MH batteries for storage applications, Appl. Energy 106 (2013) 307–313.
[9] S.U. Jeon, J.-W. Park, B.-K. Kang, H.-J. Lee, Study on battery charging strategy of electric vehicles considering battery capacity, IEEE Access 9 (2021) 89757–89767, http://dx.doi.org/10.1109/ACCESS.2021.3090763.
[10] S. Farhad, A. Nazari, Introducing the energy efficiency map of lithium-ion batteries, Int. J. Energy Res. 43 (2018) 931–944.
[11] K. Mamadou, A. Delaille, Method for calibrating an electrochemical battery, 2010, European patent, nr. EP2449392B1, US patent, nr. US 9, 075, 117 B2.
[12] K. Mamadou, E. Lemaire, A. Delaille, D. Riu, S. Hing, Y. Bultel, Definition of a state-of-energy indicator (SoE) for electrochemical storage devices: Application for energetic availability forecasting, J. Electrochem. Soc. 159 (2012) A1298–A1307.
[13] E. Fernandez, T. Delaplagne, R. Franchi, k. Mamadou, Method for determining a state-of-energy of the basis of data originating from the processing method, 2013, European patent, nr. EP2856187B1.
[14] X. Liu, J. Wu, C. Zhang, Z. Chen, A method for state of energy estimation of lithium-ion batteries at dynamic currents and temperatures, J. Power Sources 270 (2014) 151–157.
[15] W. Zhang, W. Shi, Z. Ma, Adaptive unscented Kalman filter based state of energy and power capability estimation approach for lithium-ion battery, J. Power Sources 289 (2015) 50–62.
[16] X. Shen, L. Zhang, Q. Chen, P. Xiao, R. Long, Energy management strategy for model predictive control of hybrid electric vehicle considering battery life and efficiency, in: 2021 5th CAA International Conference on Vehicular Control and Intelligence (CVCI), Tianjin, China, 2021, pp. 1–6, http://dx.doi.org/10.1109/CVCI54083.2021.9661238.
[17] G.L. Plett, Extended Kalman filtering for battery management systems of LiPB-based HEV battery packs, Part 2. Modeling and identification, J. Power Sources 134 (2004) 262–276.
[18] S. Abu-Sharkh, D. Doerffel, Rapid test and non-linear model characterisation of solid-state lithium-ion batteries, J. Power Sources 130 (2004) 266–274.
[19] M. Safoutin, J. Cherry, J. McDonald, S. Lee, Effect of Current and SOC on Round-Trip Energy Efficiency of a Lithium-Iron Phosphate (LiFePO4) Battery Pack, SAE Technical Paper 2015-01-1186, 2015.
[20] J. Kang, F. Yan, P. Zhang, C. Du, A novel way to calculate energy efficiency for rechargeable batteries, J. Power Sources 206 (2012) 310–314.
[21] F. Yang, D. Wang, Y. Zhao, K. Tsui, S.J. Bae, A study of the relationship between coulombic efficiency and capacity degradation of commercial lithium-ion batteries, Energy 145 (2018) 486–495.
[22] E. Redondo-Iglesias, P. Venet, S. Pelissier, Efficiency degradation model of lithium-ion batteries for electric vehicles, IEEE Trans. Ind. Appl. 55 (2) (2018) 1932–1940.
[23] H. Bašić, H. Pandžić, M. Miletić, I. Pavić, Experimental testing and evaluation of lithium-ion battery cells for a special-purpose electric vacuum sweeper vehicle, IEEE Access 8 (2020) 216308–216319.
[24] T. Trogrlić, M. Beus, Development of a battery management system for centralized control of a battery cluster, J. Energy 71 (2) (2022) 3–9.
[25] T. Barlow, S. Latham, I. McCrae, P. Boulter, A Reference Book of Driving Cycles for Use in the Measurement of Road Vehicle Emissions: Version 3, IHS, Bracknell, U.K., 2009.

batteries

Article

Determination of Lithium-Ion Battery Capacity for Practical Applications

Hrvoje Bašić, Vedran Bobanac and Hrvoje Pandžić *

University of Zagreb Faculty of Electrical Engineering and Computing, 10000 Zagreb, Croatia; hrvoje.basic@fer.hr (H.B.); vedran.bobanac@fer.hr (V.B.)
* Correspondence: hrvoje.pandzic@fer.hr

Abstract: Batteries are becoming highly important in automotive and power system applications. The lithium-ion battery, as the fastest growing energy storage technology today, has its specificities, and requires a good understanding of the operating characteristics in order to use it in full capacity. One such specificity is the dependence of the one-way charging/discharging efficiency on the charging/discharging current. This paper proposes a novel method for the determination of battery capacity based on experimental testing. The proposed method defines battery energy capacity as the energy actually stored in the battery, while accounting for both the charging and discharging losses. The experiments include one-way efficiency determination based on multiple cycles conducted under different operational and ambient conditions, the goal of which is to acquire the charging/discharging energies. The measured energies are corrected for one-way efficiencies to obtain values actually stored in a battery during charging or actually extracted from the battery during discharging. The proposed method is tested in a laboratory and compared against two existing baseline methods at different ambient temperatures. The results indicate that the proposed method significantly outperforms the baseline methods in terms of the accuracy of the determined battery energy capacity and state-of-energy. The prime reason for the good performance of the proposed method is that it accounts for both the operational (efficiency) and the ambient (temperature) conditions.

Keywords: battery capacity; energy capacity; state-of-charge; state-of-energy; round-trip efficiency; one-way efficiency

Citation: Bašić, H.; Bobanac, V.; Pandžić, H. Determination of Lithium-Ion Battery Capacity for Practical Applications. *Batteries* **2023**, *9*, 459.https://doi.org/10.3390/batteries9090459

Academic Editor: Jinhao Meng, Shunli Wang, Jiale Xie, Yi Xie, Fei Feng and Rui Ling

Received: 13 August 2023
Revised: 2 September 2023
Accepted: 7 September 2023
Published: 11 September 2023

1. Introduction

Battery systems are often considered as a source/sink with defined operational capabilities and fixed limitations in available capacity. In reality, battery systems consist of different connection combinations of battery cells with characteristics that depend on both the operational and the ambient conditions.

In the following subsections, we first explain the common terms used to describe the battery characteristics, then we present our literature review, define the present paper's contribution and, finally, present the organization of the rest of the paper.

1.1. Battery Parameters

Battery capacity is a measure of a battery's ability to store a certain amount of charge or energy. It represents the amount of electricity or energy generated due to electrochemical reactions in the battery. It can be defined as battery charge capacity, measured in Ah, or as battery energy capacity, measured in Wh. It is important to distinguish between the nominal average battery capacity defined by the manufacturer and the actual battery capacity. The nominal capacity is defined for a new battery used under controlled conditions. The actual available battery capacity depends on the operational and environmental conditions, as well as the age and state-of-health of the battery.

Battery state-of-charge is a measure of the amount of charge currently stored in a battery with respect to the fully charged battery. On the other hand, battery state-of-energy is a measure of the amount of energy currently stored in a battery with respect to the fully charged battery. Finally, battery state-of-health is a measure of the overall battery condition:

$$SOH = \frac{Q^{\mathrm{m}}}{Q^{\mathrm{n}}} \cdot 100\%, \tag{1}$$

where Q^{m} is the capacity of cycle number m in Ah, while Q^{n} is the nominal capacity of the battery in Ah [1].

C-rate is a ratio of the charging or discharging electrical current in Amperes and the nominal charge capacity of a battery in Ampere-hours. At 1C, the battery (dis)charges with the current corresponding to its Ah rating (e.g., 1C for a 10 Ah battery is 10 A, 0.5C is 5 A, etc.). On the other hand, P-rate is a ratio of the charging or discharging power in Watts and the nominal energy capacity of a battery in Watt-hours. At 1P, the battery (dis)charges with the power corresponding to its Wh rating (e.g., 1P for a 10 Ah battery with 10 V nominal voltage is 100 W, 0.5P is 50 W, etc.).

Battery efficiency can be defined as a measure that accounts for the losses occurring during battery charging and discharging. Since the only quantities that can be measured are the charging/discharging current, the battery voltage, and the heat losses, the efficiency can be determined and evaluated in the following ways:

- Battery Coulombic efficiency—based on the current measurements [2];
- Battery voltaic efficiency—based on the voltage measurements [2];
- Battery energy efficiency—based on both the current and the voltage measurements [3,4] or based on the heat loss measurements [5].

As mentioned above, in industry applications, the measures of power and energy (P-rate) are more convenient than measures of current and charge capacity (C-rate), as the appliances (consumers) are defined by the consumption of power and energy. Thus, this work considers the energy capacity and energy efficiency parameters.

Furthermore, battery efficiency can be calculated as round-trip efficiency or as one-way (charging/discharging) efficiency.

Round-trip energy efficiency can be calculated as the ratio of the energy discharged from the battery and the energy charged into the battery over the same SOC range:

$$\eta^{\mathrm{cycle,E}} = \eta^{\mathrm{ch,E}} \cdot \eta^{\mathrm{dis,E}} = \frac{E^{\mathrm{dis}}}{E^{\mathrm{ch}}}, \tag{2}$$

where $E^{\mathrm{ch}} = U^{\mathrm{ch}} \cdot I^{\mathrm{ch}}$ and $E^{\mathrm{dis}} = U^{\mathrm{dis}} \cdot I^{\mathrm{dis}}$ are determined by experimental measurements taken across battery terminals. This means that neither the exact amount of energy stored in the battery, nor the exact amount of energy available to extract from the battery, can be determined. As the round-trip efficiency can be defined as the charging times the discharging efficiency ($\eta^{\mathrm{cycle,E}} = \eta^{\mathrm{ch,E}} \cdot \eta^{\mathrm{dis,E}}$), one-way efficiencies are, in the literature, sometimes defined as the square root of round-trip efficiency, which would imply that one-way charging and discharging efficiencies are equal [6,7]. Additionally, in many studies, it can be seen that the charging efficiency is neglected, i.e., it is set to 1, while the one-way discharge efficiency takes over the entire value of the round-trip efficiency [8]. In both cases, an error in determining the battery capacity is inevitable because the one-way efficiency of both charging and discharging depends on factors such as operating and ambient conditions. Also, a battery cannot have 100% charging efficiency regardless of the power rate.

One-way efficiency can be determined in three ways:

- Using heat loss measurements;
- Using open-circuit voltage vs. state-of-charge characteristics;

- using voltage/current measurements and the solution of the nonlinear optimization problem that consists of several measured round-trip efficiencies.

As stated in [5], it is possible to measure the heat released from the battery and calculate the one-way efficiency of the battery under different operational and environmental conditions. However, as the total heat release from the battery is the sum of the irreversible and reversible heat generation, the efficiency determined in this way neglects the effects of reversible heat generation.

One-way battery energy efficiency can be determined based on the open-circuit voltage vs. state-of-charge characteristics [3]. The advantages of this method are its simplicity and the possibility to determine the one-way efficiency dependence on the state-of-charge level. The downside of this method is that it neglects Coulombic losses.

Another method for the determination of one-way energy efficiencies, presented in [4], is based on the solution of the nonlinear optimization problem that consists of several round-trip to one-way efficiency relationships, where round-trip efficiencies are experimentally determined parameters. One-way energy efficiencies determined in this way account for both the voltaic and the Coulombic losses. The downside of this method is that it ignores the nonlinearity of the charging/discharging characteristics.

Operational conditions are primarily related to the rate of charging and discharging current/power of the battery. Power and energy are the primary values of interest in the power system industry and the automotive industry, as opposed to the current and charge values. Thus, this work focuses on battery power characteristics that can easily be translated into energy characteristics. Ambient temperature has the greatest effect on the battery performance characteristics as compared to other ambient parameters such as humidity and vibrations [9], which is the reason for including the temperature effect in our work.

1.2. Literature Review

Different methods for the estimation of the battery cell energy capacity are evaluated in a large number of industry and scientific works [10]. The most common method is the calculation of the remaining battery energy capacity (in Wh) as a multiplication of the nominal energy capacity ($E^{\mathrm{n}} = U^{\mathrm{n}} \cdot Q^{\mathrm{n}}$, where U^{n} is the nominal voltage of the battery in V and Q^{n} is the nominal charge capacity of the battery in Ah, both determined by the manufacturer) and the state-of-charge (SOC) determined by Coulomb counting [11,12], as expressed in (3). However, this method neglects voltage charging and discharging characteristics, dynamic processes and battery capacity dependence on the power, the state-of-charge, the state-of-health, the ambient parameters, etc.

$$E_{\mathrm{SOC}}^{\mathrm{remaining}}(t) = E^{\mathrm{n}} \cdot SOC(t). \tag{3}$$

Another common method is defining the remaining battery energy capacity (in Wh) as a multiplication of the state-of-energy (SOE) and the nominal energy, where the state-of-energy is determined as a ratio of the integrated charged or discharged power ($P^{\mathrm{ch}} = U^{\mathrm{ch}} \cdot I^{\mathrm{ch}}$, $P^{dis} = -U^{dis} \cdot I^{dis}$, in W) and the nominal or maximum energy of the battery (in Wh) [7,13–15]:

$$E_{\mathrm{SOE}}^{\mathrm{remaining}}(t) = E^{\mathrm{n}} \cdot SOE(t), \tag{4}$$

$$SOE(t) = SOE(t-1) + \frac{1}{E^{\mathrm{n}}} \cdot \int_{\mathrm{t}-1}^{\mathrm{t}} P^{\mathrm{ch/dis}}(\tau) d\tau. \tag{5}$$

Both common methods neglect the energy capacity dependence on operational and environmental parameters. To reduce the error of operational losses, fixed operational round-trip efficiency is commonly accounted for in the method presented in [16]. Many other more complex methods have been developed for the determination of the remaining energy; for example, equivalent circuit models with implemented information about

electrolyte characteristics [17], impedance and resistance experimental measurements [18], and other methods based on experimental and historical data [19]. Equivalent circuit models are highly dependent on input data (usually collected from controlled laboratory environments), so their application in real dynamic operations may result in inaccurate estimations of the remaining energy.

On the other hand, methods that use Kalman filters are able to provide more accurate results in dynamic situations. In [20], an online capacity estimation method based on enhanced Coulomb counting with the adaptive Kalman filter was applied to eliminate the capacity estimation error. The Kalman filter updates the covariance and noise from the error, and the capacity estimation is performed by the fusion of the Gaussian probability density functions of the predicted value (based on state-of-health estimation) and the measured capacity value. The reduced error in estimation is experimentally verified. A method for SOE estimation based on SOC estimation with an extended Kalman filter upgraded with current, voltage, and temperature response prediction is presented in [21]. The presented method accounts for the full life cycle of the battery. Additionally, the authors presented a method for the estimation of the entire battery pack state-of-energy. A dual forgetting factor-based adaptive extended Kalman filter for SOC estimation is presented in [22]. The authors combined the existing extended Kalman filter for online SOC estimation [13,23–25] with the SOE estimation method [12] to obtain reliable SOC and SOE estimations.

Methods with prediction algorithms are often limited to capacity estimation under given conditions. The authors of [26] developed a prediction technique for the estimation of the remaining driving range of an electric vehicle. The proposed method considers operational dynamics, but neglects temperature variability. On the other hand, the authors of [27] presented a predictive algorithm that predicts both future operation and temperature conditions. The model for operation conditions is based on an equivalent circuit model, and temperature prediction is based on historical data.

Methods with neural networks that use historical data may consider environmental and operational impact on capacity, but they highly depend on the quantity and choice of historical data and the methods used for the training of the models [28,29]. Similarly, fuzzy logic models are able to provide highly precise estimations based on historical and experimental data under given operational and environmental conditions [30]. Machine learning model [31] has proved that the diversity of feasible data is critical for estimation with high accuracy. The presented model uses a multichannel technique based on voltage, current, and temperature profiles, and our results show that it outperforms the conventional method, which only uses voltage profile.

As stated in [32], the disadvantages of complex models are the accuracy dependence on training/historical data, computational costs, and development complexity.

1.3. Contribution

The conducted literature review indicates that the existing baseline methods for battery capacity determination neglect the influence of the charging and discharging current/power rate on one-way efficiencies, and thus on the determination of the battery capacity value. Moreover, in most cases, the influence of ambient temperature on the battery characteristics is also neglected, which limits the possibility of applying these methods in varying ambient conditions. To overcome this research gap, this paper offers the following contributions:

- It proposes a method for determining battery capacity that considers charging/discharging (one-way) efficiencies, as well as different ambient temperatures;
- To verify the proposed method, an experimental comparison is performed to compare it with the baseline methods.

1.4. Organization of the Paper

The rest of the paper is organized as follows. The novel method for battery capacity estimation is presented and elaborated in Section2. Section3presents the experimental

setup, a description of the baseline methods, a case study, and the experimental results. Finally, an overview of the presented work is given in Section4.

2. Proposed Method for Determination of Average Battery Energy Capacity and State-of-Energy

This section describes the proposed method for battery energy capacity determination step-by-step, as shown in Figure1.

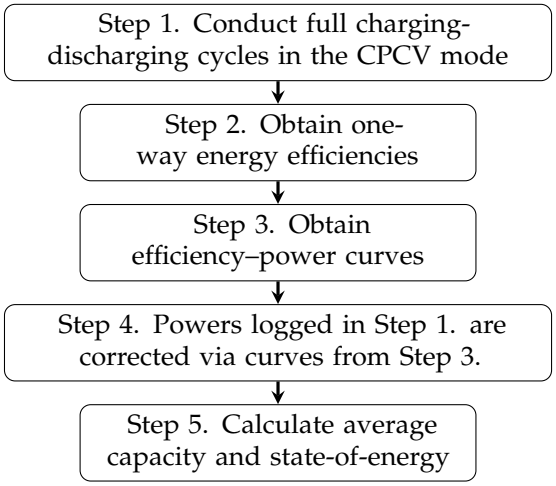

Figure 1. Algorithm for the determination of average battery energy capacity and state-of-energy in the method *Proposed* .

In the first step, the battery is cycled with the aim of obtaining the charging and discharging energies for a number of full cycles. Cycles are always started at a fully depleted battery (a fully depleted battery means that a non-depleted battery is discharged until the battery's low-voltage limit has been reached and the current has dropped below the specified cut-off value) (0% SOE), while each charging and discharging process is terminated when the current drops below the low cut-off threshold (an end-of-charge current specified by the manufacturer). Full cycles in the constant power–constant voltage (CPCV) mode are conducted, always using the same charging/discharging P-rate within a cycle. In CPCV mode, the battery is charged and discharged at constant power until the effect of voltage saturation, where the battery voltage reaches the high (for charging) or the low (for discharging) voltage limit. In that moment, the constant voltage mode begins and the power consequently decreases. The set of K full cycles is repeated at each considered ambient temperature, in order to obtain the efficiency–power characteristics for different ambient temperature conditions.

The second step is the one-way efficiency determination. As Coulombic losses for the observed lithium-ion battery cell are less than 1% [33], their effect is neglected in this research. Thus, one-way efficiencies are determined from the open-circuit voltage vs. state-of-charge (OCV-SOC) characteristic (in this work, the OCV-SOC characteristic is also determined for each considered ambient temperature), according to [3]:

$$\eta_{\mathrm{k}}^{\mathrm{Prop,ch,E}} = \frac{\int_0^{T^{\mathrm{ch}}} U^{\mathrm{OC}}(soc) \cdot I_{\mathrm{k}}^{\mathrm{ch}}(\tau) d\tau}{\int_0^{T^{\mathrm{ch}}} U_{\mathrm{k}}^{\mathrm{ch}}(\tau) \cdot I_{\mathrm{k}}^{\mathrm{ch}}(\tau) d\tau}, \tag{6}$$

where $k \in [1 \ldots K]$, $U^{\mathrm{OC}}(soc)$ is an OCV-SOC characteristic and $I_{\mathrm{k}}^{\mathrm{ch}}(\tau)$ is the charging current, and

$$\eta_{\mathrm{k}}^{\mathrm{Prop,dis,E}} = \frac{\int_0^{T^{\mathrm{dis}}} U_{\mathrm{k}}^{\mathrm{dis}}(\tau) \cdot I_{\mathrm{k}}^{\mathrm{dis}}(\tau) d\tau}{\int_0^{T^{\mathrm{dis}}} U^{\mathrm{OC}}(soc) \cdot I_{\mathrm{k}}^{\mathrm{dis}}(\tau) d\tau}, \tag{7}$$

where $I_k^{dis}(\tau)$ is the discharging current. In this way, it is possible to determine one-way charging and discharging efficiencies $\eta_k^{Prop,ch,E}$ and $\eta_k^{Prop,dis,E}$ for all K P-rates. Here, only the CP mode of each cycle (for both charge and discharge) is used to determine the efficiencies, so that the one-way efficiencies correlate with the P-rates.

Battery efficiency is a nonlinear function depending on operating conditions (power rate). To approximate this nonlinearity, an efficiency–power curve is introduced in the third step based on linear interpolation between K determined one-way efficiencies in the whole range of the operating powers, as shown in Figures2and3.

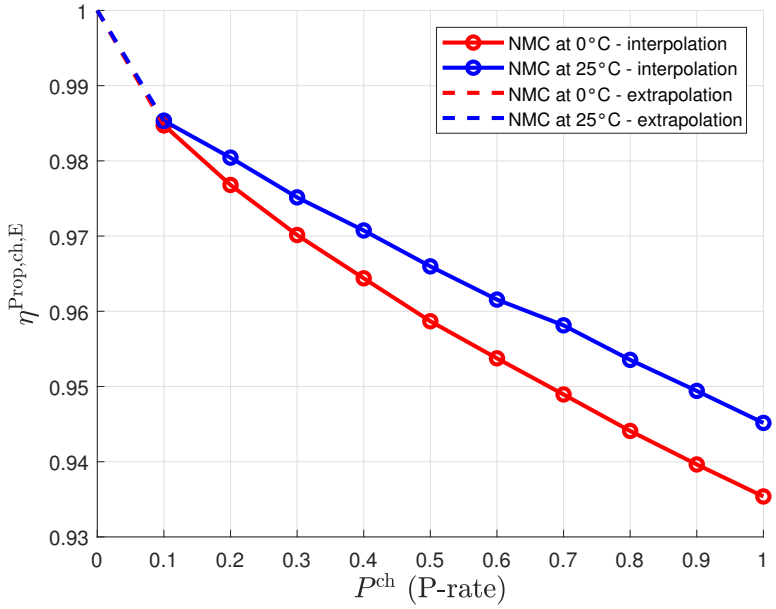

Figure 2. Charging efficiencies depending on the P-rate in the CP mode.

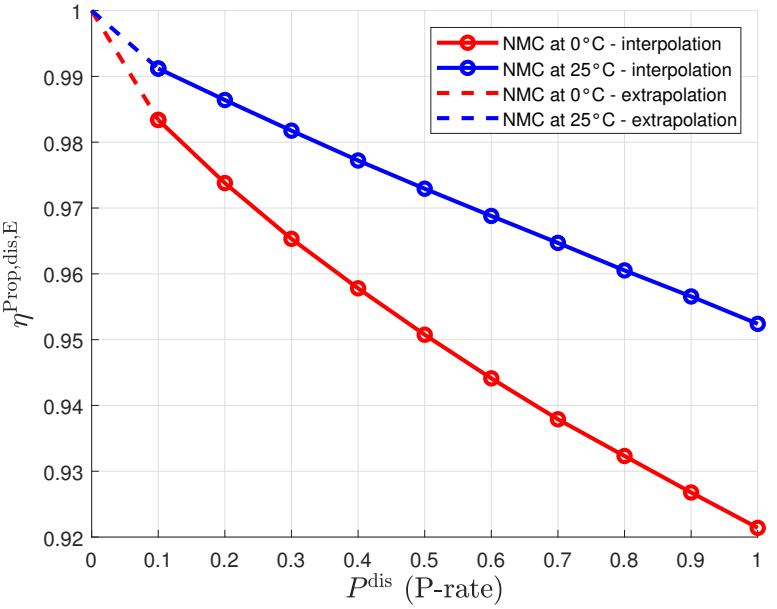

Figure 3. Discharging efficiencies depending on the P-rate in the CP mode.

In the fourth step, for every full cycle (out of K full cycles in the CPCV mode), the logged powers ($P_{\mathrm{k}}^{\mathrm{ch}}(t)$ and $P_{\mathrm{k}}^{\mathrm{dis}}(t)$) are corrected for one-way energy efficiencies by using the determined efficiency–power curves:

$$P_{\mathrm{k}}^{\mathrm{Prop,ch}}(t) = \eta^{\mathrm{Prop,ch,E}}(P^{\mathrm{ch}}) \cdot P_{\mathrm{k}}^{\mathrm{ch}}(t), \tag{8}$$

$$P_{\mathrm{k}}^{\mathrm{Prop,dis}}(t) = \frac{P_{\mathrm{k}}^{\mathrm{dis}}(t)}{\eta^{\mathrm{Prop,dis,E}}(P^{\mathrm{dis}})}, \tag{9}$$

where $\eta^{\mathrm{Prop,ch,E}}(P^{\mathrm{ch}})$ and $\eta^{\mathrm{Prop,dis,E}}(P^{\mathrm{dis}})$ are charging and discharging efficiency–power curves from Figures2and3, respectively.

Finally, in the fifth step, by integrating the corrected powers, K values of $E_{\mathrm{k}}^{\mathrm{Prop,ch}} = \int_0^{T^{\mathrm{ch}}} P_{\mathrm{k}}^{\mathrm{Prop,ch}}(\tau)d\tau$ and K values of $E_{\mathrm{k}}^{\mathrm{Prop,dis}} = \int_0^{T^{\mathrm{dis}}} P_{\mathrm{k}}^{\mathrm{Prop,dis}}(\tau)d\tau$ are obtained, representing the energy stored in a battery during charging and energy extracted from a battery during discharging, respectively. In an ideal case, values of the corrected energies $E_k^{\mathrm{Prop,ch}}$ and $E_k^{\mathrm{Prop,dis}}$ are all the same, representing the energy that can be stored in a battery. In reality, due to various effects and uncertainties (various electrochemical phenomena, e.g., loss of lithium ions due to lithium plating, as well as measurement uncertainties), these values slightly vary, and the battery energy capacity is declared to be the mean of all the corrected energies:

$$E_{\mathrm{av}}^{\mathrm{Prop}} = \frac{\sum_{k=1}^{K} E_{\mathrm{k}}^{\mathrm{Prop,ch}} + \sum_{k=1}^{K} E_{\mathrm{k}}^{\mathrm{Prop,dis}}}{2 \cdot K}. \tag{10}$$

Expression (10) represents the fifth and last step of the *Proposed* method, where state-of-energy is defined as

$$SOE(t) = SOE(t-1) + \frac{1}{E_{\mathrm{av}}^{\mathrm{Prop}}} \cdot \left(\int_{\mathrm{t}-1}^{\mathrm{t}} P^{\mathrm{Prop,ch}}(\tau)d\tau - \int_{\mathrm{t}-1}^{\mathrm{t}} P^{\mathrm{Prop,dis}}(\tau)d\tau \right), \tag{11}$$

where $P^{\mathrm{Prop,ch}}(t)$ and $P^{\mathrm{Prop,dis}}(t)$ are corrected powers, given by (8) and (9), for the time frame $\langle t-1, t]$.

3. Experimental Verification of the Proposed Method for Determination of Battery Energy Capacity and State-of-Energy

3.1. Experimental Setup

A lithium nickel manganese cobalt oxide (NMC) battery cell type is tested. The manufacturer's specifications of this cell are listed in Table1. Battery cells used in the experiments are displayed in Figure4. To reduce the error due to inconsistent cell parameters, the experimental procedure described in Section3.3was applied to six identical battery cells, the specifications of which are given in Table1. Since similar results were obtained for all cells, the verification was successful, and only one set of results is presented in the present paper.

The experiments were conducted using a professional Itech IT-M3413 bidirectional DC power supply (inverter) with the following voltage and current characteristics: 0∼150 V, −12∼12 A [34]. The control was set up using in-house developed NI LabVIEW software (https://www.ni.com/en/support/documentation/release-notes/product.labview.html, accessed on 6 September 2023). A compressor-cooled Memmert ICP110 incubator with a working temperature range of −12∼+60 °C was used to create specific testing environments. The experimental setup is displayed in Figure5, where the bidirectional DC power supply used for charging and discharging of the battery cells is located in the middle of the figure, the battery cells under test are located in a compressor-cooled incubator on the right-hand side, while a graphical interface of the in-house developed control program is presented on the left-hand side of the figure.

Figure 4. Battery cells under test.

Table 1. Specifications of the tested battery cell.

Parameter \ Battery Cells	NMC
Type	18,650
Nominal capacity	3.0 Ah
Nominal energy capacity	10.8 Wh
Nominal voltage	3.6 V
Charging voltage	4.2 V
Discharge cut-off voltage	2.5 V
Cut-off current	0.05 A
Max. charge current	1.33 C
Max. discharge current	6.67 C

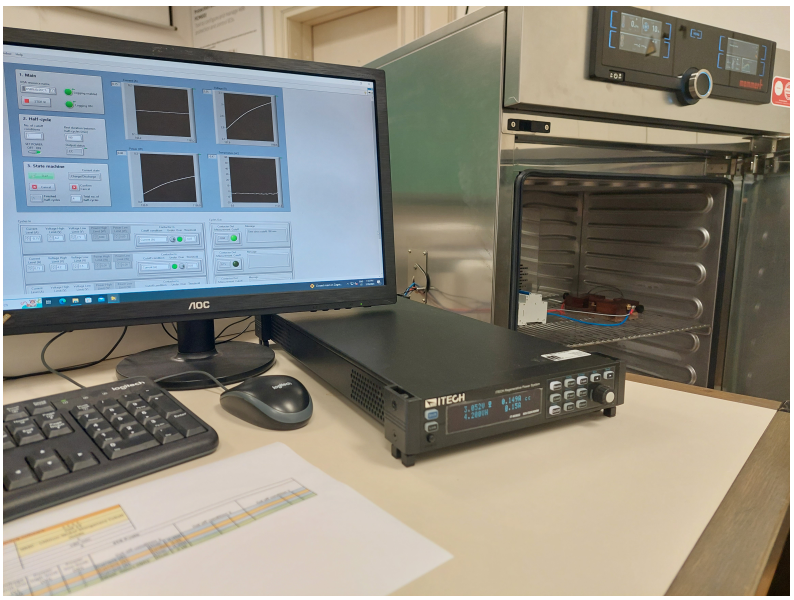

Figure 5. Experimental setup.

3.2. Compared Methods for Determination of Battery Energy Capacity and State-of-Energy

Building on the existing state-of-the-art techniques, this paper presents a novel method for determining the capacity and state-of-energy of the battery, with the aim of outperforming the existing baseline methods in terms of accuracy. As described in Section2, the *Proposed* method is based on one-way efficiencies, and considers the effect of different operating and environmental conditions.

Two established (baseline) methods for battery energy capacity and state-of-energy calculation are compared with the *Proposed* method: method *Nominal*, where the determination of the state-of-energy is based on the manufacturer's data only, and method *Conventional*, where the determination of the state-of-energy is based on the measured round-trip efficiency.

3.2.1. Method *Nominal*

Nominal average voltage is defined as U^{n} in V and nominal Coulombic capacity as Q^{n} in Ah. Both values are specified by the battery manufacturer, who may also specify the nominal average energy capacity under different ambient temperatures. On the other hand, energy efficiency is usually not defined by the manufacturer. Thus, the average energy capacity of the battery estimated with the method *Nominal* is $E_{\mathrm{av}}^{\mathrm{Nom}} = U^{\mathrm{n}} \cdot Q^{\mathrm{n}}$ at ambient temperature 25 °C, and for other ambient temperatures, the average energy capacity is as defined by the manufacturer.

The manufacturer's data for the battery under test are the following: $E_{\mathrm{av}}^{\mathrm{Nom}} = 10.8$ Wh at 25 °C, $E_{\mathrm{av}}^{\mathrm{Nom}} = 8.64$ Wh at 0 °C. Energy efficiencies are not defined, so round-trip and one-way efficiencies are defined as follows: $\eta^{\mathrm{Nom,ch,E}} = \eta^{\mathrm{Nom,dis,E}} = \eta^{\mathrm{Nom,cycle,E}} = 1$.

3.2.2. Method *Conventional*

To account for the energy losses while estimating energy capacity, in method *Conventional*, the round-trip efficiency is determined experimentally, whereby a fully depleted battery (0% SOE) is fully charged (to 100% SOE) and then fully discharged under given operating and environmental conditions. The charging and discharging energies are defined as $E^{\mathrm{Conv,ch}} = \int_0^{T^{\mathrm{ch}}} U^{\mathrm{ch}}(\tau) \cdot I^{\mathrm{ch}}(\tau) d\tau$ and $E^{\mathrm{Conv,dis}} = \int_0^{T^{\mathrm{dis}}} U^{\mathrm{dis}}(\tau) \cdot I^{\mathrm{dis}}(\tau) d\tau$. The round-trip efficiency is then calculated as

$$\eta^{\mathrm{Conv,cycle,E}} = \frac{E^{\mathrm{Conv,dis}}}{E^{\mathrm{Conv,ch}}}. \tag{12}$$

One-way charging and discharging efficiencies are calculated as square roots of the round-trip efficiency to account for charging and discharging losses separately:

$$\eta^{\mathrm{Conv,ch,E}} = \eta^{\mathrm{Conv,dis,E}} = \sqrt{\eta^{\mathrm{Conv,cycle,E}}}. \tag{13}$$

The average battery capacity is calculated as an average of the charging and discharging energies from an experimental full round-trip cycle (0–100% SOE) with one-way efficiencies accounted for:

$$E_{\mathrm{av}}^{\mathrm{Conv}} = \frac{E^{\mathrm{Conv,ch}} \cdot \eta^{\mathrm{Conv,ch,E}}}{2} + \frac{E^{\mathrm{Conv,dis}}}{2 \cdot \eta^{\mathrm{Conv,dis,E}}}. \tag{14}$$

In the experimental verification below, the fixed round-trip efficiency measured for a 1.0P charging/discharging cycle at an environmental temperature of 0 °C is $\eta_{0°\mathrm{C}}^{\mathrm{Conv,cycle,E}} = 0.8648$, while at an environmental temperature of 25 °C, it amounts to $\eta_{25°\mathrm{C}}^{\mathrm{Conv,cycle,E}} = 0.8991$. According to (13), one-way efficiency in this method is determined as the square root of round-trip efficiency. Thus, for 0 °C, $\eta_{0°\mathrm{C}}^{\mathrm{Conv,ch,E}} = \eta_{0°\mathrm{C}}^{\mathrm{Conv,dis,E}} = \sqrt{\eta_{0°\mathrm{C}}^{\mathrm{Conv,cycle,E}}} = 0.9300$, while for 25 °C, $\eta_{25°\mathrm{C}}^{\mathrm{Conv,ch,E}} = \eta_{25°\mathrm{C}}^{\mathrm{Conv,dis,E}} = \sqrt{\eta_{25°\mathrm{C}}^{\mathrm{Conv,cycle,E}}} = 0.9482$.

In this method, the battery capacity is defined as in (14); see Table2for specific numbers.

Table 2. Estimated average battery energy capacities.

Method \ Temperature	0 °C	25 °C
Nominal	8.64 Wh	10.80 Wh
Conventional	9.86 Wh	10.53 Wh
Proposed	10.05 Wh	10.68 Wh

3.2.3. Method *Proposed*

In method *Proposed*, the battery energy capacity is obtained with one-way efficiencies and ambient temperature accounted for. The efficiency–power curves are determined as described in Section2. Ten P-rates ($K = 10$) are chosen to cover the expected battery's operational range. Thus, the battery is fully cycled from a 0.1 P-rate to a 1.0 P-rate with 0.1P steps at ambient temperatures 0 °C and 25 °C. The obtained charging and discharging efficiencies are shown in Table3and in Figures2and3. The cells under test are significantly more efficient at higher environmental temperatures; this is especially the case for the discharging efficiency. At 1P, the discharging efficiency at 25 °C is over 0.95, while at 0 °C, it is just above 0.92. The charging efficiencies are much closer, at 0.945 and 0.935.

Table 3. One-way energy efficiencies for NMC battery cell.

Conditions \ P-Rate	0.0P	0.1P	0.2P	0.3P	0.4P	0.5P	0.6P	0.7P	0.8P	0.9P	1.0P
Charging at 0 °C	1	0.985	0.977	0.970	0.964	0.959	0.954	0.949	0.944	0.940	0.935
Discharging at 0 °C	1	0.983	0.974	0.965	0.958	0.951	0.944	0.938	0.932	0.927	0.921
Charging at 25 °C	1	0.985	0.980	0.975	0.971	0.966	0.962	0.958	0.954	0.949	0.945
Discharging at 25 °C	1	0.991	0.986	0.982	0.977	0.973	0.969	0.965	0.961	0.957	0.952

The proposed average battery energy capacity is then determined according to (10) and related equations; see Table2for specific numbers.

A graphical comparison of battery energy capacities determined in charging and discharging cycles, with and without one-way efficiencies accounted for, is presented in Figure6for the ambient temperature of 25 °C. Here, it is evident that the measured discharging energy (E^{dis}) is always lower than the measured charging energy (E^{ch}) within the cycle, the difference being greater for higher P-rates. This is normal and expected, since current/voltage measurements are taken across battery terminals. When correction for one-way efficiencies is applied (see Section2), the values of $E^{\mathrm{Prop,dis}}$ and $E^{\mathrm{Prop,ch}}$ are obtained, representing the estimated values of energies actually stored in the battery. As presented in Figure6, their values are approximately the same, indicating that charging/discharging energy losses are accurately described by one-way efficiencies.

3.3. Case Study

In the manufacturer's product specification of the battery under test, nominal quantities are defined with standard charge at 0.5 C-rate and with standard discharge at 0.2 C-rate. To be in line with these data, the experimental test is arranged accordingly. The considered methods for battery energy capacity and state-of-energy determination (the proposed method and the baseline methods) are compared by applying them to the full charge/discharge cycle depicted in Figure7. The battery under test is first fully depleted. Then, the battery is fully charged at 0.5 P-rate in time frame $[t_1, t_2]$, and, finally, fully discharged at 0.2 P-rate in time frame $[t_2, t_3]$ (see Figure7). Both charging and discharging are performed in the CPCV mode, which means they are terminated after a specified

voltage limit has been reached and the current has dropped below a specified cut-off value. Therefore, at the end of discharge (at t_3) the battery is at $SOE = 0\%$, and this value is used as a benchmark for the comparison of the accuracies of the three methods. Since charging and discharging rates are different, the battery cells are tested under different operating conditions. To test the methods under different environmental conditions, all the tests are performed in a compressor-cooled incubator at two different temperatures: 0 °C and 25 °C.

At the end of the case study cycle, states-of-energies are calculated as follows:

- In methods *Nominal* and *Conventional*, state-of-energy is defined as (15)

$$SOE(t) = SOE(t-1) + \frac{1}{E_{\text{av}}} \cdot \left(\int_{\text{t}-1}^{\text{t}} \eta^{\text{ch,E}} \cdot P^{\text{ch}}(\tau) d\tau - \int_{\text{t}-1}^{\text{t}} \frac{P^{\text{dis}}(t)}{\eta^{\text{dis,E}}} d\tau \right), \quad (15)$$

  where $P^{\text{ch}}(t)$ and $P^{\text{dis}}(t)$ are powers measured from the side of the inverter in time frame $\langle t-1, t]$, while triplets $(E_{\text{av}}, \eta^{\text{ch,E}}, \eta^{\text{dis,E}})$ are either $(E_{\text{av}}^{\text{Nom}}, \eta^{\text{Nom,ch,E}}, \eta^{\text{Nom,dis,E}})$ or $(E_{\text{av}}^{\text{Conv}}, \eta^{\text{Conv,ch,E}}, \eta^{\text{Conv,dis,E}})$.
- In method *Proposed*, state-of-energy is calculated according to (11).

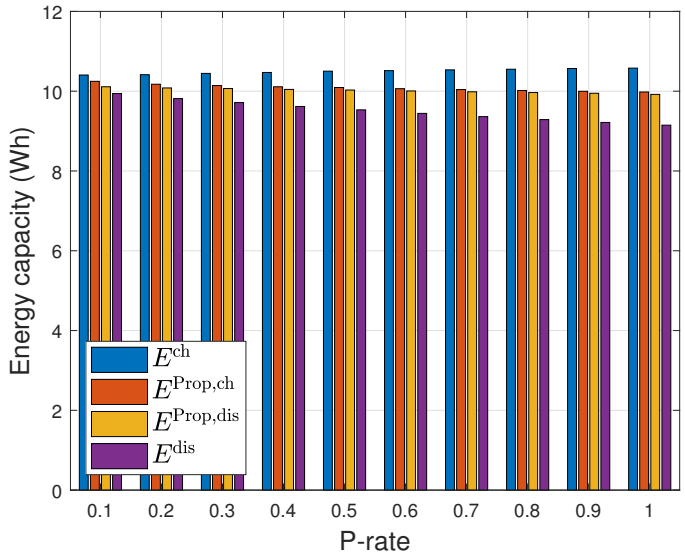

Figure 6. Charging and discharging battery energy capacities at 25 °C.

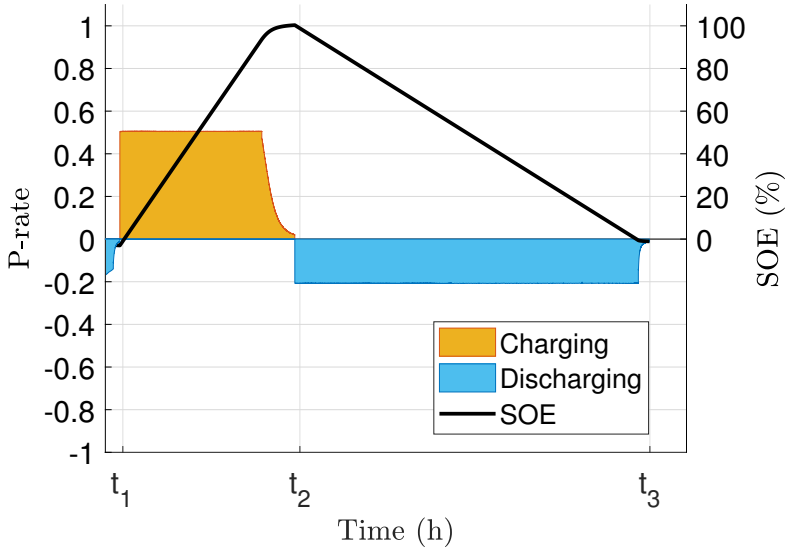

Figure 7. Case study cycle.

3.4. Results

An overview of the estimated average energy capacities is presented in Table2.

As mentioned in Section3.3, the experiments were conducted at two different temperatures: 0 °C and 25 °C. The nominal value of the average battery energy capacity at an ambient temperature of 25 °C is 10.8 Wh. As the battery completed a certain number of cycles through experimental testing, the capacity degraded, as expected. Methods *Conventional* and *Proposed* use data from experimental measurements, so the estimated capacity is lower than the nominal capacity. The nominal value of the average battery energy capacity at an ambient temperature of 0 °C is declared as 80% of the average nominal capacity at 25 °C. This estimate seems exaggerated because higher values were determined by experimental measurements with the *Conventional* and the *Proposed* methods. Namely, the estimated capacity at 0 °C is 96.6% for method *Conventional* and 94.1% for method *Proposed* compared to the estimated values at 25 °C.

An overview of the determined states-of-energies at the end of the case study cycle is presented in Table4.

The real value of the state-of-energy at the end of the case study cycle is 0%, i.e., the battery is fully depleted, as described in Section3.3(thus explaining the 0% values in the row *Measured*). Values in rows *Nominal*, *Conventional*, and *Proposed* were calculated from the expressions (15) and (11), respectively (thus, they are directly dependent on the accuracy of the capacity and one-way efficiency values used). The results demonstrate that, in this case study, the method *Proposed* provides much more accurate estimations for both ambient temperatures as compared to estimations with methods *Nominal* and *Conventional*. This is because the method *Proposed* uses battery parameters determined under different ambient temperature and operating conditions. The most important distinction compared to the two baseline methods is that the *Proposed* method uses variable one-way efficiencies (adapted to the power rate), as well as the battery capacity averaged over a wide range of cycles conducted at different rates. Although the method *Conventional* uses battery parameters determined under different ambient temperatures as well, its disadvantage is that only one fixed battery energy efficiency is used, which is based on a single fixed charging/discharging power rate at a given temperature. Therefore, this model cannot be adapted to different operating conditions, and thus, the estimation is less accurate. Method *Nominal* uses values determined by the manufacturer, and thereby neglects operational effects, as well as the state-of-health of the battery. Therefore, the estimations with the method *Nominal* are the least accurate.

Table 4. Estimated states-of-energies at the end of the case study cycle.

Method \ Temperature	0 °C	25 °C
Measured	0%	0%
Nominal	11.11%	6.56%
Conventional	9.05%	6.38%
Proposed	2.73%	1.84%

4. Conclusions

In this work, we analyze battery capacity and state-of-energy estimation, along with their dependence on the operational and ambient conditions. The operational conditions are related to the charging and discharging current/power rates, while the ambient conditions are related to the ambient temperatures at which the batteries are used. Both operational and ambient conditions affect the efficiency and the health of the batteries to different extents, depending on the range of observed conditions. The established (baseline) methods for the estimation of battery capacity and state-of-energy either consider only nominal values given by the manufacturer, or neglect the variable operational and/or ambient conditions. Our work presents a novel method that considers both the variable

operational and ambient conditions. It is based on the experimental determination of one-way (charging and discharging) efficiencies for different current/power rates under different ambient conditions. Prerequisites for implementing the presented method (at each given temperature) are as follows: (i) conduct a set of full charging/discharging cycles, (ii) determine one-way efficiencies, (iii) determine efficiency–power characteristics, and finally, (iv) calculate energies actually stored in the battery during each full charging (and energies actually extracted from the battery during each full discharging). The method estimates the current state of the battery (for the given ambient temperature); thus, it is recommended that the procedure is repeated periodically in order to take into account the battery's aging effects.

The accuracy of the proposed method is proven by testing NMC cells. Laboratory tests demonstrated that the proposed method is significantly more accurate than the baseline ones. At the end of the case study battery cycle, the real state-of-energy was 0%, i.e., the battery was fully depleted. With the proposed method, the estimated value of the state-of-energy is 2.7% at the ambient temperature of 0 °C and 1.8% at the ambient temperature of 25 °C, which is considerably more accurate than the baseline methods, where the results range from 6.4% to 11.1%.

Author Contributions: Conceptualization, H.B. and V.B.; Data curation, H.B., V.B. and H.P.; Formal analysis, H.B. and V.B.; Funding acquisition, H.P.; Investigation, H.B. and V.B.; Methodology, H.B., V.B. and H.P.; Project administration, H.B., V.B. and H.P.; Resources, H.B., V.B. and H.P.; Software, H.B. and V.B.; Supervision, V.B. and H.P.; Validation, H.B., V.B. and H.P.; Visualization, H.B., V.B. and H.P.; Writing—original draft, H.B.; Writing—review and editing, H.B., V.B. and H.P. All authors have read and agreed to the published version of the manuscript.

Funding: This work was supported by the European Union through the European Regional Development Fund Operational Programme Competitiveness and Cohesion 2014–2020 of the Republic of Croatia under Grant KK.01.1.1.07 *Universal Communication and Control System for Industrial Facilities.*

Institutional Review Board Statement: Not applicable.

Informed Consent Statement: Not applicable.

Acknowledgments: This work was supported by the European Union through the European Regional Development Fund Operational Programme Competitiveness and Cohesion 2014–2020 of the Republic of Croatia under Grant KK.01.1.1.07 *Universal Communication and Control System for Industrial Facilities.*

Conflicts of Interest: The authors declare no conflicts of interest.

Nomenclature

The following nomenclature is used in this manuscript:

E^{ch}	Charging energy obtained by integration of P^{ch}
E^{dis}	Discharging energy obtained by integration of P^{dis}
$E_{\mathrm{av}}^{\mathrm{Nom}}$	Average battery capacity estimated with method *Nominal*
$E_{\mathrm{av}}^{\mathrm{Conv}}$	Average battery capacity estimated with method *Conventional*
$E_{\mathrm{av}}^{\mathrm{Prop}}$	Average battery capacity estimated with method *Proposed*
$E^{\mathrm{Prop,ch}}$	Charging energy obtained by integration of $P^{\mathrm{Prop,ch}}$ in method *Proposed*
$E^{\mathrm{Prop,dis}}$	Discharging energy obtained by integration of $P^{\mathrm{Prop,dis}}$ in method *Proposed*
$\eta^{\mathrm{cycle,E}}$	Round-trip energy efficiency
$\eta^{\mathrm{ch,E}}$	One-way charging energy efficiency
$\eta^{\mathrm{dis,E}}$	One-way discharging energy efficiency
$\eta^{n,cycle,E}$	Nominal round-trip energy efficiency defined by the manufacturer
$\eta^{Nom,ch,E}$	One-way charging energy efficiency in method *Nominal*
$\eta^{Nom,dis,E}$	One-way discharging energy efficiency in method *Nominal*
$\eta^{Conv,cycle,E}$	Round-trip energy efficiency in method *Conventional*
$\eta^{Conv,ch,E}$	One-way charging energy efficiency in method *Conventional*

$\eta^{Conv,dis,E}$	One-way discharging energy efficiency in method *Conventional*
$\eta^{Prop,ch,E}$	One-way charging energy efficiency in method *Proposed*
$\eta^{Prop,dis,E}$	One-way discharging energy efficiency in method *Proposed*
$P^{\mathrm{ch}}(t)$	Charging power measured across battery terminals
$P^{\mathrm{dis}}(t)$	Discharging power measured across battery terminals
$P^{\mathrm{Prop,ch}}(t)$	Charging power corrected via efficiency–power characteristic in method *Proposed*
$P^{\mathrm{Prop,dis}}(t)$	Discharging power corrected via efficiency–power characteristics in method *Proposed*
$SOE(t)^{\mathrm{Nom}}$	State-of-energy in method *Nominal*
$SOE(t)^{\mathrm{Conv}}$	State-of-energy in method *Conventional*
$SOE(t)^{\mathrm{Prop}}$	State-of-energy in method *Proposed*

References

1. Amir, S.; Gulzar, M.; Tarar, M.O.; Naqvi, I.H.; Zaffar, N.A.; Pecht, M.G. Dynamic Equivalent Circuit Model to Estimate State-of-Health of Lithium-Ion Batteries. *IEEE Access* **2022**, *10*, 18279–18288. [CrossRef]
2. Linden, D.; Reddy, T.B. *Handbook of Batteries*; McGraw-Hill: New York, NY, USA, 2002.
3. Bobanac, V.; Bašić, H.; Pandžić, H. One-way voltaic and energy efficiency analysis for lithium-ion batteries. In Proceedings of the Medpower2022, The 13th Mediterranean Conference on Power Generation, Transmission, Distribution and Energy Conversion, Valletta, Malta, 7–9 November 2022; p. 53.
4. Pandžić, H.; Bobanac, V.; Bašić, H. Method for Experimental Determination of Battery Parameters and Their Use. European Patent PCT/EP2022/070718, 2022.
5. Farhad, S.; Nazari, A. Introducing the energy efficiency map of lithium-ion batteries. *Int. J. Energy Res.* **2018**, *43*, 931–944. [CrossRef]
6. Lu, R.; Yang, A.; Xue, Y.; Xu, L.; Zhu, C. Analysis of the key factors affecting the energy efficiency of batteries in electric vehicle. *World Electr. Veh. J.* **2010**, *4*, 9–13. [CrossRef]
7. Mamadou, K.; Lemaire, E.; Delaille, A.; Riu, D.; Hing, S.; Bultel, Y. Definition of a State-of-Energy Indicator (SoE) for Electrochemical Storage Devices: Application for Energetic Availability Forecasting. *J. Electrochem. Soc.* **2012**, *159*, A1298–A1307. [CrossRef]
8. Pandžić, H.; Bobanac, V. An Accurate Charging Model of Battery Energy Storage. *IEEE Trans. Power Syst.* **2019**, *34*, 1416–1426. [CrossRef]
9. Zhang, L.; Mu, Z.; Gao, X. Coupling Analysis and Performance Study of Commercial 18650 Lithium-Ion Batteries under Conditions of Temperature and Vibration. *Energies* **2018**, *11*, 2856. [CrossRef]
10. Xiong, R.; Cao, J.; Yu, Q.; He, H.; Sun, F. Critical Review on the Battery State of Charge Estimation Methods for Electric Vehicles. *IEEE Access* **2018**, *6*, 1832–1843. [CrossRef]
11. Li, K.; Tseng, K.J. An equivalent circuit model for state of energy estimation of lithium-ion battery. In Proceedings of the 2016 IEEE Applied Power Electronics Conference and Exposition (APEC), Long Beach, CA, USA, 20–24 March 2016; pp. 3422–3430.
12. Zheng, L.; Zhu, J.; Wang, G.; He, T.; Wei, Y. Novel methods for estimating lithium-ion battery state of energy and maximum available energy. *Appl. Energy* **2016**, *178*, 1–8. [CrossRef]
13. Zhang, W.; Shi, W.; Ma, Z. Adaptive unscented Kalman filter based state of energy and power capability estimation approach for lithium-ion battery. *J. Power Sources* **2015**, *289*, 50–62. [CrossRef]
14. Wang, Y.; Zhang, C.; Chen, Z. Model-based state-of-energy estimation of lithium-ion batteries in electric vehicles. *Energy Procedia* **2016**, *88*, 998–1004. [CrossRef]
15. Dong, G.; Chen, Z.; Wei, J.; Zhang, C.; Wang, P. An online model-based method for state of energy estimation of lithium-ion batteries using dual filters. *J. Power Sources* **2016**, *301*, 277–286. [CrossRef]
16. Li, K.; Tseng, K.J. Energy efficiency of lithium-ion battery used as energy storage devices in micro-grid. In Proceedings of the IECON 2015-41st Annual Conference of the IEEE Industrial Electronics Society, Yokohama, Japan, 9–12 November 2015; pp. 005235–005240.
17. Bhat, C.; Channegowda, J.; Naraharisetti, K. Electrolyte based Equivalent Circuit Model of Lithium ion Batteries for Intermittent Load Applications. In Proceedings of the 2022 IEEE International Conference on Power Electronics, Smart Grid, and Renewable Energy (PESGRE), Trivandrum, India, 2–5 January 2022; pp. 1–3.
18. Bhagyasree, P.; Shah, V.A. A Simplified Method to Evaluate Equivalent Circuit Model and State of Charge of Li-ion Battery. In Proceedings of the 2019 IEEE 1st International Conference on Energy, Systems and Information Processing (ICESIP), Chennai, India, 4–6 July 2019; pp. 1–6.
19. Fonseca, J.M.L.; Sambandam Kulothungan, G.; Raj, K.; Rajashekara, K. A Novel State of Charge Dependent Equivalent Circuit Model Parameter Offline Estimation for Lithium-ion Batteries in Grid Energy Storage Applications. In Proceedings of the 2020 IEEE Industry Applications Society Annual Meeting, Detroit, MI, USA, 10–16 October 2020; pp. 1–8.
20. Ko, Y.; Cho, K.; Kim, M.; Choi, W. A Novel Capacity Estimation Method for the Lithium Batteries Using the Enhanced Coulomb Counting Method with Kalman Filtering. *IEEE Access* **2022**, *10*, 38793–38801. [CrossRef]
21. An, F.; Jiang, J.; Zhang, W.; Zhang, C.; Fan, X. State of Energy Estimation for Lithium-Ion Battery Pack via Prediction in Electric Vehicle Applications. *IEEE Trans. Veh. Technol.* **2022**, *71*, 184–195. [CrossRef]

22. Shrivastava, P.; Kok Soon, T.; Bin Idris, M.Y.I.; Mekhilef, S.; Adnan, S.B.R.S. Combined State of Charge and state-of-energy Estimation of Lithium-Ion Battery Using Dual Forgetting Factor-Based Adaptive Extended Kalman Filter for Electric Vehicle Applications. *IEEE Trans. Veh. Technol.* **2022**, *70*, 1200–1215. [CrossRef]
23. Plett, G.L. Extended Kalman filtering for battery management systems of LiPB-based HEV battery packs: Part 3. State and parameter estimation. *J. Power Sources* **2004**, *134*, 277–292. [CrossRef]
24. Mastali, M.; Vazquez-Arenas, J.; Fraser, R.; Fowler, M.; Afshar, S.; Stevens, M. Battery state of the charge estimation using Kalman filtering. *J. Power Sources* **2013**, *239*, 294–307. [CrossRef]
25. Chen, Z.; Fu, Y.; Mi, C.C. State of charge estimation of lithium-ion batteries in electric drive vehicles using extended Kalman filtering. *IEEE Trans. Veh. Technol.* **2013**, *62*, 1020–1030. [CrossRef]
26. Liu, G.; Ouyang, M.; Lu, L.; Li, J.; Hua, J. A highly accurate predictive-adaptive method for lithium-ion battery remaining discharge energy prediction in electric vehicle applications. *Appl. Energy* **2015**, *149*, 297–314. [CrossRef]
27. Ren, D.; Lu, L.; Shen, P.; Feng, X.; Han, X.; Ouyang, M. Battery remaining discharge energy estimation based on prediction of future operating conditions. *J. Energy Storage* **2019**, *25*, 100836. [CrossRef]
28. Liu, X.; Wu, J.; Zhang, C.; Chen, Z. A method for state of energy estimation of lithium-ion batteries at dynamic currents and temperatures. *J. Power Sources* **2014**, *270*, 151–157. [CrossRef]
29. Dong, G.; Zhang, X.; Zhang, C.; Chen, Z. A method for state of energy estimation of lithium-ion batteries based on neural network model. *Energy* **2015**, *90*, 879–888. [CrossRef]
30. Singh, P.; Fennie, C.; Reisner, D. Fuzzy logic modelling of state-of-charge and available capacity of nickel/metal hydride batteries. *J. Power Sources* **2004**, *136*, 322–333. [CrossRef]
31. Choi, Y.; Ryu, S.; Park, K.; Kim, H. Machine Learning-Based Lithium-Ion Battery Capacity Estimation Exploiting Multi-Channel Charging Profiles. *IEEE Access* **2019**, *7*, 75143–75152. [CrossRef]
32. Lucu, M.; Martinez-Laserna, E.; Gandiaga, I.; Camblong, H. A critical review on self-adaptive Li-ion battery ageing models. *J. Power Sources* **2018**, *401*, 85–101. [CrossRef]
33. Xiao, J.; Li, Q.; Bi, Y.; Cai, M.; Dunn, B.; Glossmann, T.; Liu, J.; Osaka, T.; Sugiura, R.; Wu, B.; et al. Understanding and applying coulombic efficiency in lithium metal batteries. *Nat. Energy* **2020**, *5*, 561–568. [CrossRef]
34. Itech, IT-M3400 Bidirectional DC Power Supply. Available online:https://www.itechate.com/uploadfiles/(accessed on 23 December 2021).

Biography

Hrvoje Bašić is an assistant at the Department of Energy and Power Systems at the University of Zagreb Faculty of Electrical Engineering and Computing. His employment has been funded by the Croatian TSO - HOPS and Croatian Science Foundation under project SIREN (Smart Integration of RENewables) (2015–2018), the European Regional Development Fund under project Electric Compact Urban Vacuum Sweeper with an ICT System Project (2017–2020), the European Regional Development Fund under project KONPRO 2 (Development of a new generation of numeric protection devices) (2019–2020), the European Regional Development Fund under project USBSE (Connected Stationary Battery Energy Storage) (2020–2021), the European Regional Development Fund under project Development of a digital platform for building Critical Infrastructure Protection Systems in Smart Industries – CIP 4 SI (2021–2023).

He received his master's degree in electrical engineering and communication technology in September 2008. He passed the supplementary teacher education program (pedagogy, psychology, methodology, didactics), University of Zagreb, Faculty of Teacher Education, Mar. 2012. He passed the following State exams: State exam of the Expert for Occupational Safety, at the Croatian Ministry of trade, work and entrepreneurship, Sep. 2010, State exam for the performance of activities in construction projects, at the Croatian Ministry of Construction and Physical planning, May 2012, State exam for the performance of activities in testing and conformity assessment of construction, at the Croatian Ministry of Construction and Physical planning, Feb. 2015. He is a member of Croatian Chamber of Electrical Engineers since Sep. 2014.

He participated in a guest program within energy engineering at Faculty of Engineering and Science, Department of Energy Technology, Power Electronic Systems, Aalborg University, Denmark, Sep. 2016 – Dec. 2016.

His research interests include testing, evaluation, and modeling of lithium-based batteries for application in energy systems and electric vehicles. Hrvoje is involved in teaching activities as a teaching assistant in the Bachelor Programme course Fundamentals of Electric and Hybrid Vehicles and the Master Programme course Control of Energy Storage Systems. He supervises bachelor and master student thesis progress.

Hrvoje is a member of professional associations IEEE and CIGRE.

Journal Papers

[J_1]H. Baši ć, V. Bobanac and H. Pandžić, "Determination of Lithium-ion Battery Capacity for Practical Applications," *Batteries* (ISSN 2313-0105), 2023, DOI: https://doi.org/10.3390/batteries9090459

[J_2]V. Bobanac, H. Baši ć and H. Pandžić, "A Method for Deriving Battery One-way Efficiencies," *Journal of Energy Storage*, 2023, DOI: https://doi.org/10.1016/j.est.2023.108815

[J_3]H. Baši ć, H. Pandžić, M. Miletić and I. Pavić, "Experimental Testing and Evaluation of Lithium-Ion Battery Cells for a Special-Purpose Electric Vacuum Sweeper Vehicle," *IEEE Access*, vol. 8, pp. 216308-216319, 2020, DOI: 10.1109/ACCESS.2020.3040206

[J_4]Z. Zbunjak, H. Baši ć, H. Pandžić, I.Kuzle, "Phase shifting autotransformer, transmission switching and battery energy storage systems to ensure n-1 criterion of stability", Journal of Energy, vol. 64, no. 3, pp. 285-298, 2016, DOI: 10.37798/2015641-4157

Conference Papers

[C_1]V. Bobanac, H. Baši ć, H. Pandžić, "One-way voltaic and energy efficiency analysis for lithium-ion batteries" in *13th Mediterranean Conference on Power Generation, Transmission, Distribution and Energy Conversion (MEDPOWER 2022)*, 2022, pp. 261–266, DOI: 10.1049/icp.2023.0003

[C_2]V. Bobanac, H. Baši ć, H. Pandžić, "Determining Lithium-ion Battery One-way Energy Efficiencies: Influence of C-rate and Coulombic Losses", in *IEEE EUROCON 2021 - 19th International Conference on Smart Technologies*, 2021, pp. 385–389, DOI: 10.1109/EUROCON52738.2021.9535542

[C_3]H. Baši ć, T. Dragičević, H. Pandžić, F. Blaabjerg, "DC microgrids with energy storage systems and demand response for providing support to frequency regulation of electrical power systems", in *2017 19th European Conference on Power Electronics and Applications (EPE'17 ECCE Europe)*, 2017, pp. P.1-P.10, DOI: 10.23919/EPE17ECCEEurope.2017.8099000

[C_4]H. Baši ć, T. Dragičević, H. Pandžić, F. Blaabjerg, "DC microgrids providing frequency regulation in electrical power system - imperfect communication issues", *2017 IEEE Second International Conference on DC Microgrids (ICDCM)*, 2017, pp. 434–439, DOI: 10.1109/ICDCM.2017.8001081

Patents

[P_1]H. Pandži ć, V. Bobanac, H. Bašić, "Method for experimental determination of battery parameters and their use", International Application No. PCT/EP2022/070718, European Patent Office, July 23, 2022

Životopis

Hrvoje Bašić je asistent na Zavodu za visoki napon i energetiku Sveučilišta u Zagrebu Fakulteta elektrotehnike i računarstva. Njegovo zaposlenje financira Hrvatski operator prijenosnog sustava i Hrvatska zaklada za znanost u sklopu programa SIREN (Napredna integracija obnovljivih izvora) (2015–2018), Europski fond za regionalni razvoj u sklopu projekta Kompaktna gradska vakuumska čistilica s univerzalnom platformom za različite vrste pogona i informacijsko komunikacijskim sustavom (2017–2020), Europski fond za regionalni razvoj u sklopu projekta KONPRO 2 (Razvoj nove generacije uređaja numeričke zaštite) (2019–2020), Europski fond za regionalni razvoj u sklopu projekta USBSE (Umreženi stacionarni baterijski spremnici energije) (2020–2023), Europski fond za regionalni razvoj u sklopu projekta Razvoj digitalne platforme za izgradnju sustava zaštite kritičnih infrastruktura u pametnim industrijama – CIP 4 SI (2021–2023).

Diplomirao je u rujnu 2008. godine na Sveučilištu u Zagrebu Fakultetu elektrotehnike i računarstva. 2012. položio je grupu pedagoških predmeta na Učiteljskom fakultetu u Zagrebu. 2012. godine položio je stručni ispit za obavljanje poslova prostornog uređenja i graditeljstva u strukovnom području elektrotehnike za obavljanje poslova sudionika u gradnji. Član je Hrvatske komore inženjera elektrotehnike od 2014. godine. 2015. godine položio je stručni ispit za obavljanje poslova prostornog uređenja i graditeljstva u strukovnom području elektrotehnike za obavljanje poslova ispitivanja i potvrđivanja sukladnosti u graditeljstvu.

Tijekom 2016. godine 3 mjeseca je proveo na znanstvenom usavršavanju na Faculty of Engineering and Science, Department of Energy Technology, Power Electronic Systems, Aalborg University, Danska.

Njegovi istraživački interesi obuhvaćaju testiranje, evaluaciju i modeliranje litij-ionskih baterija za primjenu u elektroenergetskom sustavu i električnim vozilima.

Hrvoje sudjeluje u nastavi preddiplomskog studija na predmetu Osnove električnih i hibridnih vozila i na diplomskom studiju na predmetu Upravljanje spremnicima energije. Također nadzire napredak studenata preddiplomskog i diplomskog studija tokom završnog i diplomskog rada.

Hrvoje je član stručnih udruga IEEE i CIGRE.